VALUE-ADDED PRODUCTS FROM WASTE BIOMASS

VIA THERMAL AND CATALYTIC PROCESSING

by

Matthew David Lemieux

A dissertation submitted to the faculty of
The University of Utah
in partial fulfillment of the requirements for the degree of

Doctor of Philosophy

Department of Chemical Engineering

The University of Utah

December 2017

The University of Utah Graduate School

STATEMENT OF DISSERTATION APPROVAL

The dissertation of **Matthew David Lemieux**

has been approved by the following supervisory committee members:

Swomitra K. Mohanty	, Chair	**15 June 2017** Date Approved
Manoranjan Misra	, Member	**15 June 2017** Date Approved
Eric Eddings	, Member	**16 June 2017** Date Approved
John McLennan	, Member	**15 June 2017** Date Approved
Michael Free	, Member	**26 April 2017** Date Approved

and by **Milind Deo** , Chair/Dean of

the Department/College/School of **Chemical Engineering**

and by David B. Kieda, Dean of The Graduate School.

ABSTRACT

Lignocellulosic biomass can be upgraded via pyrolysis, yielding biochar as a value-added product, in addition to condensable liquid fractions known as pyrolysis oils; however, the utilization of these pyrolysis oils is hampered by high water content, instability, and corrosiveness. Oily biomass can be upgraded by extraction of oils and subsequent conversion to biodiesel; however, shortcomings of traditional biodiesel processes include the use of harshly acidic or basic reaction environments that require costly neutralization processes, as well as the need for expensive, high-quality feedstocks. In this work, a newly-developed ionic liquid catalyst is shown to have excellent potency for the esterification of free fatty acids (FFA) to produce biodiesel, affording the use of cheaper feedstocks traditionally seen as "waste" oils. It is also shown to achieve the esterification of acids in pyrolysis oil to partially mitigate the corrosiveness and instability of the bio-oil, allowing greater opportunity for downstream processing and utilization. Kinetic models describing the behavior of both reactions are derived and compared to the data. Notably, the kinetic treatment of pyrolysis oil exhibits remarkable accuracy for its simplicity relative to the complex composition of pyrolysis oil, with integer reaction orders definitively confirmed by experimental data. A novel coprocessing scheme that applies the catalyst to both reactions without an intermediate recovery step is developed and shown to allow both pyrolysis oil mitigation and the deacidification of high-FFA triglyceride oils to proceed in a single process, demonstrating the catalyst's broad potential for the upgrading of waste biomass.

For Grandma Shirley and Kimmy Rose Lemieux

“There is no such thing as waste.

‘Waste’ is a co-product looking for an opportunity.”

—Amar Mohanty
Professor, University of Guelph

TABLE OF CONTENTS

NOMENCLATURE

$(-r_{\mathrm{FFA}})$	≡	Rate of disappearance of free fatty acid (FFA). [=] g ml^{-1} min^{-1}
k	≡	Reaction rate constant. Units depend on rate law.
$[\mathrm{C}]$	≡	Mass concentration of catalyst in reaction mixture. [=] g ml^{-1}
$[\mathrm{FFA}]$	≡	Mass concentration of FFA in reaction mixture. [=] g ml^{-1}
n	≡	Reaction order with respect to a reactant.
m	≡	Reaction order with respect to a reactant.
C^{o}_{FFA}	≡	Initial mass concentration of FFA in reaction mixture. [=] g ml^{-1}
X_{FFA}	≡	Fractional conversion of FFA.
t	≡	Reaction time. [=] min
Ψ	≡	Slope of linearized reaction rate equation.
E_a	≡	Apparent activation energy (temperature dependence) of reaction.
M_{FFA}	≡	Molar mass of FFA. [=] g mol^{-1}
M_{FAME}	≡	Molar mass of fatty acid methyl ester (FAME) product. [=] g mol^{-1}
$(-r_{H^+})$	≡	Rate of disappearance of reactable acid groups. [=] mol ml^{-1} min^{-1}
$[\mathrm{H}^+]_{\mathrm{Titration}}$	≡	Concentration of acid groups determined by titration. [=] mol ml^{-1}
$[\mathrm{H}^+]_{\mathrm{Catalyst}}$	≡	Concentration of acid groups from catalyst. [=] mol ml^{-1}
$[\mathrm{H}^+]$	≡	Concentration of reactable acid groups. [=] mol ml^{-1}
$[\mathrm{H}^+_0]$	≡	Initial concentration of reactable acid groups. [=] mol ml^{-1}
φ	≡	Fraction of titratable acid groups that will react with catalyst.
X_{H^+}	≡	Fractional conversion of titratable acid groups.
F	≡	Function that is assumed to include the reaction rate constant.
Θ	≡	Slope of a plot of the slopes of linearized rate laws**.**

ACKNOWLEDGMENTS

I first want to extend my gratitude to my advisor, Professor Bobby Mohanty, for his guidance, support, and generosity during my long tenure as his student, as well as the unique opportunities he's afforded me to build a strong skills-set for my future. I would also like to thank Professor Eric Eddings for finding a project to support me financially when funding was tight, and for lending his expertise and feedback to my work.

I am also grateful for the superior instruction I have received at the University of Utah; although coursework seems insignificant in comparison to all the lab work that has led up to this dissertation, a deep understanding of engineering fundamentals built through academics is directly responsible for my success as a researcher. This success would not have been possible without the genius and commitment of many great teachers: Professors Mikhail Skliar, Jaye Magda, Milind Deo, James Sutherland, Kevin Whitty, Jost Wendt, Richard Christiansen, John McLennan, and Rich Roehner.

Lastly, I would like to thank my family: my parents and my brothers for their continued support through my entire academic career; Grandma Shirley, Grampa Mike, and Aunt Debbie for making me always feel at home in Utah; my wife, Jessica, for always pushing me to be my best; and my daughter, Kimmy, for giving purpose to the thousands of hours of tedious labor that have finally culminated in this dissertation.

CHAPTER 1

INTRODUCTION

1.1 Motivation

There is a need for novel applications in biomass utilization, including unexplored avenues for upgrading the downstream products of existing processes, as well as alterations to existing processes in order to make better use of untapped feedstocks. Economic shortcomings of existing processes could be overcome by additional opportunities for using cheaper feedstocks and the potential for further upgrading to value-added products.

Pyrolysis of biomass yields a solid product, biochar, that can be steam-treated to produce activated carbon in addition to being a useful product in its own right. However, little use has been made of the corrosive liquid products (pyrolysis oils) also produced from these processes, and much of what has been reported in the literature has focused on energy-intensive catalytic avenues for conversion of pyrolysis liquids to conventional hydrocarbons. Mitigation of the corrosiveness of pyrolysis oil would allow for easier utilization as an alternative fuel or as a component in an alternative fuel blend.

Economic shortcomings of biodiesel processes result from the high cost of feedstocks for conventional processes, which call for oils with a very low content of free fatty acids (FFA). Additionally, the homogeneous catalysts used in these processes must

be neutralized from the biodiesel product, and thus cannot be reused. New catalysts seek to overcome these shortcomings by allowing biodiesel to be made more easily from cheaper, high-FFA feedstocks, and this research program characterizes an extremely potent novel ionic liquid catalyst for FFA esterification. Furthermore, this research program connects the two avenues of waste biomass utilization—biodiesel production and pyrolysis—by exploring the possibilities of catalytic co-processing of pyrolysis liquids with biodiesel feedstocks, which could allow the development of a unified process for creating a useful alternative fuel blend from low-quality feedstocks.

An integrated approach to upgrading biomass is proposed in Figure 1.1, which relates biodiesel and pyrolysis avenues to the appropriate feedstock types and potential value-added products. Improvements to any of the indicated processes would allow for better utilization of biomass products that remain relatively untapped as energy sources. Generally, better handling of FFA would allow more feedstocks to be economically converted to biodiesel; better downstream processing of pyrolysis oils would greatly enhance the economics of biomass pyrolysis, for which char is the only broadly recognized value-added product.

1.2 Pyrolysis as an Avenue for Biomass Utilization

Pyrolysis of lignocellulosic biomass produces biochar and gaseous byproducts, as well as liquid fractions—known as pyrolysis oils—that are rich in phenolic, acidic, and other oxygenated compounds. Depending on feedstock and processing conditions, pyrolysis liquids can account for 10–40 % of the original dry mass of the feedstock (Akhtar and Amin, 2012). Utilization of pyrolysis oils is hampered by its water content

(15–30 wt %), as well as instability and corrosiveness. Viscosity can vary widely from 35–1000 cP (at 40 °C), with bio-oils becoming more viscous with self-catalyzed polymerization reactions that occur with aging. The low pH (2–3) due to organic acids creates concerns over corrosion, especially at elevated temperatures and with higher water contents, necessitating the use of stainless steel construction for equipment (Czernik and Bridgwater, 2004).

1.2.1 Composition of Pyrolysis Liquids

Pyrolysis is a means of thermal densification of a wide range of possible feedstocks, including spent coffee grounds (Jeguirim et al., 2014), beech wood (Mahfud et al., 2007), pelletized wood (Moens et al., 2009), mallee wood (Gunawan et al., 2012), wheat straw (Wang et al., 2013), pine chips (Zhang et al., 2011), as well as pinyon pine, juniper wood, chicken litter, and shredded pallets (based on conversations with Amaron Energy, Salt Lake City, UT). The composition of pyrolysis oils will vary with feedstock choice, process conditions, and the process configuration; however, they are generally rich in water, light carboxylic acids (C_1–C_4), phenolic compounds, ketones, aldehydes, furan derivatives, and alcohols. Table 1.1 compares the elemental composition of a representative pyrolysis oil to that of heavy fuel oil, showing the markedly higher oxygen and moisture content of the bio-oil, as well as its comparatively low heating value.

The pyrolysis oil employed for this research was analyzed by GC-MS, and while the chromatograph was not used for the analysis or conclusions of this research, it is illustrative of the mix of functional groups typically observed in pyrolysis oil. Table 1.2 presents a list of selected compounds identified by mass spectrometry, separated by

relevant functional groups. Compound identification is tentative, although the classification by functional group is likely reliable. Relative peak area percentages are broadly indicative of relative mass fractions of compounds, but there is not a direct proportionality. Nonetheless, the chromatographic results reveal the wide variety of oxygenated species within a typical pyrolysis liquid. Table 1.3 similarly presents a breakdown of oxygenated species based on reported results for bio-oil derived from the pyrolysis of pine chips (Zhang et al., 2011).

1.2.2 Upgrading Pyrolysis Oil

Much work concerning the upgrading of pyrolysis liquids has focused on energy-intensive catalytic treatments for producing hydrocarbon fuels—processes that are complicated by the panoply of different functional groups present in the oil. Since pyrolysis oils are often immiscible with hydrocarbon mixtures, they cannot simply be added to refinery streams and must be pretreated to remove oxygen. Furthermore, following the removal of oxygen, a pyrolysis liquid must be sufficiently distilled to yield useful hydrocarbon fractions, adding to the upgrading costs and eliminating any supposed advantage over petroleum-derived fuel sources (Qi et al., 2007; Bridgwater, 2012). There are alternatives to fully upgrading pyrolysis oil, and these seek to mitigate the undesirable properties of PyOil without the large material and energy investments of hydrodeoxygenation and distillation. Carboxylic acids can be converted to short chain esters, increasing the shelf life and reducing the corrosiveness of the resulting oil. Hilten et al. (2010) added ethanol to uncondensed pyrolysis vapors in order to control fractionation and condensation, as well as to convert acids to ethyl esters. Pyrolysis oils

can also be blended with traditional fuels to create emulsions that make use of the heating value of PyOil while mitigating its viscosity and reactivity. PyOil emulsions with diesel have been examined and even tested in conventional diesel engines to determine the effect of the oils on engine performance and wear (Chiaramonti et al., 2003a, 2003b; Ikura et al., 2003). Blends of PyOil with biodiesel have also been explored, using alcohols as co-solvents to make use of the heating value of these oils while overcoming the undesirable aspects of using either oil on its own (Alcala and Bridgwater, 2013).

Deacidification of pyrolysis oil has been explored as a means of mitigating bio-oil corrosiveness and improving its flow properties. In addition to being the main cause of the corrosiveness of bio-oil, carboxylic acids catalyze the polymerization of oxygenated species in pyrolysis liquids (Hu et al., 2017). Reaction of pyrolysis oil with alcohols in the presence of an acidic catalyst leads to the esterification of carboxylic acids and the acetalization of aldehydes and ketones, leading to a more benign oil that is easier to handle, often having improved stability and lower viscosity (Zhang et al., 2006).

Moens et al. (2009) tested the esterification of pyrolysis oil derived from a mixture of pelletized hard and softwoods using different acid catalysts in an excess of methanol. The results of one-pot experiments without the removal of reaction products, shown in Table 1.4, reveal equilibrium limitations that are generally not overcome with greater excesses of methanol.

The acid treatment was also carried out with azeotropic water removal by continuous addition of cyclohexane, affording increases in conversion but also causing the formation of a semisolid tar fraction with poor flow characteristics. Reactive distillation with excess methanol was tested, whereby light reaction products (esters and

acetals) were selectively distilled off while leaving water in the reaction mixture. This approach allowed the isolation of low-boiling (< 65 °C) reaction products, making it possible to remove small oxygenated species in pyrolysis oil by isolating their esterification/acetalization products in a distillate phase.

Wang et al. (2013) likewise tested reactive distillation of pyrolysis acids, using tosylic acid (*p*-toluene sulfonic acid) loaded on activated carbon as the catalyst. Preliminary water removal through vacuum distillation preceded the catalytic treatment of a bio-oil (derived from either slow pyrolysis of sawdust pellets or fast pyrolysis of wheat straw powder), and the quality of the bio-oils was found to improve through the treatment. Heating values increased from 14–17 MJ/kg to 25–29 MJ/kg; however, viscosities increased and the product acidity required mitigation by the addition of base.

Gunawan et al. (2012) tested the esterification of mallee biomass-derived pyrolysis oil using Amberlyst-70 solid acid ion-exchange resin in methanol, also examining the hydrolysis and glycosidation of pyrolysis oil sugars that happens concurrently with the esterification/acetalization reactions. At temperatures above 90 °C, these reactions become significant, converting sugar compounds into more stabilized products, as well as consuming water generated from the esterification and acetalization reactions.

The use of ionic liquid catalysts in the upgrading of pyrolysis oil was examined by Xiong et al. (2008), and they found that dicationic acids could achieve reasonable levels of esterification at room temperature and that the reaction mixture would phase-separate, leaving a bio-oil layer (48 % yield) with better heating value and flow characteristics than the source oil, separate from a polar layer containing water, the ionic

liquid, and small amounts of hydrophilic compounds. Under very mild conditions, moisture and acidity of a bio-oil were mitigated using a dicationic ionic liquid catalyst.

1.3 Biodiesel Production as an Avenue for Biomass Utilization

Biodiesel is a fuel product consisting primarily of fatty acid alkyl esters, produced from the transesterification of triglycerides (TG) and the esterification of free fatty acids (FFA), using an alcohol in the presence of a catalyst. The alcohol is typically methanol or ethanol; though longer-chain alcohols have also been employed to achieve better fuel characteristics, methanol is the most common choice due to its low cost (Huber et al., 2006). Catalysts have typically been strong, homogeneous acids or bases, such as sulfuric acid (H_2SO_4) or sodium hydroxide (NaOH), although the literature now reports a variety of different catalysts that have been tested for TG transesterification and FFA esterification, such as ion-exchange resins, ionic liquids, solid-supported ionic liquids, mixed metal-oxides, and enzymes (Chouhan and Sarma, 2011).

Biodiesel shows promise as an alternative fuel to help form part of the multi-pronged future of energy solutions. There is no magic bullet for today's energy challenges: overreliance on petroleum sources that are becoming increasingly expensive to develop, the contribution of traditional combustion fuels to net increases in atmospheric CO_2 and links to anthropogenic global climate change, national security concerns over Western dependence on volatile regions of the world for energy resources, emerging economies' growing reliance on fossil fuels, and environmental hazards associated with transporting large quantities of hydrocarbon fuels around the world, among other issues. However, next-generation technologies aim to open the door to broad

utilization of a diverse portfolio of energy sources, and biodiesel production is of particular interest to the transportation fuels sector. Compared to petroleum diesel fuels, biodiesel fuels have advantages of biodegradability, reduction of exhaust emissions (other than NO_x, which are actually worse with biodiesel utilization), safer handling, and superior lubricity in engines. In the European Union, where 90 % of the world's biodiesel is produced and markets are well-suited to its growth as an industry, production is estimated at 7.9 billion gallons/year (Huber et al., 2006).

1.3.1. Chemistry of Biodiesel Production

The transesterification of triglycerides requires a basic catalyst. Although there is an acidic pathway, it is a much slower reaction that requires a concentrated strong acid for reasonable yields. In an excess of methanol under reflux conditions, a typical catalyst loading would be 0.2 wt. % NaOH (as a fraction of oil mass) to achieve near-complete conversion within 30 minutes, while the acidic pathway would require 1.0 wt. % H2SO4 to achieve only 50 % conversion over several hours (Balat and Balat, 2010). Figure 1.2 shows the overall reaction equation for TG transesterification; however, the reaction actually takes place over three transesterification events. Methanol replaces the glycerol backbone for one of the long alkyl chains, producing a methyl ester molecule and leaving behind a diglyceride (DG) molecule. The reaction repeats for one of the diglyceride chains, producing another methyl ester molecule and leaving behind a monoglyceride (MG) molecule. The monoglyceride is finally reacted to form a third methyl ester unit, leaving behind glycerol, which separates from the oil phase of the reaction mixture. Although each transesterification event is theoretically reversible, the phase-separation of

glycerol shifts the equilibrium towards the generation of products (Di Serio et al., 2008).

The esterification of free fatty acids requires an acidic catalyst. The alcohol replaces the acidic OH group of the FFA, generating the alkyl ester product and eliminating water as a byproduct, as shown in the chemical reaction equation drawn in Figure 1.3. Unlike TG transesterification, however, there is not a basic pathway for FFA esterification.

The reaction of FFA with a homogeneous base produces soap and water, as shown in the reaction equation for FFA saponification drawn in Figure 1.4. Soap generation has serious implications for a biodiesel process by affecting not only the phase-separation of glycerol from the biodiesel product, but also hampering downstream purification of biodiesel (Nakagaki et al., 2008). Processing FFA with a basic catalyst involves adding additional catalyst to make up for its consumption due to soap formation; however, if the fatty acid content of the feedstock exceeds 0.5 wt. %, saponification can lead to gel formation, increased viscosity, and higher product separation costs that severely hamper the economic viability of the overall process (Lotero et al., 2005). Because of the strict FFA specifications required for homogeneous base esterification, the feedstocks most suited to being upgraded to biodiesel—those without competing roles as food products and those which can be extracted from waste products—are off-limits to straightforward treatment with a homogeneous strong base. Table 1.5 lists some examples of biodiesel feedstocks and their FFA contents, showing the broad range of bio-oil sources that require treatment of both triglycerides and free fatty acids for efficient biofuels production. Conversion to biodiesel can be accomplished in a two-step scheme, with acid-catalyzed esterification followed by base-catalyzed transesterification

(Atadashi et al., 2012); however, catalyst separation must either be extremely energy-intensive, or the catalyst must simply be neutralized, preventing recovery and reuse. A high-FFA feedstock could also be treated with concentrated sulfuric acid to promote both reactions with the same catalyst, but this scheme also presents issues for catalyst recovery and neutralization, and the handling of concentrated, strong acids creates concerns over corrosion, necessitating costlier equipment (Kondamudi et al., 2011).

These challenges have motivated the study of alternative catalysts, aimed at being more environmentally benign, easier to recover, and more versatile. Solid heterogeneous catalysts afford easier recovery and reuse, with some catalysts having bifunctional character to effect acidic esterification and basic transesterification simultaneously (Semwai et al., 2011). Table 1.6 summarizes the reported performance of several solid catalysts on different feedstocks, along with process parameters (Chouhan and Sarma, 2011). Generally, high yields require longer reaction times, higher temperatures, and larger methanol excesses for these catalysts versus traditional catalysts.

1.3.2. Ionic Liquids as Effective Catalysts for FFA Esterification

Ionic liquids are salts with peculiarly low melting points and are generally nonflammable, remarkably stable, and have extremely low vapor pressures. The cation of an ionic liquid often consists of a ring structure with a side chain that can be modified to tune the characteristics of the ionic liquid, allowing catalysts and solvents to be designed to satisfy desired specifications. When ionic liquids are used in biodiesel production, they generally partition into the polar (water/methanol) phase, allowing easy recovery by solvent extraction and washing/drying (Andreani and Rocha 2012). They can be used in

lieu of homogeneous strong acids for the esterification of FFA prior to treating the oil with a basic catalyst for TG transesterification. Figure 1.5 shows some of the varieties of ionic liquid structures that make for effective acid catalysts; common features are a nitrogen-containing positive functional group on the large cation and an anion that is the conjugate base of a strong acid. Terminal sulfonic groups on the hydrocarbon chain of the cation are also a common feature, although the work of Li et al. (2014) indicates that it is not as crucial as other structural characteristics of the ionic liquid. Among seven ionic liquids tested, [$BHSO_3MIM$][HSO_4] was by far the most potent; however, the same catalyst without the terminal sulfonic group, [BMIM][HSO_4], exhibited performance that was still far superior to the other catalysts tested. Table 1.7 lists several ionic liquid catalysts along with homogeneous strong acids and solid-supported acids, comparing their performance in the acid-catalyzed esterification of FFA and showing that respectable conversions can be achieved at relatively mild temperatures and reaction times compared to other catalysts; although catalyst loadings are higher, note that these catalysts are more benign and easily recoverable than homogeneous strong acids.

1.3.3. Mechanism of FFA Esterification

The acid-catalyzed esterification of free fatty acids with alcohols is a classic example of Fischer-Speier esterification. The proposed mechanism for Fischer-Speier esterification widely taught in Organic Chemistry textbooks is shown in Figure 1.6. In this mechanism, protonation of the carbonyl oxygen in the carboxylic acid leaves the carbonyl carbon vulnerable to nucleophilic attack by the alcohol. Proton rearrangement leads to the elimination of water from the reactive species, allowing the acid to be

reformed, leaving the ester product (Watson, 1937).

Recent work using density functional theory (DFT) calculations to predict activation energies and transition states, however, has cast doubt on the validity of this mechanism. Shi et al. (2015) propose that the reaction proceeds via the protonation of the non-carbonyl oxygen, based on DFT calculations showing that the carbonyl-protonated carboxylic acid cannot form the necessary tetrahedral intermediates with the alcohol species, preventing the reaction from taking place by that protonation. Instead, as shown in Figure 1.7, the alcohol is first protonated by the acidic catalyst, and the resulting alkyloxonium ion protonates the non-carbonyl oxygen of the carboxylic acid in the rate-limiting step. Elimination of water from the reactive intermediate forms an acylium ion which spontaneously reacts with two alcohol molecules (or two water molecules, in the hydrolysis reaction) in a trimolecular reaction to generate the ester product. Results from electrospray ionization-mass spectrometry were used to support the proposed mechanism.

The possible mechanisms of binding and association of the reactants with an ionic liquid catalyst for this reaction remain largely unexplored. Work by Vafeezadeh and Fattahi (2015) examined esterification over silica-functionalized propylsulfonic acid, proposing two possible pathways and their transition states. Notably, however, they did not discover a conflict between DFT calculations and the classical mechanism for Fischer-Speier esterification, although they may not have questioned the viability of the alcohol's approach to the carbonyl-protonated transition state or examined the possibility of acylium ion intermediates. Certainly, one study is not sufficient justification for throwing out widely accepted organic chemistry theory; however, the discrepancies are

indicative of the difficulty of ascribing a proposed mechanism to the observed behavior of a next-generation ionic liquid catalyst.

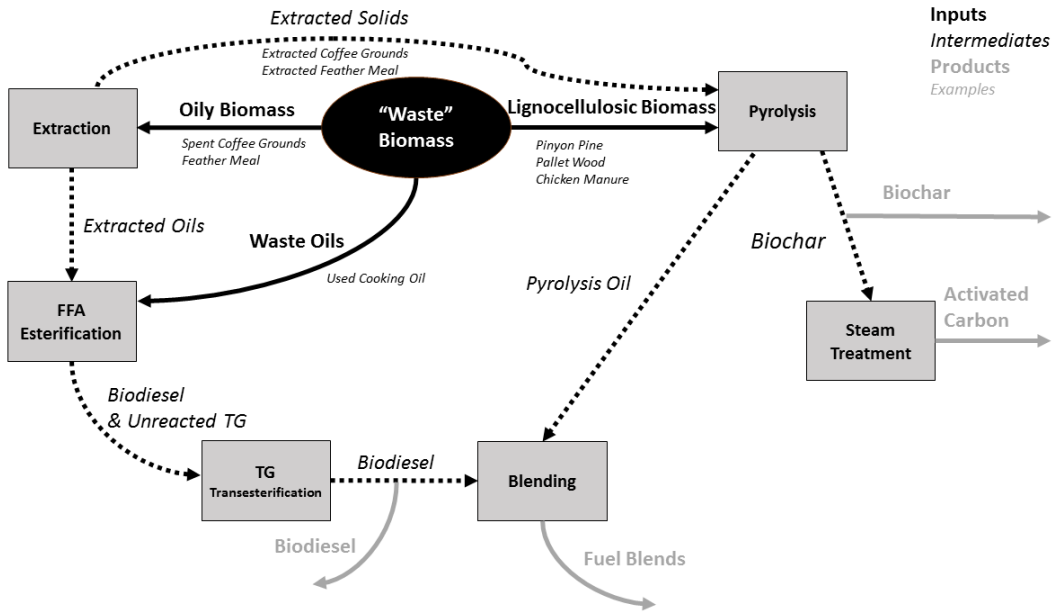

Figure 1.1. *An integrated approach to "waste" biomass utilization. Oily biomass can have its oils extracted for conversion to biodiesel, with the remaining solids pyrolyzed. Lignocellulosic biomass can be pyrolyzed as-is. Some waste oils can be converted to biodiesel as-is. Better processes for FFA esterification will allow for increased utilization of feedstocks traditionally seen as waste. New opportunities for downstream utilization of pyrolysis oil will increase the value added to biomass by densification through pyrolysis.*

Table 1.1. *Typical properties of wood pyrolysis oil and heavy fuel oil (data from Czernik and Bridgwater, 2004). The pyrolysis oil has much higher oxygen and moisture content and a significantly lower heating value relative to the fuel oil.*

Physical Property	**Bio-oil**	**Heavy Fuel Oil**
moisture content, wt %	15–30	0.1
pH	2.5	-
specific gravity	1.2	0.94
elemental composition, wt%		
C	54–58	85
H	5.5–7.0	11
O	35–40	1
N	0–0.2	0.03
ash	0–0.2	0.1
HHV, MJ/kg	16–19	40
viscosity (at 50 degC), cP	40–100	180
solids, wt%	0.2–1	1
distillation residue, wt %	up to 50	1

Table 1.2. *GC-MS analysis of pyrolysis liquid used for this work, showing selected compounds from the chromatogram, along with retention times (RT) and the compounds' associated fractions of the total chromatogram area.*

Retention Time (min)	**Compound Class** / Compound ID.	**% Tot. Area**
7.355–39.796	**Carboxylic Acids**	**25.29%**
7.355	(S)-2-Hydroxypropanoic acid	0.26%
11.365	Acetic acid	21.16%
13.533	Propanoic acid	1.05%
18.911	2-Butenoic acid, (E)-	0.30%
29.567	Pentanoic acid, 4-oxo-	0.81%
39.796	Benzeneacetic acid, 4-hydroxy-3-methoxy-	1.71%
225.855–36.601	**Sugar Derivatives**	**6.29%**
22.855	Maltol	0.90%
26.414	1,4:3,6-Dianhydro-.alpha.-d-glucopyranose	0.30%
28.483	2,3-Anhydro-d-mannosan	0.23%
30.768	1,4:3,6-Dianhydro-.alpha.-d-glucopyranose	0.94%
36.601	.beta.-D-Glucopyranose, 1,6-anhydro-	3.92%
20.68–35.697	**Phenolics**	**22.44%**
20.68	Mequinol [Phenol, 4-methoxy]	3.93%
22.659	Phenol, 2-methoxy-4-methyl-	5.97%
24.117	Phenol, 4-ethyl-2-methoxy-	2.45%
25.156	Phenol, 2-ethyl-	0.96%
25.637	Phenol, 2-methoxy-4-propyl-	0.57%
26.718	3-Allyl-6-methoxyphenol	0.58%
26.889	Phenol, 3-ethyl-	0.17%
29.974	Phenol, 2-methoxy-4-(1-propenyl)-, (E)-	0.40%
33.569	Vanillin [Phenol, 3-methoxy, 4-hydroxy-]	0.87%
34.748	Ethanone, 1-(4-hydroxy-3-methoxyphenyl)-	1.17%
35.014	Propan-2-one, 1-(4-isopropoxy-3-methoxyphenyl)-	2.24%
35.697	1,2-Benzenediol	3.13%
7.992–21.401	**Ketones**	**32.79%**
7.992	2-Propanone, 1-hydroxy- / hydroxyacetone / acetol	20.40%
9.297	2-Cyclopenten-1-one	0.49%
9.582	2-Cyclopenten-1-one, 3-methyl-	0.22%
9.651	1-Hydroxy-2-butanone	2.47%
10.16	2(1H)-Pyridinone, 3-hydroxy-	2.01%
13.144	2-Cyclopenten-1-one, 3-methyl-	0.29%
15.633	3,4-Dihydroxy-5-methyl-dihydrofuran-2-one	0.56%
16.785	2(5H)-Furanone, 5-methyl-	0.28%
17.66	2(5H)-Furanone, 3-methyl-	0.44%
18.453	2(5H)-Furanone	2.57%
20.034	2-Cyclopenten-1-one, 2-hydroxy-3-methyl-	1.96%
21.334	4-Hexen-3-one	0.94%
21.401	2-Cyclopenten-1-one, 3-ethyl-2-hydroxy-	0.17%
11.815–32.552	**Aldehydes**	**4.13%**
11.815	3-Furaldehyde	1.53%
25.265	Pentanal	0.91%
32.552	2-Furancarboxaldehyde, 5-(hydroxymethyl)-	1.68%
13.332–27.232	**Esters**	**2.22%**
13.332	Propanoic acid, ethenyl ester	0.24%
15.752	1,2-Ethanediol, monoacetate	0.83%
26.823	2-Hydroxy-gamma-butyrolactone	0.48%
27.232	1,2,3-Propanetriol, monoacetate	0.67%
4.405–22.115	**Alcohols**	**1.11%**
4.405	2-Propen-1-ol	0.13%
16.787	3-Furanmethanol	0.13%
22.115	Glycerin	0.84%

Table 1.3. *Selected oxygen-containing components of pyrolysis oil produced by fast pyrolysis of southern pine sawdust in an auger-fed reactor at 450 °C (data from Zhang et al., 2011).*

Components	Area (%)	Components	Area (%)
Acids	**12.67%**	**Alcohols**	**11.97%**
Glyoxylic acid	0.19%	Glycerin	11.17%
Formic acid	1.16%	1,2,3,4-Butanetetrol	0.59%
Acetic acid	8.84%	2,3-Dimethylcyclohexanol	0.18%
Propanoic acid	1.70%	3-Methoxy-1,2,4-butanetriol	0.03%
Butanedioic acid	0.41%	**Esters and Acetals**	**2.2%**
2-Hydroxy-3-methoxy-succinic acid	0.17%	2,2-Dimethoxypropane	0.1%
D-Araboascorbic acid	0.20%	Hexanedioic acid, monomethyl ester	0.58%
Phenols	**10.64%**	Acetic acid, 2-propyltetrahdropyran-3-yl ester	1.49%
Phenol	0.59%	**Furans**	**1.64%**
2-Methyl phenol	0.22%	2,5-Dimethylfuran	0.92%
3-Methyl phenol	0.37%	(2-Hydroxy-1-methoxy)ethylfuran	0.18%
2-Methoxyphenol	2.33%	2(5H)-Furanone	0.41%
2,6-Dimethyl phenol	0.26%	2,3-Dihydro-2,5-dimethylfuran	0.08%
2-Methoxy-4-methyl phenol	3.44%	2,5-Dimethoxytetrahydrofuran	0.05%
1,2-Benzenediol (catechol)	0.98%	**Sugars**	**51.58%**
4-Ethyl-2-methoxy phenol	0.75%	D-Arabinitol	0.17%
2-Methoxy-5-propenyl phenol	0.73%	2-Deoxy-D-arabitol	0.33%
2-Methoxy-4-propyl phenol	0.15%	2-Deoxy-D-galactose	0.54%
1-(4-Hydroxy-3-methoxyphenyl)-2-propanone	0.56%	2,2-Dimethyl-3-heptanone	0.60%
4-(3-Hydroxy-1-propenyl)-2-methoxy-phenol	0.17%	3-Deoxyglucose	0.13%
5-Hydroxy-6-methoxy-1-benzofuran-3(2H)-one	0.09%	1,4:3,6-Dianhydro-α-D-glucopyranose	0.43%
Ketones and Aldehydes	**4.66%**	2,3-Anhydro-D-galactosan	0.69%
3-Hydroxy-2-butanone	0.08%	2,3-Anhydro-D-mannosan	0.33%
1-Hydroxy-2-butanone	0.46%	3,4-Anhydro-D-galactosan	1.93%
4-Hydroxy-3-methyl-2-butanone	0.64%	D-Allose	1.46%
2-Methyl-cyclopentanone	0.14%	1,6-Anhydro-β-D-glucopyranose	44.13%
3-Methyl-1,2-cyclopentanedione	1.45%	D-Glycero-D-*galacto*-heptose	0.35%
2,2-Dimethyl-3-heptanone	0.60%	D-Glycero-d-ido-heptose	0.23%
4-Ethoxy-cyclohexanone	0.17%	Diacetonyl-D-mannosan	0.26%
4-Hydroxy-3-methoxy-benzaldehyde	0.33%	**Others**	**4.67%**
4-Hydroxy-2-methoxycinnamaldehyde	0.20%	2,3-Dihydroxy-1,4-dioxane	2.01%
2,3-Methylenedioxyanisole	0.26%	2-(2-Propenyl)-1,3-dioxolane	0.38%
Hexanedial	0.33%	Octahydro-4a(2H)-naphthalenecarboxylic acid	2.28%

Table 1.4. *Conversion of acids and carbonyl groups under different reaction conditions. RT = room temperature. Sulfuric acid was used as 1 wt. %, while the ion-exchange resins were 10 wt. %. *For this run, molecular sieves were added to absorb water. One equivalent of alcohol is the amount theoretically required to convert all carboxylic acids to esters and all carbonyl compounds into acetals. Table is adapted from Moens et al., 2009.*

Alcohol	Equivalents of alcohol	Catalyst	Temp (°C)	time (h)	Conversion of Carboxylic acids	Conversion of Carbonyl groups
MeOH	2	*no catalyst*	*RT*	29	3%	14%
MeOH	2	*no catalyst*	62	23	15%	25%
MeOH*	4*	H_2SO_4*	*RT**	21*	39%*	35%*
MeOH	2	H_2SO_4	*RT*	22	58%	31%
MeOH	4	H_2SO_4	*RT*	22	76%	29%
MeOH	6	H_2SO_4	*RT*	22	76%	31%
MeOH	8	H_2SO_4	*RT*	22	76%	37%
MeOH	2	H_2SO_4	63	21	76%	50%
MeOH	4	H_2SO_4	63	72	82%	52%
MeOH	2	Amberlyst-15	62	22	76%	41%
MeOH	2	Amberlyst-15	62–66	4 days	82%	58%
MeOH	2	Nafion SAC-13	62	4 days	27%	23%
EtOH	2	Amberlyst-15	64–72	21	58%	48%
n-BuOH	2	Amberlyst-15	70–74	19	58%	44%

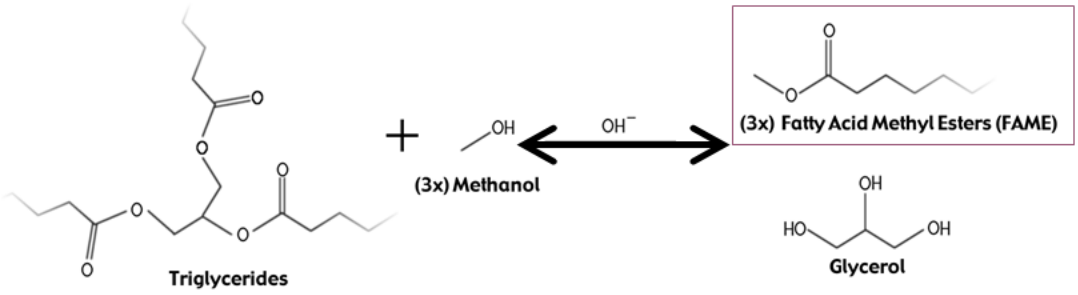

Figure 1.2. *Reaction equation for the base-catalyzed transesterification of triglycerides (TG) with methanol. The full carbon chains are not shown, as real oils will have a variety of chain lengths and unsaturated bond positions within the chains. While the reaction is generally reversible, the glycerol product phase-separates from the oil phase of the reaction mixture, shifting the equilibrium far to the products side of the reaction.*

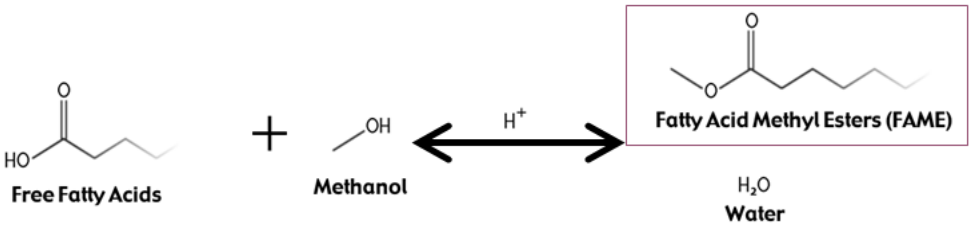

Figure 1.3. *Reaction equation for the acid-catalyzed esterification of free fatty acids (FFA) with methanol. The full carbon chains are not shown, as real oils will have a variety of chain lengths and unsaturated bond positions within the chains.*

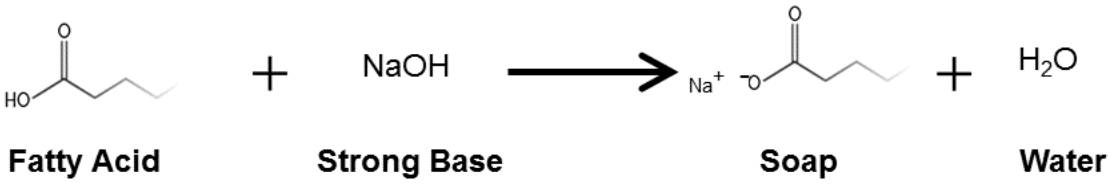

Figure 1.4. *Reaction equation for the saponification of FFA with a strong base, an undesired reaction which occurs when the transesterification of a high-FFA triglyceride feedstock is carried out with a homogeneous strong base catalyst, such as sodium hydroxide (NaOH).*

Table 1.5. *Oils extracted from biomass and their corresponding FFA contents. Waste oils and oils from non-food sources tend to have higher FFA contents, necessitating treatment of both TG and FFA for effective conversion to biodiesel.*

Bio-Oil	wt. % FFA	Reference
Canola Oil	0.04%	Leung and Guo (2006)
Soybean Oil	< 0.1%	Kouzu et al. (2008)
Tobacco Seed Oil	< 2.0%	Veljkovic et al. (2006)
Waste Cooking Oil	2.56%	Kouzu et al. (2008)
Waste Fryer Grease	5–6 %	Issariyakul et al. (2007)
Oil from Meat and Bone Meal	11%	Nebel and Mittelbach (2006)
Jatropha Curcas Oil	28%	Atadashi et al. (2012)
Oil from Spent Coffee Grounds	30%	Kondamudi et al. (2008)
Micro-algal Oil	20–50 %	Atadashi et al. (2012)
Palm Fatty Acid Distillate	93%	Chongkhong et al. (2009)

Table 1.6. *Selected heterogeneous catalysts tested on the esterification/transesterification of different oils. Adapted from the review of Chouhan and Sarma (2011).*

Oil Source	Catalyst	Temp (°C)	Alcohol:oil ratio	Catalyst Loading (wt% Oil)	Reaction Time (h)	Biodiesel Yield %	Reference
Sunflower Oil	Fe-Zn double-metal cyanide (DMC) complexes as solid catalysts.	170	15:1	3%	8	92%	Sreeprasanth et al. (2006)
Soybean Oil	ZnO loaded with Sr(NO3)2 (alkali earth metal)	65	12:1	5%	1–4	94.7%	Yoo et al. (2010)
Soybean Oil	Sulfated ZrO2	120	20:1	5%	1	98.6%	Garcia et al. (2008)
Soybean Oil	ZnO	130	55:1	5%	7	24%	Antunes et al. (2008)
Sunflower Oil	ZrO2 supported La2O3 catalyst (21% La2O3/ZrO2)	60	3:1	2%	5	84.9%	Sun et al. (2010)
Soybean Oil	TiO2/ZrO2	175–200	40:1	4.0%	4–20	95%	Furuta et al. (2006)
Waste Cooking Oil	Zinc stearate immobilized on silica gel (ZS/Si)	200	18:1	3%	10	98%	Jacobson et al. (2008)
Vegetabe oils	WO3/ZrO2 catalyst	75	19.4:1	0.2%	1	70%	Park et al. (2008)
Ethyl Propanoate/hexanoate	Heteropoly acids (H2SO4, Amberlyst-15 and Zeloites HY and H-Beta)	60	20:1	0.1%	1	84%	Alsalme et al. (2008)
Waste Cooking Oil	Zinc stearate immobilized on silica gel (ZS/Si)	200	18:1	3%	10	98%	Jacobson et al. (2008)
Vegetabe oils	WO3/ZrO2 catalyst	75	19.4:1	0.2%	1	70%	Park et al. (2008)
Coffee Oil	Sodium Quintinite (NaQ3-T)	70	12:1	10%	2	98%	Kondamudi et al. (2011)

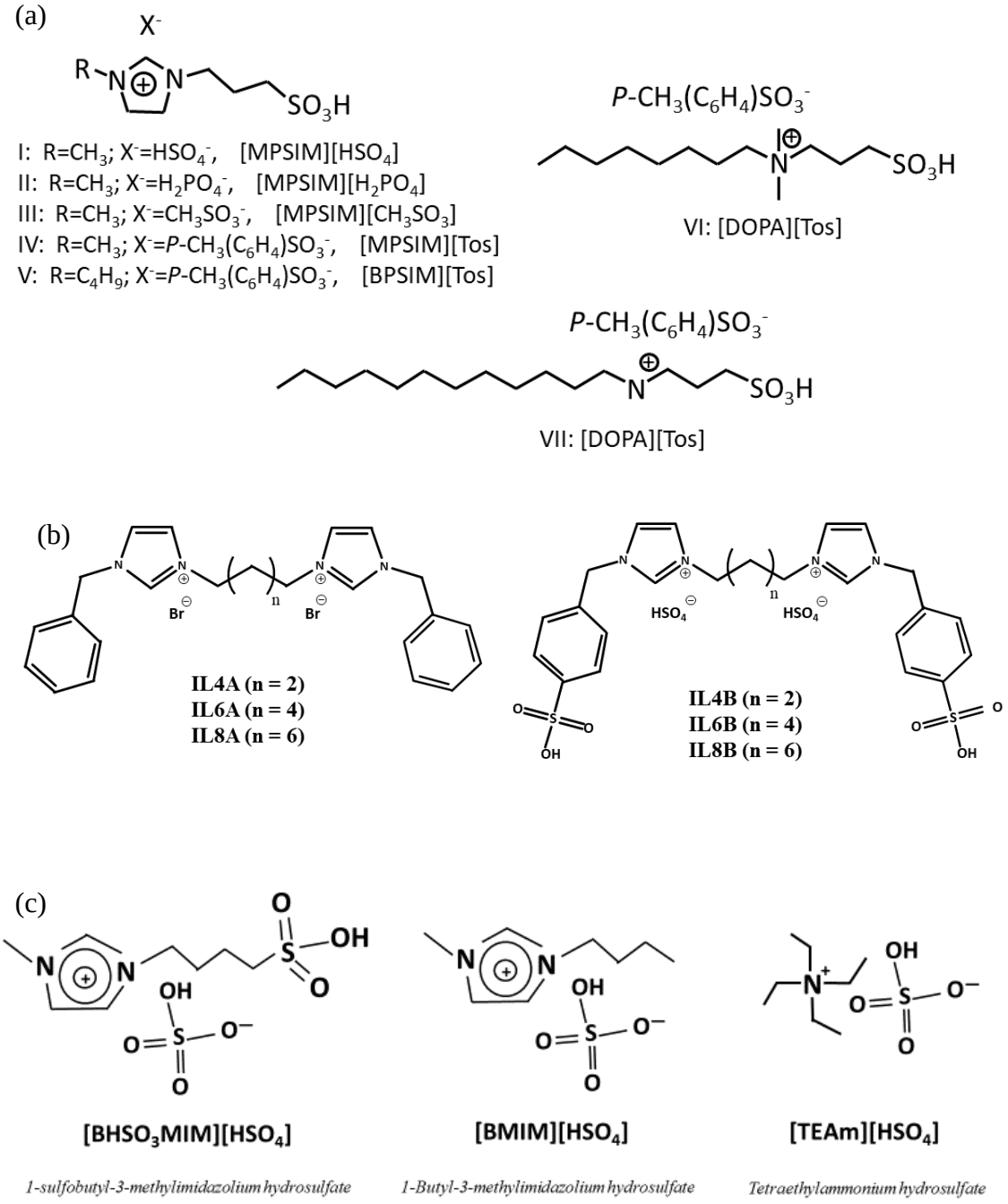

Figure 1.5. *Examples of acidic ionic liquid catalysts tested on the esterification of free fatty acids. Adapted from (a) He et al. (2012), (b) Aghabarari et al. (2014), (c) Li et al. (2014).*

Table 1.7. *Summary of different catalysts tested on the esterification of free fatty acids with methanol. "PFAD" is Palm Fatty Acid Distillate, which is primarily composed of palmitic acid and oleic acid. Catalyst loadings are on a basis of moles of catalyst per moles of FFA, except where noted.*

FFA	Catalyst Type	Catalyst	T (°C)	Cat Loading % mol FFA	MeOH:FFA	Reaction Time (h)	Conversion	Reference
Oleic	Solid	D5081 (polystyrene-supported sulfonic acid)	65	1.40%	44:1	2	85%	Andrijanto et al., 2012
Oleic	Solid	Amberlyst 15 (ion-exchange resin)	65	6.60%	44:1	2	45%	Andrijanto et al., 2012
Oleic	Solid	Relite CFS (ion-exchange resin)	85	2.70%	5.1:1	3.3	80%	Tesser et al., 2005
Stearic	Solid	EBD-100 (ion-exchange resin)	120	2.00%	2.1:1	24	100%	Russbueldt and Hoelderich, 2009
Oleic	Solid	Amorphous Carbon with SO3H groups	95	8.80%	25.8:1	4	99.9%	Nakajima and Hara, 2012
PFAD	Supported IL	Polystyrene-supported IL with terminal Trifluoromethane Sulfonic Acid group	60	7 wt %	4:1	3	61%	Heer et al., 2015
PFAD	Supported IL	Polystyrene-supported IL with terminal Tosylic Acid group	60	7 wt %	4:1	3	58%	Heer et al., 2015
PFAD	Supported IL	Polystyrene-supported IL with terminalSulfuric Acid	60	7 wt %	4:1	3	51%	Heer et al., 2015
PFAD	Strong Acid	Sulfuric Acid	60	3.00%	3:1	1	58%	Chabukswar et al., 2013
PFAD	Strong Acid	Tosylic Acid	60	1.00%	4:1	1	66%	Hayyan et al., 2012
PFAD	Strong Acid	Trifluoromethane Sulfonic Acid	60	1.00%	4:1	1	77%	Hayyan et al., 2012
Oleic	Strong Acid	4-DBSA	60	1.50%	2:1	5.5	96%	Alegria, 2015
Oleic	Ionic Liquid	IL8B	50	7.50%	2:1	6	95%	Aghabarari et al., 2013
Oleic	Ionic Liquid	IL6B	50	10%	2:1	5	80.3%	Aghabarari et al., 2013
Oleic	Ionic Liquid	IL4B	50	10%	2:1	5	76.1%	Aghabarari et al., 2013
Oleic	Ionic Liquid	[BHSO3MIM][HSO4-]	130	8.93%	4:1	4	97.7%	Li et al., 2004
Oleic	Ionic Liquid	[DDPA][Tos]	80	20%	2:1	1	97.9%	He et al., 2013
Oleic	Ionic Liquid	[BPSIM][Tos]	80	20%	2:1	2	96.0%	He et al., 2013
Oleic	Ionic Liquid	[MPSIM][HSO4]	80	20%	2:1	3	89.7%	He et al., 2013

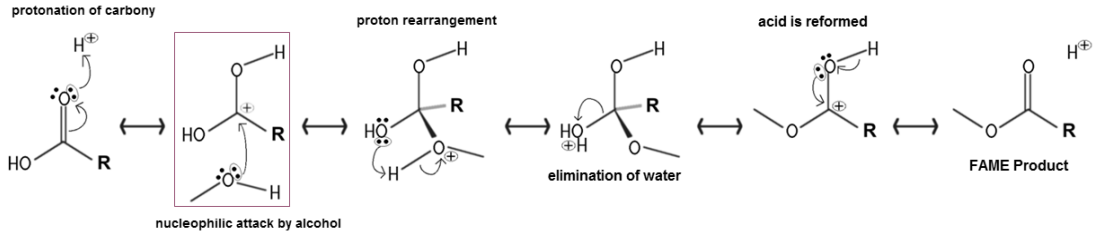

Figure 1.6. *Widely-taught mechanism for Fischer-Speier esterification of a carboxylic acid with an alcohol in the presence of an acid catalyst. Diagram is based on the work of Watson (1937).*

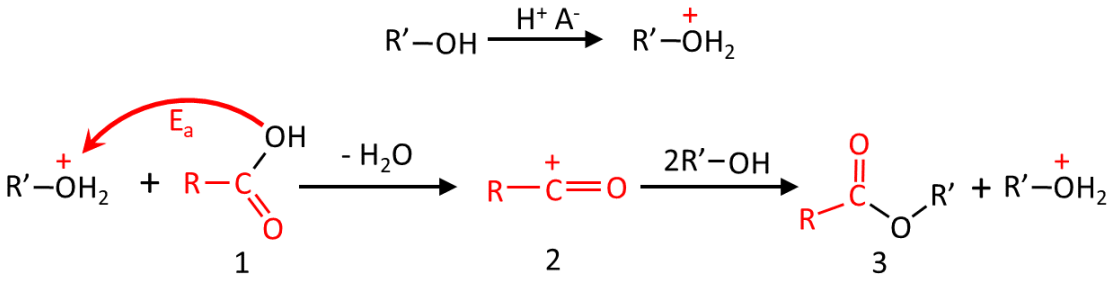

Figure 1.7. *Recently-proposed mechanism for Fischer-Speier esterification of a carboxylic acid with an alcohol in the presence of an acid catalyst, whereby the reaction proceeds via the protonation of the non-carbonyl oxygen. Adapted from the work of Shi et al. (2015).*

CHAPTER 2

IONIC LIQUID CATALYST FOR ACIDIC ESTERIFICATION OF FREE FATTY ACIDS WITH METHANOL

2.1. Abstract

Shortcomings of traditional biodiesel processes include the use of harshly acidic or basic reaction environments that require costly neutralization processes, as well as the need for expensive, high-quality feedstocks. In this chapter, we report the synthesis of an acidic ionic liquid and show that it is a potent catalyst for achieving the esterification of free fatty acids (FFAs)—a major component of oils derived from waste biomass—to produce biodiesel. Two model FFA compounds were reacted with an excess of methanol in a batch reactor setup, and kinetic parameters for applicable rate equations were derived from the measured fractional conversions. The resulting kinetic models predict FFA conversion as a function of reaction time and initial reactor loading, with a first-order dependence on FFA concentration and a first-order dependence on catalyst concentration. Fractional conversions in excess of 80% were achieved within 1 hour with catalyst loadings of only 0.83 wt % (mass of catalyst used / initial mass of FFA) at moderate temperatures (~60 °C), showing this to be a potent catalyst for acidic esterification of fatty acids. The catalyst's strong performance in the conversion of pure carboxylic acids indicates its potential utility in the deacidification of real bio-oils, such as high-FFA

biodiesel feedstocks or the acidic liquid fractions derived from biomass pyrolysis.

2.2. Introduction

Derived from renewable sources, biodiesel shows promise as a contributor to the growing alternative fuels market in the United States; however, it struggles against high production costs that prevent it from being an attractive competitor to fossil fuel-derived diesels. Shortcomings of current commercial biodiesel processes include the use of harshly acidic or basic reaction environments that require costly neutralization processes (Di Serio et al., 2008), as well as the need for expensive, high-quality feedstocks (Kondamundi et al., 2011).

Chemically, biodiesel consists of fatty acid methyl esters (FAME), which are produced through the esterification of free fatty acids (FFA) and the transesterification of triglycerides (TG), using a simple alcohol such as methanol (Huber et al., 2006). Utilizing the high-quality (low-FFA) feedstocks traditionally used in biodiesel processes—for example, corn oil and canola oil—puts an increased demand on what are otherwise food products, leading to unfavorable economics for biofuels production (Huber et al., 2006). Therefore, it will be crucial to the economic viability of biodiesel ventures to produce fuels from sources that have fewer alternative uses: lower-quality feedstocks like the oils extracted from spent coffee grounds (Kondamundi et al., 2008), algae (Huber et al., 2006), or feather meal (Nebel and Mittelbach, 2006; Kondamundi et al., 2009). These high-FFA waste products do not lend themselves well to traditional biodiesel catalytic processes, which can be complicated by soap and water formation from homogeneous base catalysts.

Ionic liquids are a new generation of nontraditional catalysts that have yet to be applied in commercial biodiesel production. The cation of an ionic liquid often consists of a ring structure with a side chain that can be modified to tune the characteristics of the ionic liquid, allowing catalysts to be designed to satisfy desired specifications (Andreani and Rocha, 2012). Different ionic liquids have been previously reported as catalysts for the esterification of free fatty acids, typically achieving respectable (~85 %) fractional conversions within 3–6 hours at mild conditions and catalyst loadings of 5–10 wt % relative to the fatty acid.

In this chapter, we present an ionic liquid having acidic character, examine its behavior in catalyzing the esterification of two saturated free fatty acids, and derive a kinetic model for those reactions to aid in the future design of a reactor employing this catalyst for the production of biodiesel from high-FFA feedstocks. The catalyst presented was found to effect relatively high conversions (50–85 % within 1 hour) at very low catalyst loadings (<1 wt %), showing it to be particularly potent for this application.

2.3. Materials and Methods

2.3.1. Materials

Palmitic acid (hexadecanoic acid, 98%, Acros Organics), Methanol (HPLC-grade, Fischer), n-Hexane (HPLC-grade, Alfa Aesar), 2-propanol (HPLC-grade, Fischer), docosane (99%, Alfa Aesar), and nonanoic acid (97%, Alfa Aesar) were used as received.

2.3.2 Catalyst Preparation

Figure 2.1 summarizes the catalyst preparation scheme. The Brønsted acid ionic liquid catalyst was synthesized by coupling 1-allyl imidazolium-containing zwitterion salt with CF_3SO_3H slowly at 0 °C and then stirring in an oil bath at 60 °C for 12 hours (Quiao et al., 2006). The zwitterionic salt was prepared by adding imidazole with 1,4-butane sultone in a flask, slowly at 0 °C. The solution was stirred for 24 hours at room temperature to convert the contents of the flask to solid which was then washed with ether and filtered under vacuum. A Fourier Transform Infrared (FTIR) spectrum of the compound showed two specific characteristic peaks at 1647 $cm^{-1}$and 2565 cm^{-1} corresponding to doubly bonded carbon-carbon vibration peaks indicating the formation of the compound.

2.3.3 Catalytic Testing

To test the catalytic esterification of palmitic acid with methanol, 12.0 g of palmitic acid were added to a three-neck, 250 ml round-bottom flask along with 30.2 g of methanol. These reactants were heated in a temperature-controlled oil bath to the reaction temperature (35–60 °C) for 30 minutes, under stirring, with an attached condenser to reflux evaporating methanol. Meanwhile, 0.05 g or 0.10 g of the catalyst was dissolved in 1.0 g of methanol before being added to the round-bottom flask to begin the experiment.

To test the catalytic esterification of nonanoic acid with methanol, 7.4 g of nonanoic acid were added to a three-neck, 250 ml round-bottom flask along with 30.2 g of methanol; hence, the molar ratio of methanol:FFA is the same as in the palmitic acid experiments. The lower bubble point of this reaction mixture made it necessary to run

this reaction at a lower temperature to ensure reliable sample collection. These reactants were heated in a temperature-controlled oil bath to the reaction temperature for 30 minutes, under stirring, with an attached condenser to reflux evaporating methanol. Meanwhile, 0.05 g or 0.10 g of the catalyst was dissolved in 1.0 g of methanol before being added to the round-bottom flask to begin the experiment.

During the experiment, samples were removed (roughly 200–400 µl each, deposited in 1.5 ml vials containing a solvent mixture) at reaction times of 1, 5, 7.5, 10, 15, 20, 25, 30, 45, and 60 minutes. The masses of collected samples were recorded for normalization of measured reactant concentrations during data analysis. At the end of each run, the remaining reaction charge was poured into a graduated cylinder and weighed in order to determine the density of the reaction mixture.

2.3.4 Sample Analysis

Each vial for sample collection was prepared with 1250 µl of a 4:5 (vol/vol) mixture of hexane and 2-propanol, also containing 0.05 g/ml of docosane for use as an internal standard. Vials were weighed at each stage of preparation to keep track of solvent and sample mass. After sample collection, 50 µl of each diluted mixture were further diluted by adding 1500 µl of n-hexane. To ultimately determine the fatty acid concentration in the reaction mixture at time *t*, these samples were analyzed on a gas chromatograph – mass spectrometer (Shimadzu GCMS-QP2010 Ultra) equipped with a Restek RTX-5MS capillary column. Injections of standard solutions of the fatty acid and docosane at different concentrations were used to calibrate the response of the mass spectrometer to the concentration of analyte in solution. Inconsistencies in the first

dilution were accounted for using the weights of solvent and sample. Inconsistencies in the second dilution were accounted for using the measured concentration of docosane in this final dilution. Running the experiment in the absence of any catalyst was found not to result in ester formation or consumption of the free fatty acid, so catalyst performance was evaluated based on fractional conversion of the free fatty acid.

Additional data were needed to confirm the reaction order and reliably determine the activation energy of the reaction. These experiments were performed as before, but the samples were removed every 15 minutes and then analyzed through a revised method that was found to be more reliable; the approximately 1.0 g aliquots were diluted with approximately 10 g of a homogenizing solvent (hexane in 2-propanol, 1:3 volume ratio), and approximately 0.5 g of the first dilution were added to approximately 20 g of methanol. Weights were recorded for every sample at every stage of dilution, allowing a dilution factor to be calculated for each sample. The GC-MS was calibrated for both nonanoic acid and methyl nonanoate, so that fractional conversion could be estimated based on consumption of FFA as well as generation of FAME.

2.4. Theory

A generalized reaction equation for FFA esterification with methanol is shown below:

$$\mathrm{FFA} + \mathrm{Methanol} \rightleftarrows \mathrm{FAME} + \mathrm{Water} \qquad (2.1)$$

The following form of the reaction rate equation is assumed (Roberts, 2009), based on the

reaction system having an “excess” of methanol—this work employs a 20:1 molar ratio of methanol to FFA

$$(-r_{\mathrm{FFA}}) = k[\mathrm{C}]^n[\mathrm{FFA}]^m \tag{2.2}$$

Or, expressed in terms of FFA conversion:

$$(-r_{\mathrm{FFA}}) = k(C^o_{\mathrm{FFA}})^m[\mathrm{C}]^n(1 - X_{\mathrm{FFA}})^m \tag{2.3}$$

This form of the rate expression neglects the reverse reaction; however, the excess of methanol allows this simplification except at the highest fractional conversions. It will be assumed that this reaction takes place in a constant-density liquid. Experimentally, the density of the liquid was found to change by less than 2% over the course of the reaction. The performance equation for a constant-volume, liquid batch reactor (Roberts, 2009) is expressed, in terms of fractional conversion of FFA, as:

$$\frac{dX_{FFA}}{dt} = \frac{(-r_{\mathrm{FFA}})}{C^o_{\mathrm{FFA}}} = k_1 {C^o_{\mathrm{FFA}}}^{m-1}[\mathrm{C}]^n(1 - X_{\mathrm{FFA}})^m \tag{2.4}$$

If the reaction is first-order with respect to FFA, as will be shown experimentally, then the above equation can be integrated to give the following:

$$-\ln(1 - X_{\mathrm{FFA}}) = k_1[\mathrm{C}]^n t \tag{2.5}$$

which means that a plot of $-\ln(1 - X_{\mathrm{FFA}})$ versus time will produce a line with a slope of $\Psi = k\,[\mathrm{C}]^n$ and an intercept of zero. The slope, Ψ, for such a model can be used to determine reaction order with respect to catalyst loading. If these slopes are calculated for two data sets that differ in catalyst loading only (other parameters being equal), then it follows that the reaction order with respect to catalyst loading, *n*, is given by:

$$n = \frac{\ln(\Psi_1/\Psi_2)}{\ln([\mathrm{C}]_1/[\mathrm{C}]_2)} \tag{2.6}$$

Once *n* has been determined, the rate constant *k* can be calculated from the slope of a first-order linear fit, according to Equation 2.7:

$$k = \frac{\Psi}{[\mathrm{C}]^n} \tag{2.7}$$

2.5. Results and Discussion

Linear regression parameters were determined assuming that the reaction is first-order with respect to the free fatty acid. Table 2.1 summarizes the experimental conditions and their resulting linear fits.

Figure 2.2 shows the first-order fit for the esterification of nonanoic acid over a 2-hour period. Linearity holds up fairly well until conversion appears to level off around 92%, indicating that this reaction is first-order with respect to fatty acid concentration until equilibrium limitations manifest at high fractional conversions.

Equation 2.6 estimates the reaction order with respect to catalyst concentration

from the slopes of two linear fits for different catalyst loadings with the same fatty acid feedstock and reaction temperature. Table 2.2 shows the results of estimating *n* from three different pairs of linear fits.

The spread is relatively narrow considering how sensitive the calculation is to the errors of the slopes. A cursory analysis indicates that the error of *n* will be roughly 170–180 % of the difference in the errors in the slopes (i.e., if the slopes skew the same direction, they partially cancel out). A pair of slopes skewing 3–4 % in opposite directions would easily result in a 10–15 % error in *n.* Therefore, based on the results' proximity to unity, it can reasonably be asserted that the reaction is first-order with respect to catalyst concentration, and the rate equation is simplified as shown in Equation 2.8:

$$(-r_{\mathrm{FFA}}) = k[\mathrm{C}][\mathrm{FFA}] \tag{2.8}$$

Equation 2.7 estimates the rate constant *k* from the slopes of the first-order linear fits, provided *n* is known. The rate constant was calculated from the data for different catalyst loadings with a given FFA and temperature, and the results were averaged. The relative differences in *k* between the two loadings were 3.0 % for both nonanoic acid (at 55 °C) and palmitic acid (at 60 °C). Activation energy was calculated using Arrhenius plots, whereby a plot of ln(*k*) versus 1/*T* yields a line whose slope is $-E_a/R$. The Arrhenius plot for the esterification of nonanoic acid is shown in Figure 2.3.

For palmitic acid, data from only two different temperatures were available due to the limited range of temperatures that could be effectively tested; solidification of

palmitic acid presented significant problems for sample collection at lower operating temperatures, and the volatility of methanol puts a ceiling on the temperatures that can be reliably maintained under atmospheric pressure (~0.85 atm absolute pressure where this work was performed). Additionally, as shown in Figure 2.4, the temperatures tested were too close together for the data to exhibit the kind of separation that would be necessary to calculate a trustworthy activation energy using data from only two temperatures. Since the calculated value is comparable to the more reliable value for nonanoic acid esterification, it is still presented in this work; however, the result should be considered in light of these limitations.

For nonanoic acid esterification:

$$k(55\ ^\circ\mathrm{C}) = 14.52\,\frac{\mathrm{ml}}{\mathrm{g}_{\mathrm{cat}} \cdot \mathrm{min}} \tag{2.9}$$

$$E_a = 34.4\ \mathrm{kJ/mol} \tag{2.10}$$

For palmitic acid esterification:

$$k(60\ ^\circ\mathrm{C}) = 18.06\,\frac{\mathrm{ml}}{\mathrm{g}_{\mathrm{cat}} \cdot \mathrm{min}} \tag{2.11}$$

$$E_a = 32.9\ \mathrm{kJ/mol} \tag{2.12}$$

Solving Equation 2.5 for fractional conversion allows the predictions of the kinetic model to be compared with the experimental data, as shown in Figures 2.5, 2.6, 2.7, and 2.8.

$$X_{FFA} = 1 - \exp(-k[\mathrm{C}]t) \quad (2.13)$$

Since the different FFAs were tested at different temperatures, the model was used to compare the relative performance of palmitic acid and nonanoic acid. Figure 2.9 shows the model's predictions for the esterification of palmitic acid at 60 °C and a catalyst concentration of 1.83 mg/ml (100 mg loading) compared to the kinetic model's prediction for nonanoic acid conversion at the same temperature and catalyst concentration. Because of the conditions used in this comparison, the palmitic acid curves are the model's fit to actual data, while the nonanoic acid curves are the model's extrapolation to untested conditions, allowing the questionable figure for the palmitic acid's apparent activation energy to not be an issue in the comparison. Generally, ionic liquid catalysts perform more favorably with longer-chain FFAs, and the comparison appears to fit this trend to a small degree, indicating that this catalyst should perform comparably well with the variety of chain lengths in high-FFA waste oils.

For the 2-hour experiment (*N-Long*) and the experiments at different temperatures (*T-1, T-2,* and *T-3),* the GC-MS was calibrated to measure the product concentration, and not just the reactant concentration, so there is additional data for determining fractional conversion, and conversion can be calculated based on measured FFA or measured FAME. Averaging the results of the two methods should be seen as a reasonable practice since the errors of the two measurements will trend in opposite directions for a given error in the sample collection and dilution. For example, if the amount of reaction mixture injected to the GC column is less than what was calculated, then there will be less FFA observed, causing conversion to be overestimated, but there will also be less

FAME observed, causing conversion to be underestimated.

The dilution factor was taken as the mass fraction of reaction mixture in the sample injected onto the GC column. GC-MS results for diluted samples were related to concentrations in the reaction mixture by the dilution factor and the density of the solvent used in the final dilution. Based on the uncertainty of the equipment used (taken as ±0.005 g), the error in the dilution factor should range between ±1.5 %. This treatment attributes more uncertainty to the balance than there ought to be as a means of accounting for measurement uncertainty due to the volatility of the hot reaction mixture and the solvents used to dilute it. As can be seen in Figure 2.10, the errors of the fractional conversions calculated by the two methods trend in opposite directions and tend to cancel each other out when the conversions are averaged, leading to a better estimation of fractional conversion over a broad range of conversions (approximately 20–75 % conversion for a 1.5 % error in dilution factor).

2.6. Conclusion

A novel ionic liquid catalyst has been used for the acid-catalyzed esterification of two different fatty acids with methanol, reactions relevant to the production of biodiesel from low-quality, high-FFA oils. Catalyst concentrations on the order of 1 mg/ml were found to effect 80–90% conversion to biodiesel within an hour at relatively mild reaction conditions, and this behavior was modeled as a first-order reaction with respect to reactant concentration in an excess of methanol (20:1 molar ratio). The reactions were found to be first-order with respect to catalyst concentration as well, and rate constants were determined for the esterification of palmitic acid at 60 °C and of nonanoic acid at

55 °C, along with activation energies. The model compares well to the experimental data at different conditions, and catalyst performance is comparable between the two FFAs.

Future work should examine the recovery of this catalyst from appropriate reaction systems. In a practical biodiesel process, the transesterification of triglycerides produces a second liquid phase of aqueous glycerol, into which the catalyst is likely to partition (Andreani and Rocha, 2012); however, in this work, the minute amount of catalyst precluded simple recovery by phase separation. Recovery of the excess methanol by distillation may also yield a two-liquid system from which the catalyst can be more readily recovered.

The catalyst's strong performance in the conversion of pure carboxylic acids indicates its potential utility in bio-oil deacidification. Future work should apply the catalyst towards the esterification of carboxylic acids in real bio-oil mixtures, such as high-FFA biodiesel feedstocks or the acidic liquid fractions derived from biomass pyrolysis, as the demonstrated potency of the catalyst indicates broad applicability for biomass upgrading.

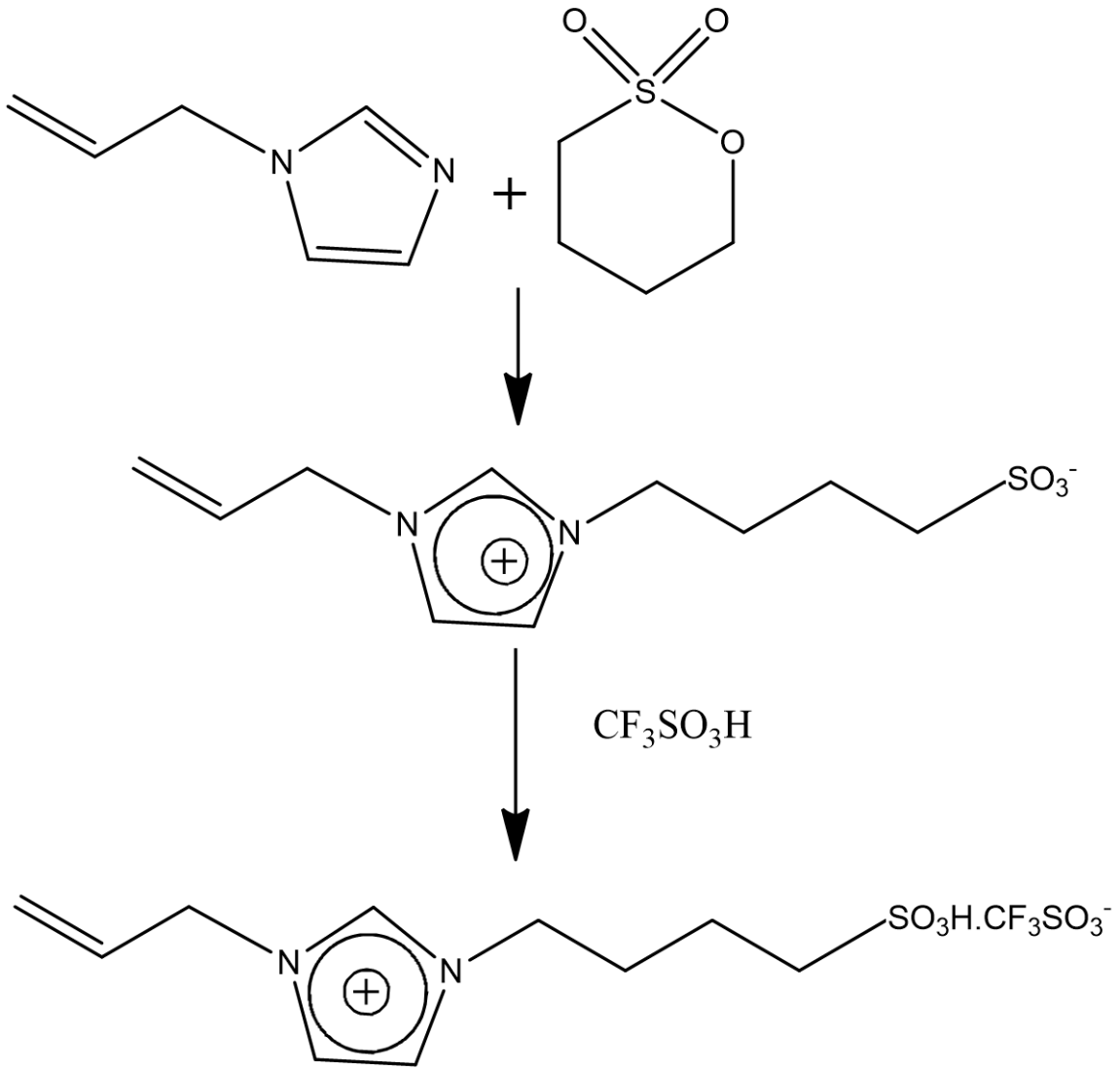

Figure 2.1. *Synthesis scheme for Brønsted acid ionic liquid catalyst [BHSO₃AIM][CF₃SO₃], or 1-sulfobutyl-3-allylimidazolium triflate. First, the zwitterion is prepared by adding 1-allyl imidazole with 1,4-butane sultone in a flask, slowly, at 0 °C. Then, the ionic liquid is made by coupling the zwitterion with triflic acid (CF_3SO_3H) at 0 °C and then stirring in an oil bath at 60 °C for 12 hours, as described in the work of Quiao et al. (2006).*

Table 2.1. *Reaction conditions tested and the first-order linear fits for the data. The four experiments below the horizontal rule were collected and analyzed differently (and more reliably) than the others, as described previously.*

Parameters					Reactor Loading			1st Order Fit
ID	**Acid**	**Temp °C**	**[C] mg/ml**	**C^{o}_{FFA} mg/ml**	**Catalyst (mg)**	**FFA (g)**	**MeOH (g)**	**Slope min^{-1}**
N-C1	Nonanoic	50	2.09	151.0	100.0	7.4	31.2	0.0305
N-C2	Nonanoic	50	1.05	151.0	50.0	7.4	31.2	0.0151
P-C1	Palmitic	60	1.83	218.8	100.0	12.0	31.2	0.0320
P-C2	Palmitic	60	0.91	218.8	50.0	12.0	31.2	0.0170
P-T	Palmitic	56	0.91	218.8	50.0	12.0	31.2	0.0147
N-Long	Nonanoic	55	1.57	151.0	75.0	7.4	31.2	0.0235
N-T1	Nonanoic	55	1.05	151.0	50.0	7.4	31.2	0.0147
N-T2	Nonanoic	45	1.05	151.0	50.0	7.4	31.2	0.0113
N-T3	Nonanoic	35	1.05	151.0	50.0	7.4	31.2	0.0065

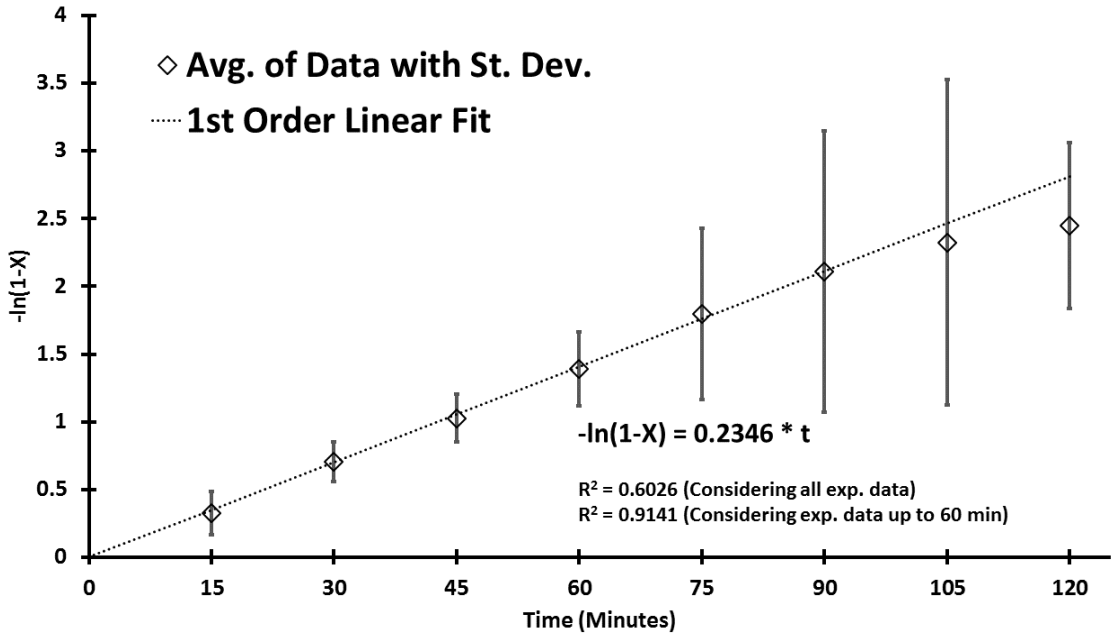

Figure 2.2. *Linear fit for the esterification of nonanoic acid at 55 °C and 0.075 g catalyst loading, showing the trend expected for first-order behavior with respect to fatty acid concentration. Linearity holds up well for 90 minutes, and the deviation occurs as fractional conversion appears to level off around 92%.*

Table 2.2. *Estimated reaction order with respect to catalyst concentration, calculated from three different pairs of data sets. The results' narrow spread and proximity to unity strongly suggest that the reaction is first-order with respect to catalyst concentration.*

ID 1	ID 2	Acid	Temp (°C)	$n = \frac{\ln(\Psi_1/\Psi_2)}{\ln([C]_1/[C]_2)}$
N - Long	N - T1	Nonanoic	55	1.15
N - C1	N - C2	Nonanoic	50	1.01
P - C1	P - C2	Palmitic	60	0.91
				Average = 1.02

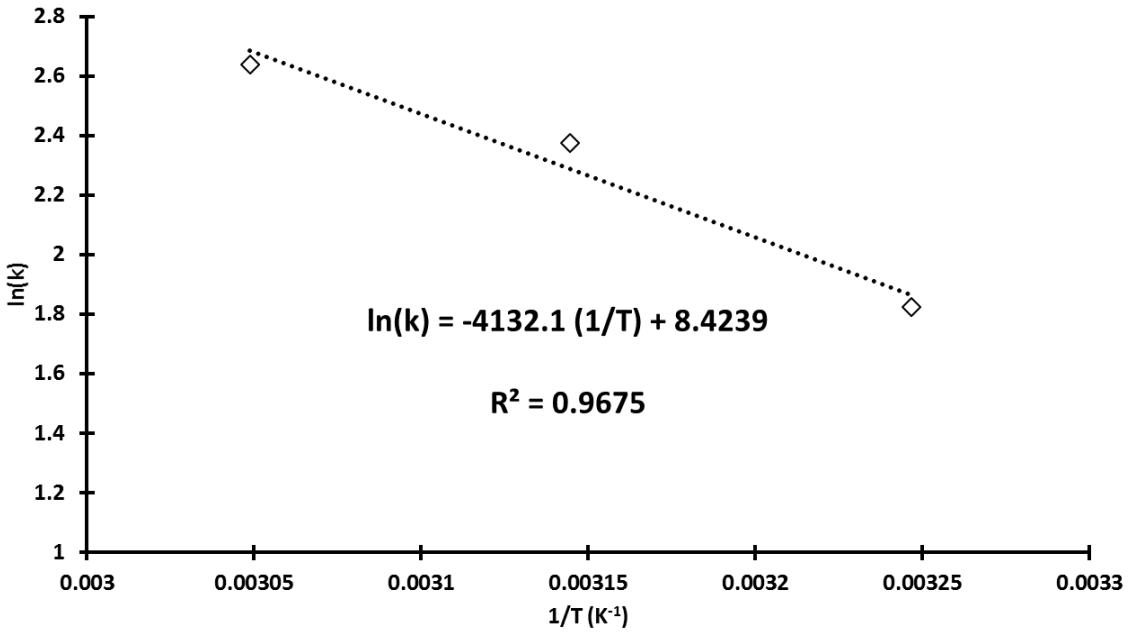

Figure 2.3. *Arrhenius plot for the esterification of nonanoic acid, using data from experiments N-T1, N-T2, and N-T3, indicating an activation energy of 34.4 kJ/mol.*

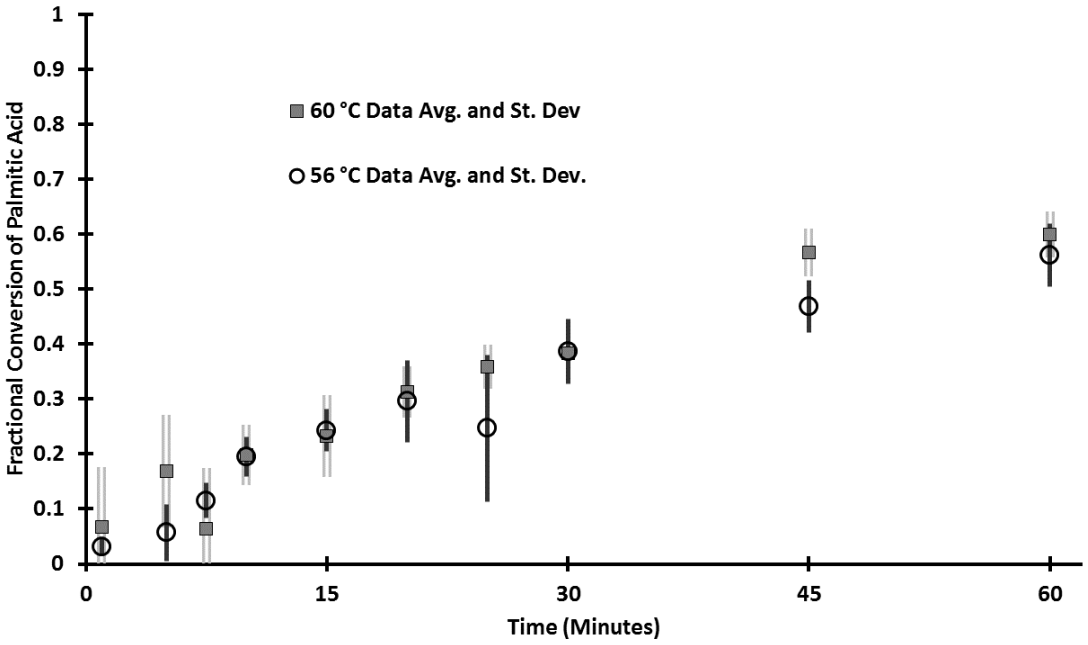

Figure 2.4. *Fractional conversion of palmitic acid at 56 °C (P-T) and 60 °C (P-C2) with catalyst loading of 50 mg. Poor separation between the data sets suggests that the calculated activation energy is questionable; however, the value of 32.9 kJ/mol is presented because it is still comparable to the more reliable value calculated for nonanoic acid esterification, 34.4 kJ/mol.*

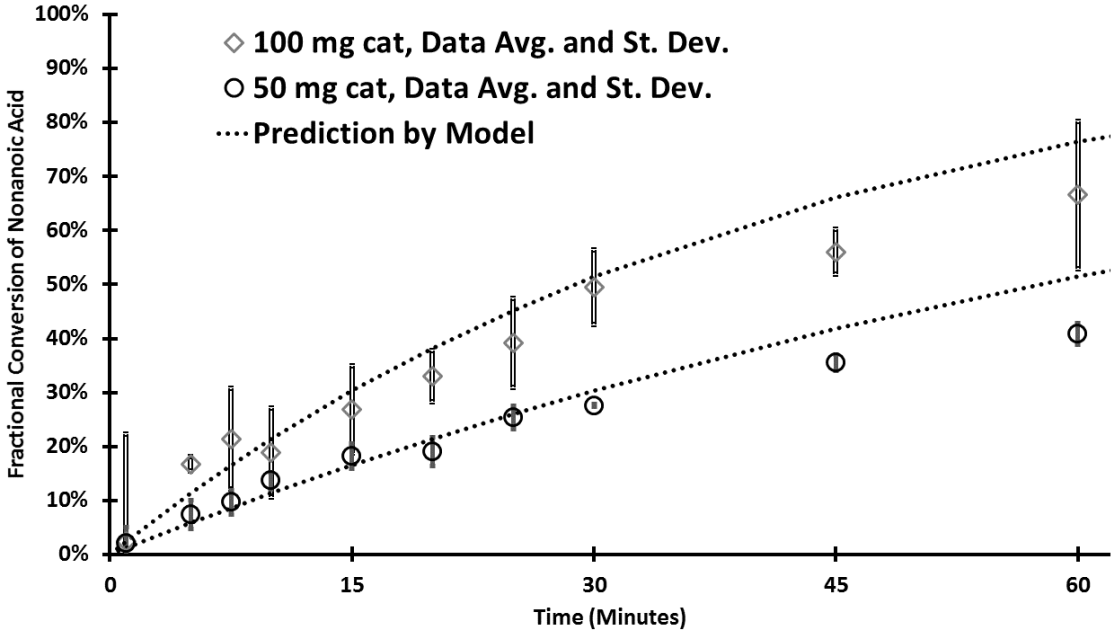

Figure 2.5. *Fractional conversion of nonanoic acid at 50 °C and two catalyst loadings: 100 mg (N-C1) and 50 mg (N-C2). Higher loadings lead to improved conversion, with a first-order dependence on catalyst loading.*

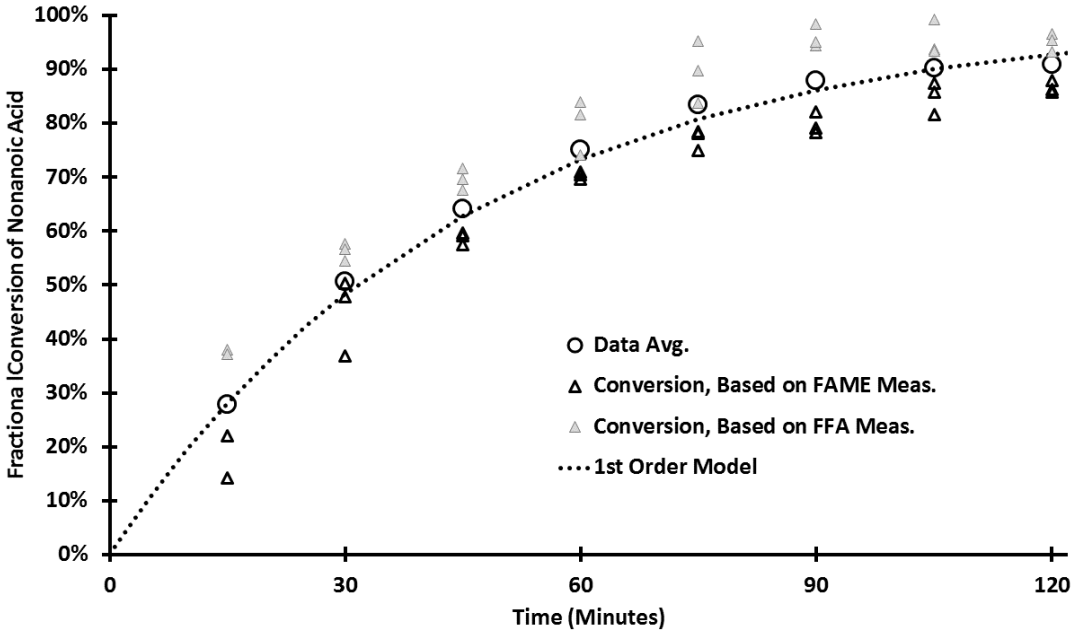

Figure 2.6. *Fractional conversion of nonanoic acid at 55 °C and 75 mg catalyst loading (N-Long). Individual data points are shown, categorized by which measurement was used to calculate fractional conversion.*

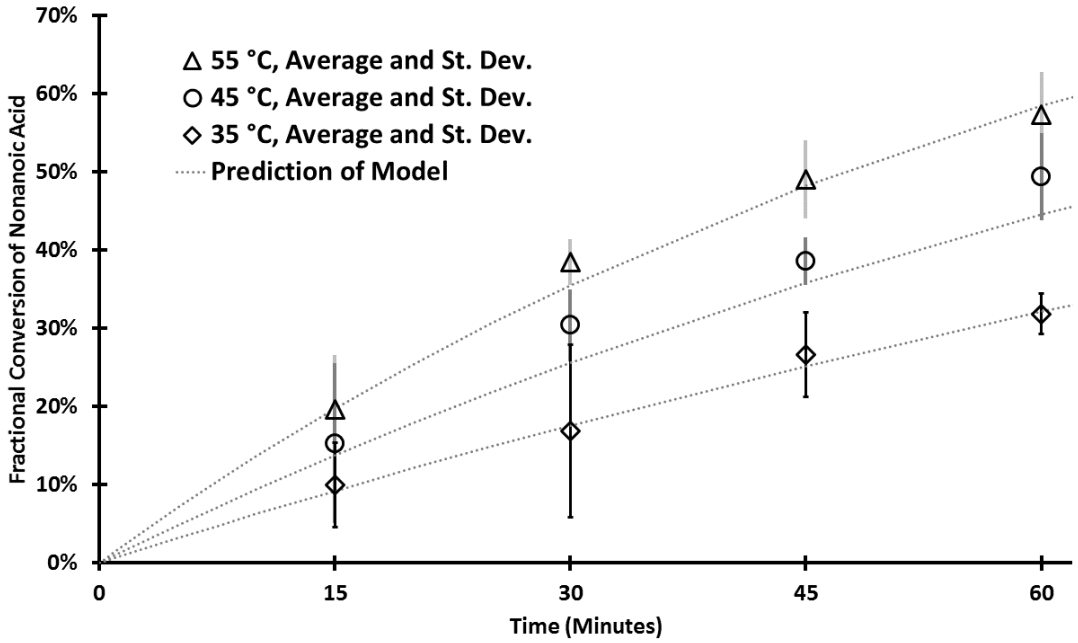

Figure 2.7. *Fractional conversion of nonanoic acid at 50 mg catalyst loading and different temperatures: 55 °C (N-T1), 45 °C (N-T2), and 35 °C (N-T1). Higher temperatures improve reaction performance.*

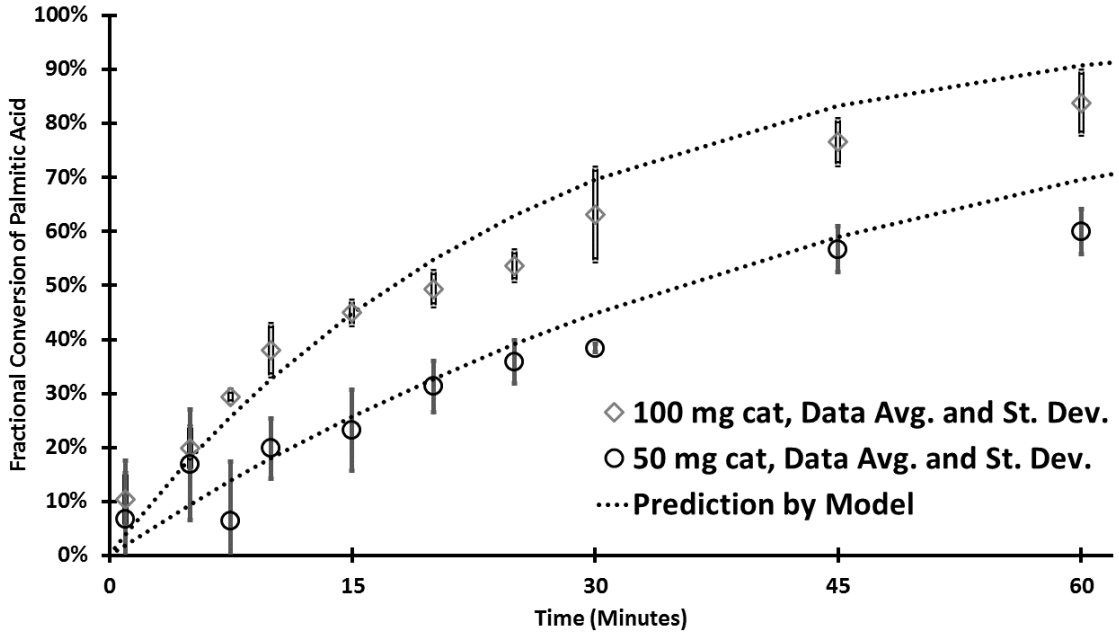

Figure 2.8. *Fractional conversion of palmitic acid at 60 °C and two catalyst loadings: 100 mg (P-C1) and 50 mg (P-C2). Higher catalyst loadings improve reaction performance, with a first-order dependency on catalyst concentration.*

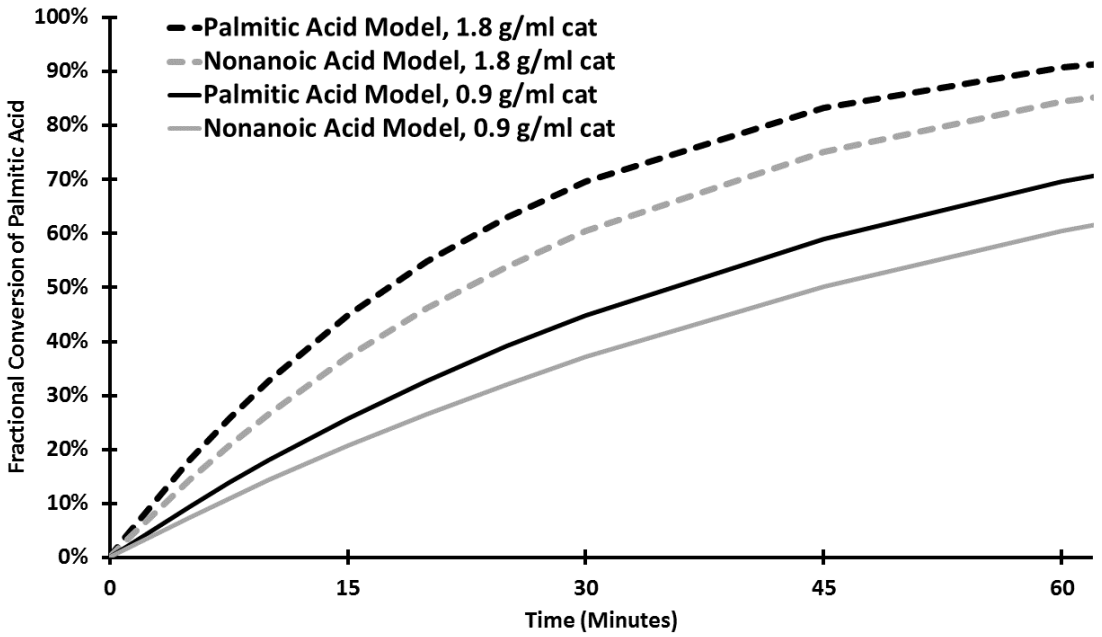

Figure 2.9. *Model predictions for fractional conversion of the two fatty acids at 60 °C and two different catalyst loadings. The conditions are the same as were tested for palmitic acid, so the black curves show model's fit to the data, rather than an extrapolation. The model was used to extrapolate nonanoic acid conversion to the conditions tested on palmitic acid, since the activation energy calculated for nonanoic acid is likely more reliable. Catalyst performance is comparable between the different carbon chain lengths (sixteen and nine, respectively) and is slightly better for the longer chain FFA, as is usually the trend for ionic liquid performance in FFA esterification.*

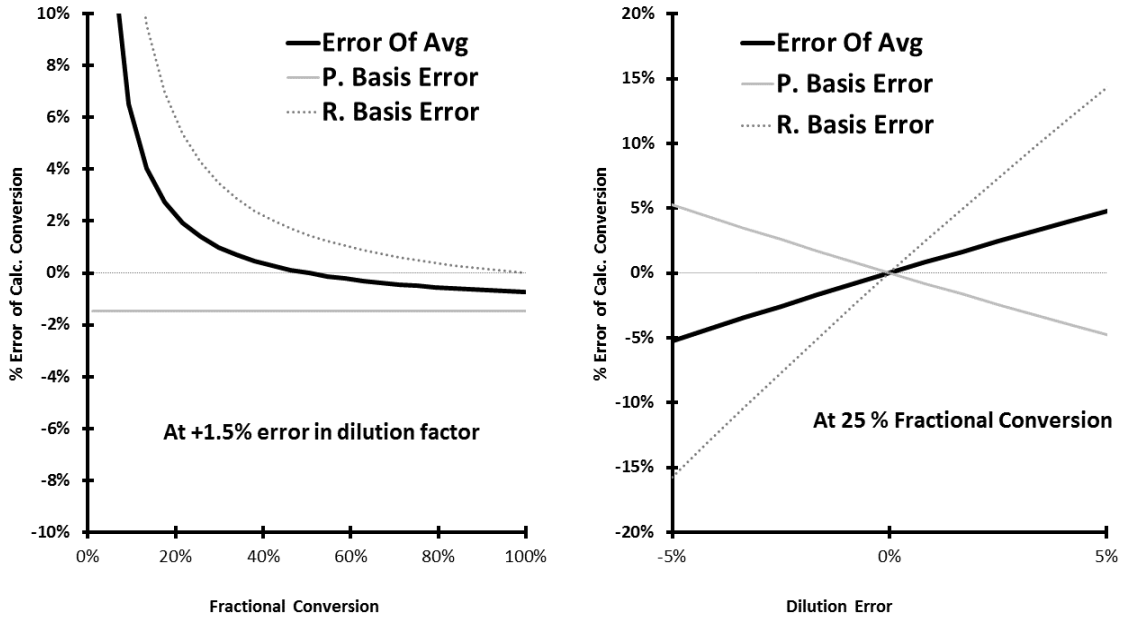

Figure 2.10. *Effect of dilution error on fractional conversion calculation, showing the benefit of averaging the results of product and reactant measurements.*

CHAPTER 3

MITIGATION OF PYROLYSIS OIL ACIDITY VIA ESTERIFICATON WITH METHANOL AND SUBSEQUENT COPROCESSING WITH HIGH-FFA TRIGLYCERIDE OIL

3.1. Abstract

Pyrolysis of lignocellulosic biomass yields condensable liquid fractions that contain a significant fraction of the original mass of the feedstock (10–40 %); however, utilization of these pyrolysis oils is hampered by high water content, as well as instability and corrosiveness caused by high concentrations of phenolic, acidic, and other oxygenated compounds. In this chapter, we report the use of an ionic liquid catalyst in the esterification of the carboxylic acids in a pyrolysis oil to produce methyl esters, in order to mitigate the corrosiveness and instability inherent to pyrolysis oil. The ratio of catalyst to pyrolysis oil is determined to be the most relevant predictor of reaction performance, and a semi-empirical kinetic model is derived to describe the reaction, which was found to be second-order with respect to the acids concentration and second-order with respect to the ratio of catalyst to acids. The possibility of using the catalyst to react both pyrolysis oil acids and the free fatty acids (FFA) from a low-quality triglyceride feedstock was explored, with two candidate coprocessing schemes being tested. If the reactants are all mixed at once (a one-step, one-pot scheme), then only the FFAs react; however, if the

pyrolysis oil is reacted first, with the triglyceride feedstock subsequently added to the hot reaction mixture (the two-step, one-pot scheme), appreciable conversion of the acids from both feedstocks is observed, although the performance is markedly worse than the processing of either bio-oil on its own. Despite the noted shortcomings of the schemes tested, this work demonstrates the early feasibility of a novel approach to the coprocessing of a pyrolysis liquid with a low-quality biodiesel feedstock, using the same catalyst and no intermediate recovery steps, in order to both deacidify the biodiesel feedstock and to mitigate the undesirable properties of the pyrolysis liquid.

3.2. Introduction

Pyrolysis of lignocellulosic biomass produces biochar and gaseous byproducts, as well as liquid fractions—known as pyrolysis oils—that are rich in phenolic, acidic, and other oxygenated compounds. Utilization of pyrolysis oils is hampered by its water content (as much as 30 wt %), as well as instability and corrosiveness. Much work concerning the upgrading of pyrolysis liquids has focused on energy-intensive catalytic treatments for producing hydrocarbon fuels—processes that are complicated by the panoply of different functional groups present in the oil. Since pyrolysis oils are often immiscible with hydrocarbon mixtures, they cannot simply be added to refinery streams and must be pretreated to remove oxygen. Furthermore, following the removal of oxygen, a pyrolysis liquid must be sufficiently distilled to yield useful hydrocarbon fractions, adding to the upgrading costs and eliminating any supposed advantage over petroleum-derived fuel sources (Qi et al., 2007; Bridgewater, 2012).

There are alternatives to fully upgrading pyrolysis oil, and these seek to mitigate

the undesirable properties of PyOil without the large material and energy investments of hydrodeoxygenation and distillation. Carboxylic acids can be converted to short chain esters, increasing the shelf-life and reducing the corrosiveness of the resulting oil. Hilten et al. (2010) added ethanol to uncondensed pyrolysis vapors in order to control fractionation and condensation, as well as to convert acids to ethyl esters. Pyrolysis oils can also be blended with traditional fuels to create emulsions that make use of the heating value of PyOil while mitigating its viscosity and reactivity. PyOil emulsions with diesel have been examined and even tested in conventional diesel engines to determine the effect of the oils on engine performance and wear (Chiaramonti et al., 2003a, 2003b; Ikura et al., 2003). Blends of PyOil with biodiesel have also been explored, using alcohols as co-solvents to make use of the heating value of these oils while overcoming the undesirable aspects of using either oil on its own (Alcala and Bridgewater, 2013).

This chapter demonstrates that the ionic liquid catalyst shown, in Chapter 1, to achieve the esterification of pure carboxylic acids with methanol can be effectively applied to the esterification of pyrolysis oil acids for the purpose of mitigating corrosiveness and instability. A kinetic model is derived to describe the fractional conversion of acids in an actual pyrolysis liquid (not a surrogate), showing that the reaction proceeds as second-order with respect to acid concentration and second-order with respect to the catalyst loading (as the ratio of catalyst to pyrolysis oil), despite the complexity of the mixture. The catalyst is then tested in two candidate coprocessing schemes to explore the possibility of coupling pyrolysis oil acids mitigation with the deacidification of a high-FFA biodiesel feedstock. The process is not optimized by any means, but the results demonstrate promise in this novel approach to biomass treatment.

3.3. Materials and Methods

3.3.1. Pyrolysis Oil

Pyrolysis oil was provided by Amaron Energy (Salt Lake City, UT), generated as illustrated in the scheme shown in Figure 3.1. The oil was known to be one fraction of condensable pyrolysis products collected from a system of condensers on the back-end of a fast pyrolysis unit. Woody biomass was fed to a rotating pipe operated under slight vacuum and heated by burners. Pyrolysis vapors were fed to a system of two condensers; the first condenser collected a water-rich fraction called "C1" that was allowed to settle in a barrel. A solids-rich layer settled to the bottom, and the top layer, "C1 Top," was the oil employed for this work. It was received in a large plastic tub and poured into a 4-liter glass container for storage, and solids—presumably comprised of mostly lignin—were allowed to settle in the bottom of the container. Since diesel fuel was used as a startup feed to the condenser, a small amount was present in the pyrolysis oil, so the pyrolysis oil was decanted into a separatory funnel to remove the diesel. After settling, the aqueous (bottom) layer was used for catalyst testing while remaining stored in the separatory funnel. When the separatory funnel was emptied of pyrolysis oil, the remaining diesel and dregs would be poured out of the top, and it would be replenished from the material in the glass container. Prior to catalyst testing, the pyrolysis oil in the separatory funnel was titrated to ensure reliable calculation of fractional conversions. On average, the pyrolysis oil contained 2.02 mol/kg of NaOH-titratable functional groups, with a relative standard deviation of 2.31 %.

3.3.2. Catalyst Preparation

The Brønsted acid ionic liquid catalyst was synthesized by coupling 1-allyl imidazolium-containing zwitterion salt with CF_3SO_3H slowly at 0 °C and then stirring in an oil bath at 60 °C for 12 hours (Quiao et al., 2006). The zwitterionic salt was prepared by adding imidazole with 1,4-butane sultone in a flask, slowly at 0 °C. The solution was stirred for 24 hours at room temperature to convert the contents of the flask to a solid which was then washed with ether and filtered under vacuum. A Fourier Transform Infrared (FTIR) spectrum of the compound showed two specific characteristic peaks at 1647 $cm^{-1}$and 2565 cm^{-1} corresponding to doubly bonded carbon-carbon vibration peaks indicating the formation of the compound.

Two different batches of the catalyst were employed for this work. Batch A had been employed for prior work concerning the esterification of pure FFAs in methanol and was utilized for the tests of pyrolysis oil esterification at different temperatures, as well as short-run experiments to determine the early behavior of the reaction. This batch was found to contain 3.35 mol/kg of NaOH-titratable acid. Batch B was utilized for the other tests of pyrolysis oil esterification, as well as for the coprocessing experiments. This batch was found to contain 3.07 mol/kg of NaOH-titratable acid, indicating different purities between the batches. Furthermore, both values differ from the 2.45 mol/kg predicted by the catalyst's molecular weight. The discrepancy could be attributable to numerous possible factors beyond the scope of this work; titration results were merely used to correct measured acid concentrations in reacted pyrolysis oil samples to reliably calculate fractional conversion.

3.3.3. Esterification of Pyrolysis Oil Acids in Methanol

The esterification of pyrolysis oil acids was tested in a bench-scale batch reactor, as outlined in Figure 3.2. Depending on the desired operating parameters, different amounts of pyrolysis oil and methanol were added to a 250 ml round-bottom flask which was attached to a condenser before being submerged in an oil bath (already heated to temperature, 35–55 °C) on a temperature-controlled hot plate. The thermocouple from the oil bath was removed, cleaned and dried, and then inserted into the reaction mixture through the top of the condenser, so that the temperature controller would target the set point for the actual reaction mixture. The reaction mixture was stirred at a constant 500 RPM for the duration of the experiment. After nominally 15 minutes (more than sufficient time to reach the reaction temperature), a predetermined amount of catalyst mixture (52.4 wt% in methanol) was added to the flask to initiate the reaction. Samples were collected at 1 hr, 2 hr, and 3 hr reaction times and then titrated to determine the acid content, in terms of moles of acid per gram of reaction mixture. Fractional conversion was calculated based on the initial moles of acid from pyrolysis oil and the measured amount of acid, corrected for the acid contribution from the catalyst (also determined by titration).

To vary the weight ratio of pyrolysis oil to methanol, the amounts of the two were varied while keeping the estimated volume constant, so that the catalyst concentration (rather than the catalyst/acid ratio) would remain consistent. To vary the catalyst loading, different amounts of the catalyst mixture were used, and the initial methanol loading was changed to account for the amount of methanol in the catalyst mixture.

3.3.4. One-Step, One-Pot Coprocessing of Pyrolysis Oil and FFA

Preliminary experiments were carried out to assess the feasibility of performing the esterification of both pyrolysis oil and FFA in a single step, as outlined in Figure 3.3. While the experiments were not repeated, they include five very similar tests, and the insights gleaned from their results form the justification for subsequent testing of a one-pot, two-step scheme.

In these experiments, 50 g of a triglyceride oil comprised of 20 wt % nonanoic acid in canola oil were added to a 250 ml round-bottom flask along with 19.5 g of methanol and a variable amount of pyrolysis oil (0, 1.0, 2.5, 5.0, 7.5, and 10.0 g). A condenser was applied to the flask, and the flask was submerged in an oil bath at 60 °C. The thermocouple from the oil bath was removed, cleaned and dried, and then inserted into the reaction mixture through the top of the condenser, so that the temperature controller would target the set point for the actual reaction mixture. The reaction mixture was stirred at a constant 500 RPM for the duration of the experiment. After 15–20 minutes, 1.0 g of a catalyst mixture (52.4 wt % in methanol) was added to the flask to begin the reaction. After 2 hours, the reaction mixture was quenched by running cool water over the outside of the flask, and the reaction mixture was decanted into a separatory funnel to isolate the two liquid phases. After settling for one day, the two phases were drained off separately, weighed, and titrated to determine acid content. Since the mass recovered was slightly less than the initial mass in the reaction mixture, the recovered mass of each liquid phase was proportionally scaled up in order to relate the titration results to a total acid content for the purpose of calculating fractional conversion. An additional experiment—utilizing 10.0 g of pyrolysis oil, the same methanol and

catalyst amounts as the other experiments, and none of the triglyceride oil—was performed to compare the one-step coprocessing to the esterification of only pyrolysis oil at these conditions.

3.3.5. Two-Step, One-Pot Coprocessing of Pyrolysis Oil and FFA

The two-step, one-pot coprocessing scheme is outlined in Figure 3.4. Nominally 5 g of PyOil were added to 9.5 g of methanol in a 250 ml round-bottom flask which was attached to a condenser before being submerged in a 55 °C oil bath on a temperature-controlled hot plate. The thermocouple from the oil bath was removed, cleaned and dried, and then inserted into the reaction mixture through the top of the condenser, so that the temperature controller would target the set point for the actual reaction mixture. The reaction mixture was stirred at a constant 500 RPM for the duration of the experiment. After approximately 30 minutes, 1.0 g of a catalyst mixture (52.4 wt% in methanol) was added to the flask to begin the reaction of the PyOil. Two hours after the initial addition of the catalyst, nominally 25 g of 10 wt% nonanoic acid in canola oil were added, and this moment was taken as t = 0 minutes. Due to the viscosity of the TG/FFA oil, its beaker was weighed before and after its addition to the reaction flask to ensure an accurate recording of the amount of fatty acid ultimately added to reaction mixture. 1–2 g aliquots of the reaction mixture were removed at t = 30, 60, 90, 120, 180, and 240 minutes.

Care was taken to ensure that during sampling, the reaction mixture continued mixing thoroughly, and the sample was removed near the stir bar, where turbulence was greatest. This consideration was necessary, as the reaction mixture is a two-phase liquid,

and it was observed that a consistent distribution of the two phases could be extracted from the flask in this manner. Samples were diluted with approximately 10 g of a homogenizing solvent (hexane in 2-propanol, 1:3 volume ratio), and this initial dilution was titrated to determine the total acid content. For GC-MS analysis, approximately 0.5 g of the first dilution were added to approximately 30 g of HPLC-grade methanol. Weights were recorded for every sample at every stage of dilution, allowing a dilution factor to be calculated for each sample.

3.3.6. Sample Analysis by GC-MS

To determine the fatty acid and methyl ester concentrations in the reaction mixture at time *t*, samples diluted for GC-MS were analyzed on a Shimadzu GCMS-QP2010 Ultra equipped with a Restek RTX-5MS capillary column. The GC-MS was calibrated using standard solutions with known concentrations (g/ml) of nonanoic acid and methyl nonanoate dissolved in HPLC-grade methanol, allowing the concentration of each analyte in the final dilution of each sample to be determined. The density of methanol was used to convert these concentrations to mass fractions, and the dilution factors for each sample related these mass fractions to the mass fractions of the analytes in the reaction mixture at time *t*.

Fractional conversion was calculated with two methods. First, by using the measured mass fraction of nonanoic acid and comparing it to the known mass fraction at the beginning of the reaction, a fractional conversion was calculated on a *reactant basis*. Second, by converting the measured mass fraction of methyl nonanoate to an equivalent mass of consumed nonanoic acid (via the ratio of their molecular weights), a fractional

conversion was calculated on a *product basis*. The second method assumes 100 % selectivity to methyl nonanoate, and while the generation of side products cannot be unequivocally ruled out, there is no evidence from the chromatograms to suggest that nonanoic acid is converted to anything else.

$$X(\text{Reactant Basis}) = \frac{\text{Initial Mass of FFA} - \text{Mass of FFA at Time } t}{\text{Initial Mass of FFA}} \tag{3.1}$$

$$X(\text{Product Basis}) = \frac{\text{Mass of FAME} \cdot \frac{M_{FFA}}{M_{FAME}}}{\text{Initial Mass of FFA}} \tag{3.2}$$

While the average conversion at time *t* shows a discrepancy between the two methods, there is reasonable agreement within the spread of the data.

3.3.7. Sample Analysis by Titration

Titrations were performed to determine the total acid content of various reaction mixtures. The titrant solution was prepared by diluting ~7.4 g of NaOH to 1000 ml with 2-propanol in a volumetric flask. NaOH is known to be hygroscopic and to gradually lose its basicity (per unit mass) by absorbing moisture and CO_2 from the atmosphere, so a titration of nonanoic acid was performed to determine a corrected molar concentration of NaOH in the solution. The molar hydroxide concentration, predicted by the mass of NaOH used, had to be corrected downward by 6–8 %, depending on the batch of titrant prepared. While this corrected value may not be entirely correct itself, it allows all titration results to be effectively compared to the acidity of the FFA used in the

experiments.

Titration involved partially filling a 10 ml burette with the titrant solution. A small amount of titrand (reaction mixture) was added to a beaker and weighed, then diluted with approximately 40 ml 2-propanol. The exact amount of the dilution does not matter, although samples containing pyrolysis oil had to be dilute enough to ensure that the color change could be appropriately observed. Three drops of indicator solution (1 wt % phenolphthalein in 2-propanol) were added to the beaker, along with a stir bar. The titrand mixture was stirred while adding titrant solution, dropwise, until the color change characteristic of phenolphthalein could be observed: a pale pink tinge that persists for at least 1 minute. The volume of titrant necessary to effect this color change was used to calculate the moles of acid present in a given mass of titrand. Each titration was performed three times, and the average of the results was taken as the amount of acid in a given sample.

For experiments involving the esterification of only pyrolysis oil acids, 0.100–0.300 g of reaction mixture were titrated at a time. For experiments involving the co-processing of pyrolysis oil with FFA/TG, 1.000–4.000 g of reaction mixture were titrated at a time. These ranges allowed a reasonable amount of titrant to be used to get an accurate result without requiring excessive amounts of solvent to thin out the pyrolysis oil’s dark color.

The color of pyrolysis oil must be considered when titrating samples containing pyrolysis oil. Not only does it darken the clear solvent (to a pale brown or grey), making the phenolphthalein color change more difficult to observe, but pyrolysis oil exhibits its own color change with the addition of base. As the titration proceeds, the pyrolysis oil

gradually becomes more grey and less brown (a very subtle change), until a point where it begins to turn a strong amber, reminiscent of human urine. This change occurs comparatively quickly, and it invariably happens “a few drops” before the phenolphthalein changes color. However, if the pyrolysis oil is too concentrated in the titrand solution, the pyrolysis oil merely appears to darken, the amber color is not observed, and at some point, the solution appears to become increasingly purple without it having been evident when the phenolphthalein first changed color.

This work did not consider whether the pyrolysis oil’s intrinsic color change could serve as its own indicator of something important, and this consideration could be something useful to explore in future work. Pyrolysis oil is rich in phenolics, some of which react with NaOH (as phenol itself does), without themselves being the sort of acids that contribute majorly to the corrosive properties of the pyrolysis oil. It may be the case that the color change to amber indicates the consumption of carboxylic acids and would provide a measure of acidity that is more relevant to this work’s aim of esterifying those acids with methanol; then the phenolphthalein color change would indicate the consumption of other acidic species.

3.4. Results and Discussion

3.4.1. Esterification of Pyrolysis Oil Acids in Methanol

The conditions used to test the esterification of pyrolysis oil with methanol are shown in Table 3.1. In the first series of tests, the ratio of methanol to pyrolysis oil was varied while keeping the liquid volume and catalyst concentration constant. Next, the catalyst concentration was varied while keeping the ratio of methanol to pyrolysis oil

constant. The data were plotted to observe that higher catalyst loadings and higher methanol ratios both lead to higher fractional conversions; however, the effect of methanol loading was uncharacteristically large, given the molar excess of methanol at all conditions, suggesting that some more relevant parameter was being varied. The ratio of catalyst to pyrolysis oil was determined to be the parameter most relevant to reaction performance, and a semi-empirical kinetic model was derived to account for the observed second-order dependence on pyrolysis oil and second-order dependence on the ratio of catalyst to pyrolysis oil. Experiments conducted at different temperatures were used to determine the activation energy, and experiments conducted to collect data from 30 minutes and before were used to definitively confirm the reaction's second-order behavior with respect to pyrolysis oil concentration.

3.4.1.1. Effect of Methanol/PyOil Ratio at Constant Catalyst Concentration

Figure 3.5 shows the effects of varying the ratio of methanol to pyrolysis oil while keeping the volume and catalyst concentration constant. Note that methanol is in molar excess at all conditions; a 1:1 weight ratio of methanol to pyrolysis oil is equivalent to a 15.5:1 molar ratio of methanol to titratable acid groups. Therefore, it is unlikely that greater excesses of methanol are responsible for the marked improvement in conversion across the three lowest methanol ratios. It is also unusual that conversion would be observed to decrease between 2 and 3 hours at the highest methanol loading; however, at this loading, the reaction mixture is 86 % methanol by mass. The observed decrease in conversion may be a result of the reaction mixture concentrating itself as the evaporation of methanol outstrips the condenser's ability to overcome it, an effect that would not be

observed in mixtures whose vapor pressures are more depressed by the water and other compounds in pyrolysis oil. Nonetheless, what is seen is a diminishing returns effect from higher methanol ratios and an apparent upper limit to the performance of this reaction, more apparent when the data are plotted as in Figure 3.6.

3.4.1.2. Effect of Catalyst Loading at Constant MeOH/PyOil Ratio

Figure 3.7 shows the effect of varying the catalyst loading while keeping the amounts of methanol and pyrolysis oil constant. Across the three lowest catalyst loadings, it appears that a ~20 % increase in fractional conversion can be effected by an approximately twofold increase in the amount of catalyst. The 60-minute data for the lowest catalyst loading suggest an induction period prior to which the reaction does not appreciably occur; however, this result may only be the case for very low catalyst loadings, as such a phenomenon is not apparent from short-run data at a higher catalyst loading. When the data are plotted as shown in Figure 3.8, a diminishing returns effect is again apparent, and conversions beyond 60 % are not achieved from any of the conditions tested.

3.4.1.3. Effect of Catalyst/PyOil Ratio

While catalyst concentration is reasonably expected to be relevant to the kinetics of esterification, it seems unlikely that the magnitude of the excess of methanol would have such similarly pronounced effects. The data from Figure 3.6 and Figure 3.8 are plotted together in Figure 3.9 versus the mass ratio of catalyst to pyrolysis oil. A 1:1 weight ratio of catalyst to pyrolysis oil is equivalent to a 1.2:1 molar ratio of catalyst to

titratable acid groups; under no conditions is the catalyst in molar excess. The apparent continuity of the curves drawn by connecting the data points suggests that the catalyst ratio was the parameter actually being tested by varying the methanol ratio and keeping the catalyst concentration constant. Both data sets share a base case in common, and there is notable agreement in how data from the lowest methanol ratio fit in between the results of varying the catalyst concentration. Furthermore, there is remarkable agreement between the two data sets where their catalyst ratios are nearly the same (*C3* has a ratio of 0.1043:1 while *M2* has a ratio of 0.1045:1), strongly indicating that catalyst ratio is the most relevant parameter to reaction performance.

3.4.1.4. Effect of Reaction Temperature

The effect of varying temperature was also studied; however, these experiments used a different, stronger batch of the ionic liquid catalyst. While such variation is not ideal for deriving a kinetic model, it should not affect the calculation of activation energy, nor the determination of reaction order. Since experiment *T3* shares all conditions with the base case other than the batch of catalyst, the two batches could be compared, as shown in Figure 3.10.

Figure 3.11 shows the results of running the reaction at three different temperatures. As expected, conversion increases with temperature; however, in order to determine an activation energy, some function of *k* must be known. Usually, this function is the slope of a linear fit based on the reaction order with respect to the reactant; therefore, the calculated activation energy relies on the derivation of a kinetic model.

3.4.1.5. Early-Time Behavior of Reaction

In order to determine the reaction order with respect to pyrolysis oil, data from sampling at earlier reaction times were paired with later-run data under identical conditions (using the same batch of catalyst), as shown in Figure 3.12. These data would be treated as a single set for this purpose.

3.4.1.6. Kinetic Model Derivation and Comparison with Data

Based on the observation that the ratio of catalyst to pyrolysis oil was the parameter most relevant to reaction performance, a semi-empirical model was constructed to fit the data, assuming the following form:

$$-r_{H^+} = F\left(\frac{[\mathrm{C}]}{[\mathrm{H}_0^+]}\right)^n [\mathrm{H}^+]^m \tag{3.3}$$

The concentration of acids and the ratio of catalyst to initial acids are raised to the power of their respective reaction orders, and *F* is some expression that includes the rate constant *k*. A mechanistic basis for assuming the catalyst dependency to be a function of the ratio, rather than merely the concentration, is lacking; however, this assumption produces a model with predictive power at different pyrolysis oil loadings in an excess of methanol. It is possible that the $[\mathrm{H}_0^+]^n$ factor in the denominator is not a dependency on the initial acids concentration, but rather a dependency on the concentration of some species or class of compounds in the pyrolysis oil that inhibits the performance of the catalyst; this concentration would be proportional to the acids concentration in the reaction mixture, leading to the appearance that the catalyst ratio is the dependency that

matters.

Since fractional conversion was calculated on the basis of titratable acid content, rather than reactable acid content, the parameter φ was introduced to relate the measured fractional conversion of total acids to the conversion of reactable acids, as shown in Equation 3.4:

$$[\mathrm{H}^+] = \varphi\left([\mathrm{H}^+]_{\mathrm{Titration}} - [\mathrm{H}^+]_{\mathrm{Catalyst}}\right) \tag{3.4}$$

φ is the fraction of titratable acids that can be consumed in the esterification reaction, and for this analysis, it is assumed to be 0.60. This value not only produces the best fit for the model, but the data strongly suggest that this is the maximum possible conversion of titratable acids, irrespective of parameters that should enhance equilibrium conversion, such as higher temperatures or methanol loadings. The performance equation for a batch reactor with this reaction is therefore given by:

$$\frac{-r_{H^+}}{[\mathrm{H}_0^+]} = \frac{dX_{\mathrm{H}^+}}{dt} = \varphi\left(1 - \frac{X_{\mathrm{H}^+}}{\varphi}\right)^m F[\mathrm{C}]^n[\mathrm{H}_0^+]^{m-n-1} \tag{3.5}$$

Integrating this differential equation yields different results, depending on the value of *m*.

For *m* = 1,

$$-\ln\left(1-\frac{X_{\mathrm{H}^+}}{\varphi}\right)=\frac{F}{\varphi}\left(\frac{[\mathrm{C}]}{[\mathrm{H}_0^+]}\right)^n t \tag{3.6}$$

For m > 1,

$$(m-1)\left[\left(1-\frac{X_{\mathrm{H}^+}}{\varphi}\right)^{1-m}-1\right]=(F[\mathrm{C}]^n[\mathrm{H}_0^+]^{m-n-1})\,t \tag{3.7}$$

If the reaction were first-order with respect to acid concentration, then a plot of $-\ln(1-X_{\mathrm{H}^+}/\varphi)$ versus time would be linear; however, for no value of φ was this found to be remotely the case. For the reaction to be second-order with respect to acid concentration, a plot of $(X_{\mathrm{H}^+}/\varphi)\ /\ (1-X_{\mathrm{H}^+}/\varphi)$ versus time should produce a line that passes through the origin, and $\varphi = 0.60$ produced the best fit for this model:

$$\frac{X/\varphi}{1-X/\varphi}=\Psi t \tag{3.8}$$

The slope contains the catalyst and rate constant dependencies:

$$\Psi = F[\mathrm{H}_0^+]\left(\frac{[\mathrm{C}]}{[\mathrm{H}_0^+]}\right)^n \tag{3.9}$$

Such a plot is shown in Figure 3.13, demonstrating the linearity of the data over the course of the reaction. Linear fits were generated for the different catalyst loadings, and the fits for the models are summarized in Table 3.2. Using the second-order fits for

the experimental data at different catalyst loadings, a plot of the *n*th root of the slopes versus the catalyst ratio (g cat / mol H^+) should also yield a line that passes through the origin:

$$\Psi^{-n} = \Theta\left(\frac{[\mathrm{C}]}{[\mathrm{H}_0^+]}\right) \tag{3.10}$$

The slope, Θ, is given by:

$$\Theta = (F\,[\mathrm{H}_0^+])^{-n} \tag{3.11}$$

Rearranging yields an expression for *F*:

$$F = \frac{\Theta^n}{[\mathrm{H}_0^+]} \tag{3.12}$$

Since *F* was assumed to be a function of the rate constant *k*, and $[\mathrm{H}_0^+]$ varies with the reactor loading, for the purpose of this analysis, the rate constant will be taken as the following:

$$k = \Theta^n = \Psi\left(\frac{[\mathrm{C}]}{[\mathrm{H}_0^+]}\right)^{-n} \tag{3.13}$$

Figure 3.14 shows the best-fit linear regression for $n = 2$. While noninteger values

for *n* can yield better R^2 values, they ultimately make the model a poorer fit for the fractional conversion over time, so the reaction will be treated as second-order with respect to the ratio of catalyst to initial pyrolysis oil loading. Treating the reaction as second-order with respect to catalyst concentration (rather than the catalyst ratio) also produces a model that fit these data; however, such a model breaks down when compared against data from different pyrolysis oil concentrations, indicating that the catalyst dependency is indeed second-order, but that there is another dependency that must be accounted for by deriving the model in terms of the catalyst ratio.

Therefore, the rate equation for the esterification of pyrolysis oil acids is given by:

$$-r_{H^+} = k\left(\frac{[\mathrm{C}]}{[\mathrm{H}_0^+]}\right)^2 [\mathrm{H}^+]^2 \tag{3.14}$$

For the purpose of comparing the model to the experimental data, the rate constant *k* was taken as the square of the slope, Θ, of the plot shown in Figure 3.14, although each slope, Ψ, from the linear fits at different catalyst loadings would yield a value of *k* as well. While the catalyst batch employed in the experiments at different temperatures differed slightly from the batch used in the experiments at different catalyst loadings, the apparent activation energy E_a should be the same regardless; this apparent activation energy was calculated as shown in the Arrhenius plot in Figure 3.15.

Now the relevant parameters for the model have been determined:

$$k(55\ ^\circ\mathrm{C}) = 876.5\ \frac{\mathrm{ml}\cdot\mathrm{mmol\ H}^+}{\mathrm{kg_{cat}}\cdot\mathrm{hr}} \tag{3.15}$$

$$E_a = 71.41 \text{ kJ/mol} \tag{3.16}$$

To compare the predictions of the model to experimental results, the fractional conversion over time as a function of the rate constant and catalyst ratio is given by:

$$\frac{X}{\varphi} = \frac{k\frac{[\mathrm{C}]^2}{[\mathrm{H}_0^+]^2}t}{1 + k\frac{[\mathrm{C}]^2}{[\mathrm{H}_0^+]^2}t} \tag{3.17}$$

Equation 3.17 allows the fractional conversion of titratable or reactable acids to be easily calculated. The results of the model are plotted against the experimental data in Figures 3.16 and 3.17, showing strong predictive power except at very high ratios of methanol to pyrolysis oil. The deviation is likely due to methanol attrition over the 3-hour run; at the highest methanol ratio, the reaction mixture is 86 wt. % methanol, which would cause its vapor pressure to be markedly higher than the other reaction mixtures tested.

3.4.1.7. Predictions of Kinetic Model

While the data employed here are mainly from long reaction times, the kinetic model can be used to predict the behavior of the reaction for shorter reaction times at different conditions, allowing the conditions to be tuned for a desired level of acids mitigation in a pyrolysis liquid. Temperature and catalyst ratio are the only parameters to be tuned within the model; however, the amounts of methanol and pyrolysis oil employed

are not irrelevant to the real-world performance of the reaction. Higher temperatures will lead to better performance, but methanol must remain in molar excess in the liquid phase, and higher concentrations of methanol will raise the vapor pressure of the reaction mixture, limiting the temperatures that can be effectively maintained at atmospheric pressure. Therefore, the predictions of the model must be considered in light of the potential effects of varying the methanol concentration.

Figure 3.18 shows the model's prediction for the fractional conversion of *reactable acids* at different temperatures and reaction times, with a catalyst loading of 10 wt % relative to the pyrolysis oil. The desired level of acids mitigation will depend on the final application of the pyrolysis oil, but it is apparent that even short reaction times of 5–10 minutes would have a significant impact on the instability and corrosiveness of this pyrolysis liquid. Figure 3.19 shows the model's prediction at different catalyst loadings, with a temperature of 60 °C. Above loadings of 10 wt %, a temperature change of 10 °C appears to have an effect on reaction performance similar to a catalyst ratio change of 5 wt %, an observation that allows a simple optimization of reaction parameters if the utility costs of heating, condensation, and catalyst recovery can be compared.

3.4.2. One-Step One-Pot Coprocessing of PyOil

Based on the strong performance of the catalyst in the esterification of either fatty acids or the acids in pyrolysis oil, coprocessing of the oils was explored as an avenue for upgrading. The most obvious approach was to mix the oils together with methanol, heat to temperature, and add the catalyst. Because the results did not show promise for this

approach, these experiments were not repeated; however, since all were very similar experiments and the results yielded useful insights, their data are presented here. Figure 3.20 shows the results of coprocessing different amounts of pyrolysis oil with a fixed amount of high-FFA triglyceride oil; fractional conversion of total acids was determined by titration.

In the absence of pyrolysis oil, acids are completely converted in 2 hours. With the addition of pyrolysis oil, the fraction of acids contributed by the pyrolysis oil go unconverted in 2 hours. The experiment using none of the triglyceride oil showed 53 % conversion of acids, indicating that the pyrolysis oil is indeed prone to esterification by this catalyst, but that something inhibits the reaction when the triglyceride oil is present before kicking off the reaction. While this result suggests that the catalyst may preferentially partition into the organic phase—leaving the pyrolysis oil untouched—a study of the phase partitioning of the catalyst shows that it prefers polar phases (water and methanol) to triglyceride. Such a contradiction implies that this behavior may have a mechanistic explanation; i.e., the interaction of the catalyst with reactive species results in intermediates with different liquid-liquid phase partitioning than the catalyst alone.

It is worth noting that the amount of pyrolysis oil affected the order in which the phases settled; for 5.0 g and below, the nonpolar layer (TG and FAME) was the bottom phase, while the polar layer (MeOH and PyOil, if present) was the top phase. For 7.5 g and above, the phases were inverted, although the exact break point between 5.0–7.5 g was not determined. This result is easily explainable by the triglyceride oil's density being between those of methanol and the pyrolysis oil, but it will be an important consideration for the design of any process that involves a PyOil/FFA coprocessing

scheme.

3.4.3. Two-Step One-Pot Coprocessing of PyOil with high-FFA Triglyceride Oil

The failure of the one-step, one-pot coprocessing scheme to convert pyrolysis oil acids motivated the testing of a two-step scheme, whereby the pyrolysis oil is reacted with methanol and the catalyst, presumably close to completion (60 % conversion of titratable acids), before a high-FFA triglyceride oil is added to the flask to react with the methanol and catalyst. Table 3.3 shows a summary of the reactor loading tested to demonstrate the possibility of using the ionic liquid catalyst in the esterification of both pyrolysis oil and a high-FFA triglyceride oil without an intermediate recovery step.

The conditions were chosen to ensure near-complete conversion of pyrolysis oil acids over 2 hours before adding a sufficient amount of TG/FFA oil to avoid possible equilibrium limitations due to the water in the pyrolysis oil and produced from the esterification reaction. The conversion of FFA following its addition to the reaction mixture is shown in Figure 3.21. While this performance is competitive with other ionic liquid catalysts in the literature, it compares poorly to the case of esterifying pure FFA, or even FFA mixed with TG, with this particular catalyst.

Fractional conversion versus time shows a linear trend, as shown in Figure 3.22, indicating that the reaction is behaving as zero-order with respect to FFA concentration at these conditions. Zero-order performance implies that the catalyst is the limiting factor and that FFA is in excess, suggesting that the catalyst is failing to partition effectively into the TG/FFA oil phase. This result is interesting in the context of the observation that a one-step, one-pot approach prevents the catalyst from converting the pyrolysis oil acids

effectively, while the catalyst will partition into the polar phase of nonreactive mixtures of corn oil and a polar solvent.

Figure 3.23 shows the conversion of total titratable acids for the same set of experiments. By subtracting the total titratable acids from the FFA at time *t* (determined either by measuring FFA or by inference from measure FAME), the conversion of pyrolysis oil acids could be estimated, as shown in Figure 3.24. The data appear to show stability over the first 2 hours, with hydrolysis of the pyrolysis oil esterification products becoming apparent towards the end of the run. This apparent reversal of the reaction is likely due to water from the FFA esterification concentrating in the polar phase, causing an equilibrium shift that neither affects the FFA esterification in the nonpolar phase, nor manifests during the esterification of pyrolysis oil on its own.

Recalling that 60 % is the fraction of titratable acids that will actually esterify, and these carboxylic acids are generally the main problem with pyrolysis oil in terms of corrosion and instability, it can reasonably be concluded that respectable levels deacidification of both pyrolysis oil and high-FFA triglyceride oil can be achieved through this process.

3.5. Conclusion

An ionic liquid catalyst, previously tested on the esterification of free fatty acids with methanol, has been used to effect the esterification of acidic compounds in a pyrolysis liquid, using an excess of methanol. The behavior of this reaction was demonstrated to be second-order with respect to the concentration of reactable acids, taken as a known fraction (0.60) of the total titratable moles acid in pyrolysis oil, and a

kinetic model was developed to fit the observation that the ratio of catalyst to pyrolysis oil was the most relevant parameter in predicting reaction performance. Catalyst dependency was found to be second-order, and a rate constant and activation energy were calculated as well. The model predicts that a 10 % weight ratio of catalyst to pyrolysis oil should achieve 80 % mitigation of the acids in pyrolysis oil within 15 minutes if the reaction mixture can be maintained at 70 °C with sufficient excess of methanol. Higher temperatures and catalyst ratios should achieve better conversions, with a 10 °C increase in temperature providing roughly the same improvement as an increase 5 wt % increase in the catalyst ratio at practical conditions.

While the parameters for the model presented in this work only truly fit the particular batch of pyrolysis oil tested, the model could be extended to the use of other pyrolysis liquids with a relatively small number of experiments for a given batch or source. A base case experiment, for which early-time data are also collected, would confirm second-order dependence on pyrolysis oil and allow the fitting of an appropriate value for φ. Two additional catalyst loadings would allow the determination of k from the slope, Θ, of a plot like the one in Figure 3.14. A test at one additional temperature would provide sufficient information for calculating the activation energy even though a more reliable value would result from testing an additional two temperature. Future work could tabulate the values of k and E_a for pyrolysis liquids from different sources using only four or five experiments per feedstock.

The possibility was explored of using the catalyst to convert the fatty acids in a high-FFA triglyceride oil to biodiesel, as well as to mitigate the acidic groups of a pyrolysis oil in the same reaction vessel, without an intermediate recovery step.

Preliminary tests on a single-step one-pot scheme only showed conversion of FFA without the reaction of pyrolysis oil acids. A two-step one-pot scheme was tested, whereby a high-FFA triglyceride oil was added to a mixture of pyrolysis oil, methanol, and catalyst that had already been reacting for 2 hours. The biodiesel reaction was found to be zero-order with respect to FFA, indicating that the amount of catalyst participating in the reaction was very small compared to the amount of FFA. The contradictory results of the two coprocessing schemes demand a mechanistic explanation where one is lacking, as it is possible that the catalyst, which would ordinarily prefer one liquid phase to another (polar over nonpolar), is modified by the reactants in such a way that it preferentially partitions into the TG/FFA/biodiesel phase in one case, while preferentially partitioning into the methanol/PyOil/water phase if the same reactants are added in a different manner.

The results, however, are promising nonetheless. If a blend of biodiesel and pyrolysis oil is to be utilized for a combustion application, then it may be useful to add a surfactant or co-solvent to form a single liquid phase in a coprocessing scheme; homogenizing the reaction mixture may help to overcome the limitations observed in the coprocessing of the two oils. If sufficient conversion of FFA and pyrolysis oil acids can be achieved, then a well-tested traditional process can be employed for the transesterification of triglycerides to biodiesel. If the phase behavior limitations of the catalyst in a coprocessing scheme can be overcome, then the conversion of FFA should be effected relatively quickly, as the catalyst loadings necessary for pyrolysis oil are much higher than those necessary for the conversion of FFA to biodiesel at mild conditions.

If sufficient conversion can be reasonably achieved by alterations to the process that do not homogenize the product mixture, phase-separation of the biodiesel/TG layer from the methanol/water layer containing the mitigated pyrolysis oil would allow for subsequent upgrading or utilization of each feedstock independently.

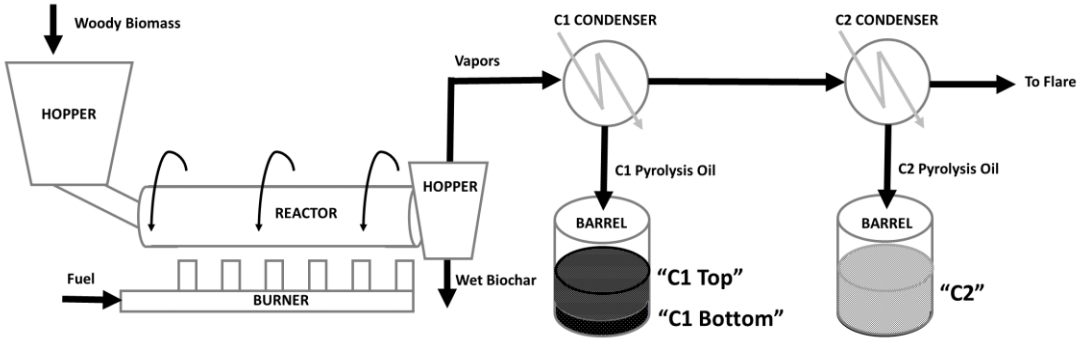

Figure 3.1. *Diagram of fast pyrolysis process used to generate the pyrolysis oil for this work. Biomass is fed to a rotating pipe operated under slight vacuum and heated by burners. As the biomass passes through the pipe, it pyrolyzes, releasing vapors and converting to char. The char collects in a hopper while the vapors pass through a system of condensers to collect pyrolysis liquids. The C1 condenser knocks out a more water-rich fraction which is allowed to settle in a collection barrel. A thick, lignin-rich layer settles to the bottom, and the liquid collected at the top of the barrel forms the "C1 Top" fraction, which was employed in this work.*

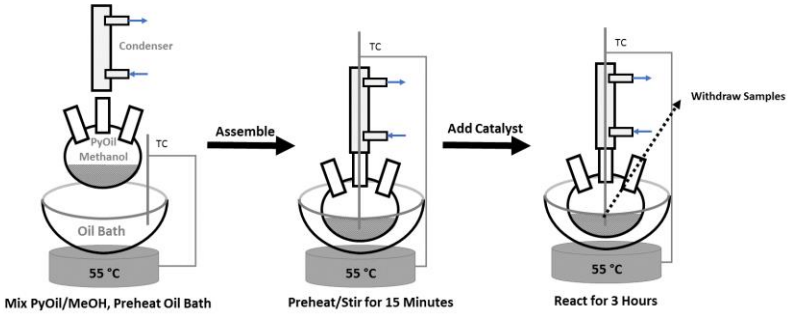

Figure 3.2. *Graphical summary of pyrolysis oil esterification procedure. The round-bottom flask was loaded on a scale with pyrolysis oil and methanol before applying a condenser and inserting into a preheated oil bath. Catalyst was added after 15 minutes of preheating, and samples were withdrawn for analysis at specified intervals throughout the run. Following collection of the last sample, the reaction mixture was disposed of.*

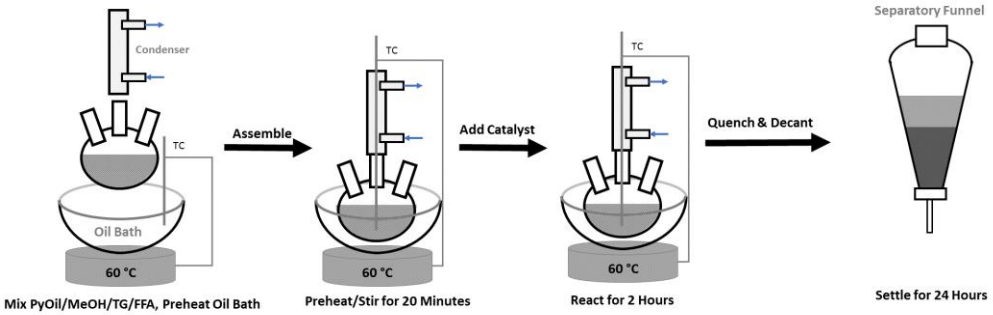

Figure 3.3. *Graphical summary of one-step, one-pot coprocessing scheme. The round-bottom flask was loaded with methanol, pyrolysis oil, and 20 wt % nonanoic acid in canola oil before applying a condenser and inserting into a preheated oil bath. Catalyst was added after 20 minutes of preheating. After 2 hours of reaction, the flask was quenched and its contents were decanted into a separatory funnel for phase separation. The liquid phases were weighed and titrated to determine acid content of the reaction mixture.*

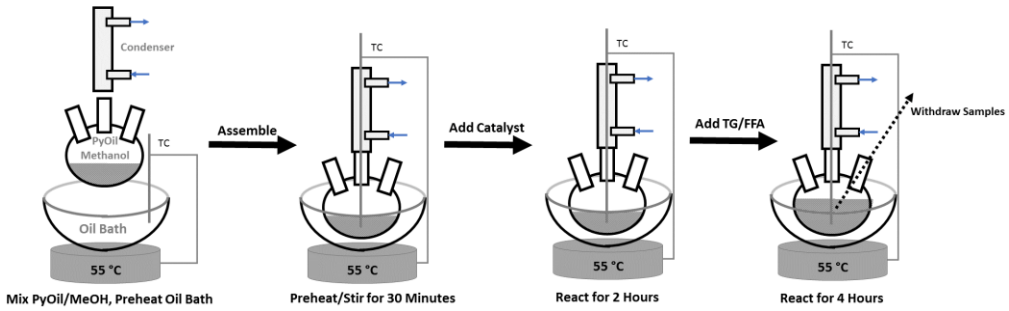

Figure 3.4. *Graphical summary of two-step, one-pot coprocessing scheme. The round-bottom flask was loaded with methanol and pyrolysis oil before applying a condenser and inserting into a preheated oil bath. Catalyst was added after 30 minutes of preheating, and the reaction was allowed to proceed for 2 hours before the addition of 10 wt % nonanoic acid in canola oil. Samples were withdrawn for analysis at specified intervals following the addition of TG/FFA. Following collection of the last sample, the reaction mixture was disposed of.*

Table 3.1 *Reaction conditions tested along with a summary of results. The base case is listed twice so that it can be seen in the context of the parameters being varied. Experiments T1, T2, T3, and SR employed a different batch of catalyst from the other experiments, which is why T3 shows different results from the base case; however, these experiments were still appropriate for calculating activation energy and for determining the rate-dependency on pyrolysis oil concentration.*

	Parameters				**Reactor Loading**			**Performance**	
ID	**T (°C)**	**MeOH/PyOil Mass Ratio**	**Cat/PyOil Mass Ratio**	**Cat. Conc. (mg/ml)**	**PyOil (g)**	**MeOH (g)**	**Catalyst (mg)**	**1 hr Conv.**	**Peak Conv.**
M1	55	**0.57**:1	0.035:1	19.3	15.0	8.5	524	33%	41%
Base	55	**1.27**:1	0.052:1	19.3	10.0	12.7	524	41%	52%
M2	55	**3.36**:1	0.105:1	19.3	5.0	16.8	524	52%	60%
M3	55	**7.53**:1	0.208:1	19.3	2.5	18.9	524	54%	57%
C1	55	1.27:1	0.013:1	**4.9**	10.0	12.7	131	1%	16%
C2	55	1.27:1	0.026:1	**9.7**	10.0	12.7	262	21%	36%
Base	55	1.27:1	0.052:1	**19.3**	10.0	12.7	524	41%	52%
C3	55	1.27:1	0.104:1	**37.8**	10.0	12.7	1047	47%	56%
T1	**35**	1.27:1	0.052:1	19.3	10.0	12.7	524	29%	39%
T2	**45**	1.27:1	0.052:1	19.3	10.0	12.7	524	35%	51%
T3	**55**	1.27:1	0.052:1	19.3	10.0	12.7	524	47%	55%
SR	**55**	1.27:1	0.052:1	19.3	10.0	12.7	524	*30-minute Run*	

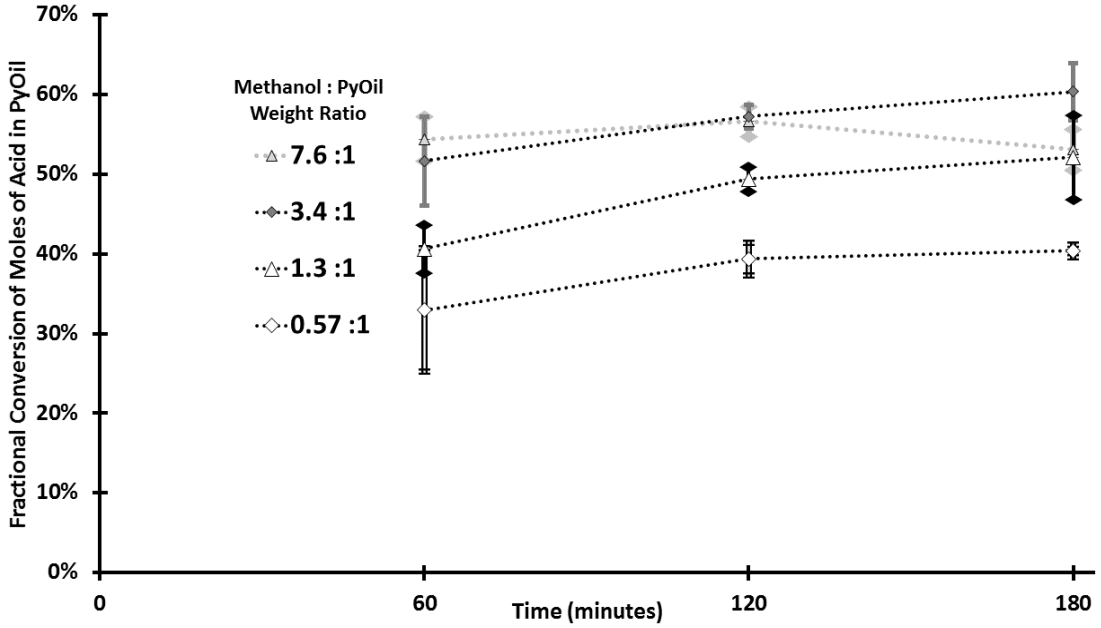

Figure 3.5. *Fractional conversion of pyrolysis oil acid over time, at different MeOH/PyOil weight ratios. Reactor charge was nominally 524 mg of catalyst with 2.5–15.0 g of pyrolysis oil and 8.5–18.9 g methanol, holding volume at a constant 27 ml. Operating temperature was 55 °C. Error bars show the standard deviation of the data.*

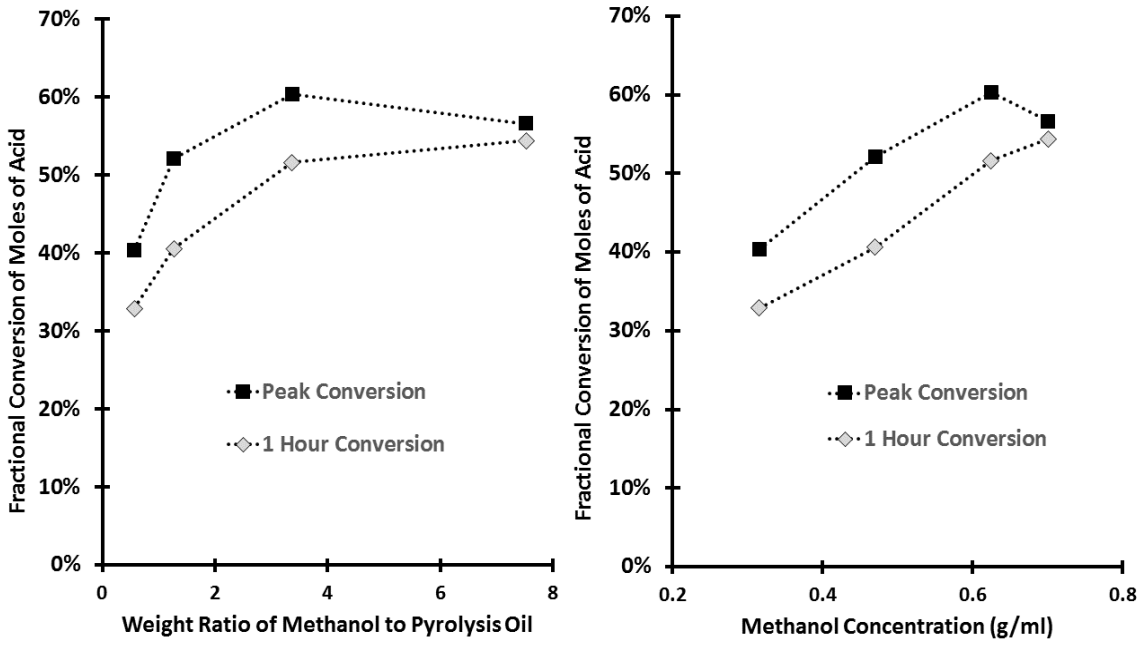

Figure 3.6. *The effect of different MeOH/PyOil weight ratios (with constant catalyst concentration) on 1-hour and peak (3-hour, except for the highest ratio) fractional conversion. The same data are plotted against different x-axes. Methanol is in excess at all conditions: a 1:1 weight ratio of methanol to pyrolysis oil is equivalent to a 15.5:1 molar ratio of methanol to titratable acid groups*

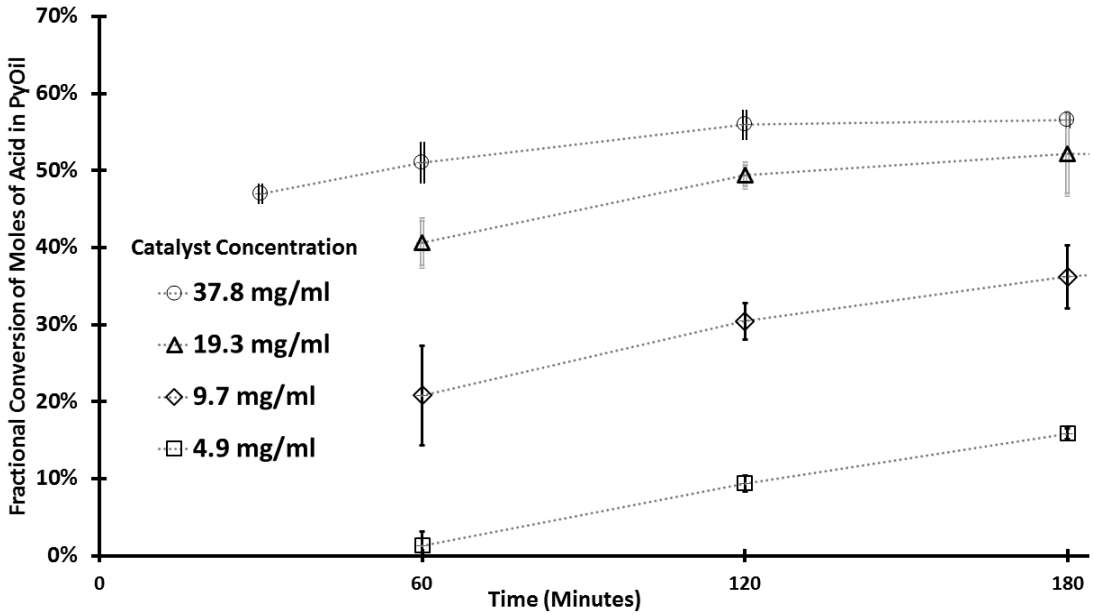

Figure 3.7. *Fractional conversion of pyrolysis oil acid over time, at different catalyst loadings. Reactor charge was nominally 10.0 g of pyrolysis oil with 12.7 g of methanol, and operating temperature was 55 °C. Error bars show the standard deviation of the data.*

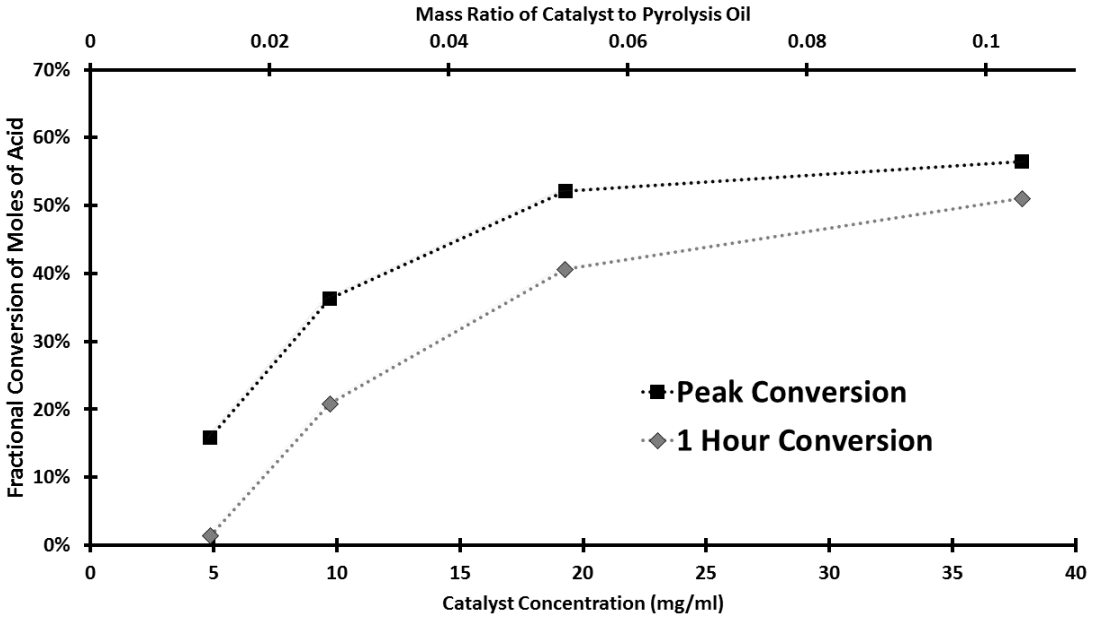

Figure 3.8. *The effect of different catalyst loadings on 1-hour and peak (3-hour) fractional conversions for different catalyst concentrations, showing diminishing returns as catalyst loading is increased.*

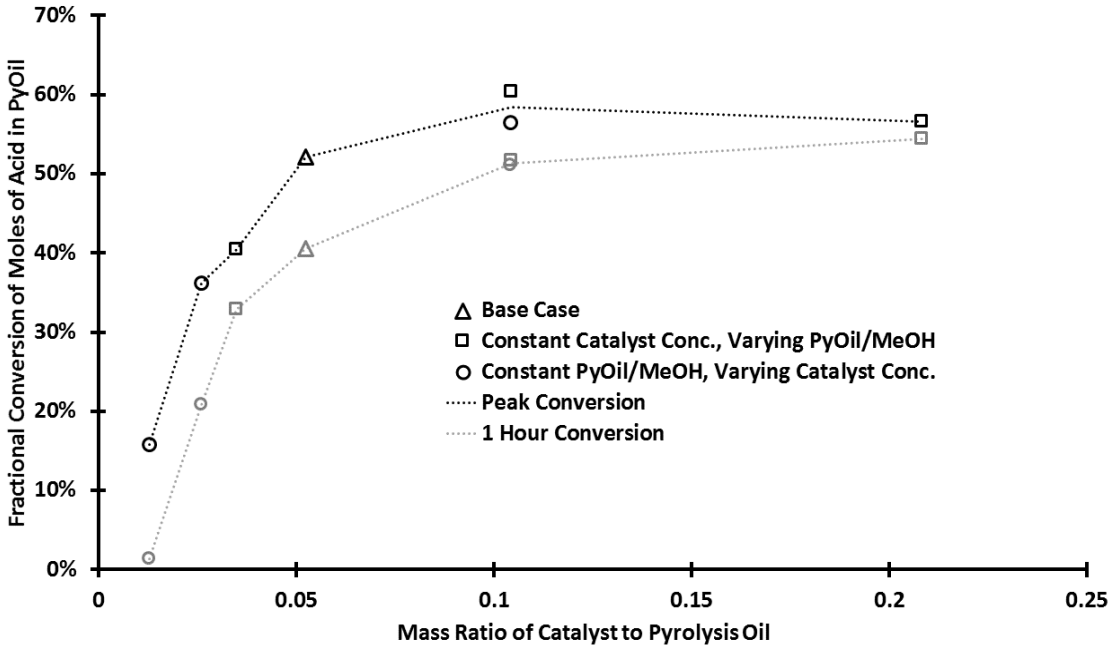

Figure 3.9. *The effect of different catalyst/PyOil weight ratios on 1-hour and peak (3-hour, except for the highest ratio) fractional conversion, plotted from the data collected to test the effects of catalyst loading and MeOH/PyOil ratio. Peak conversion was measured at 2 hours for the highest catalyst/PyOil ratio. Connecting the data points produces an apparent curve whose continuity suggests that the catalyst ratio was the relevant parameter being varied by the different reaction conditions tested.*

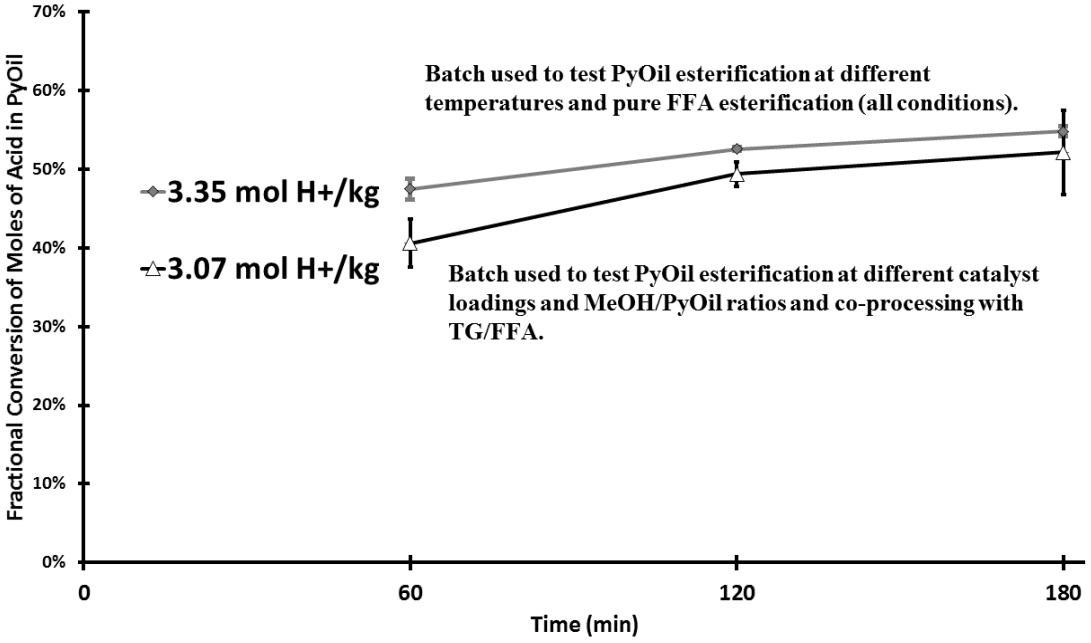

Figure 3.10. *Comparison of the two batches of catalyst used in this research. The batch used in the prior work on FFA esterification was employed to test different temperatures of pyrolysis oil esterification (to determine activation energy), as well as for the short-run data. While this batch was ~10 % stronger by titration, its performance was equivalent to using ~26% more catalyst.*

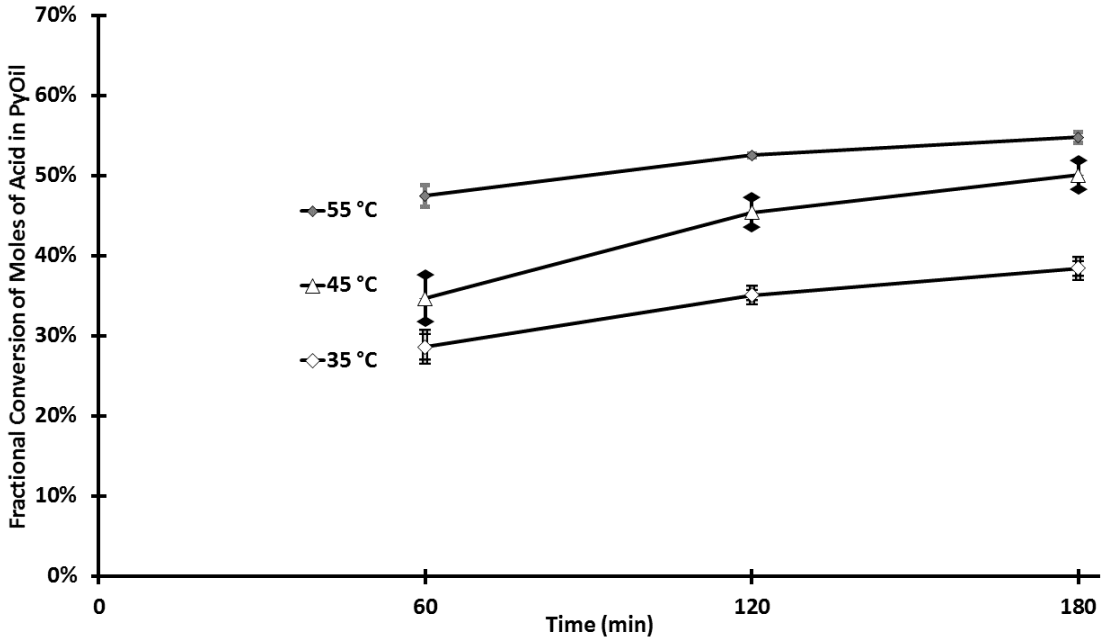

Figure 3.11. *Fractional conversion of pyrolysis oil acid over time, at different temperatures. As should be expected, conversion increases with temperature.*

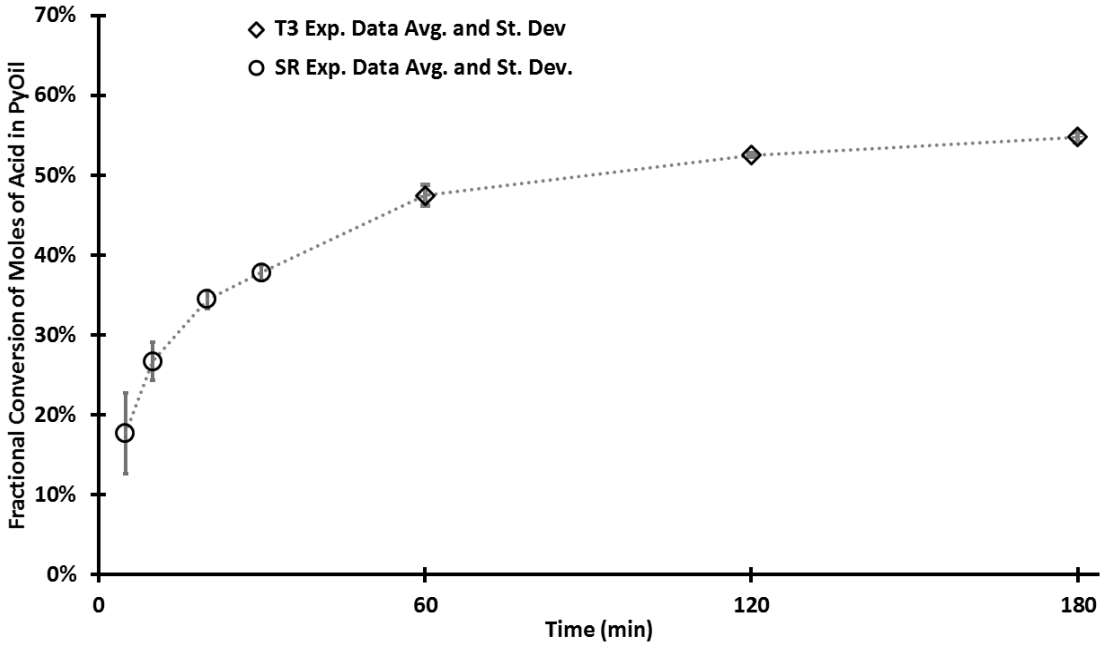

Figure 3.12. *Fractional conversion of pyrolysis oil acid over time, from two sets of data derived from identical conditions, showing the short-time behavior of the reaction.*

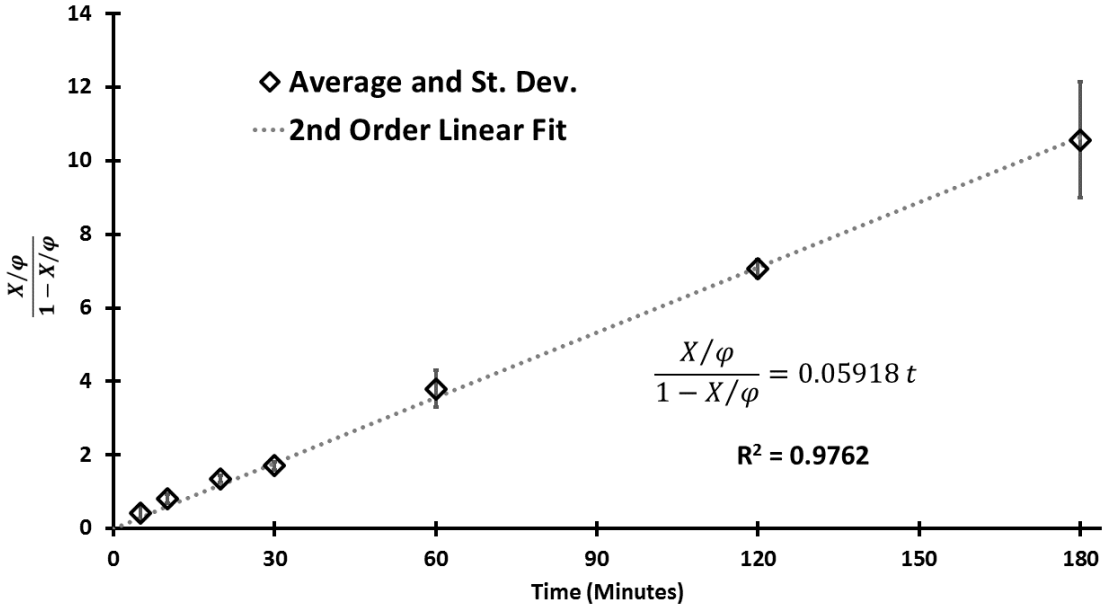

Figure 3.13. *Linear fit showing second-order behavior of pyrolysis oil esterification. Data are from the SR (up to 30 minutes) and T3 (60 minutes and after) experiment runs. All data points were considered in the calculation of* R^2.

Table 3.2. *Slope and R^2 values for second-order linear fits at different catalyst loadings. In some cases, the spread of X/(1-X) was very wide at longer reaction times while still averaging out to a value close to the best-fit line, and this observation is reflected in the differences in the R^2 values.*

ID	Catalyst Ratio (g cat / mol H^+)	Slope Ψ (min^{-1})	R^2 Based on Averages	R^2 Based on all Points
C1	10.8	0.001750	0.8349	0.8163
C2	21.6	0.008532	0.9990	0.7089
Base	43.3	0.037215	0.9941	0.2759
C3	86.2	0.098053	0.9379	0.5506

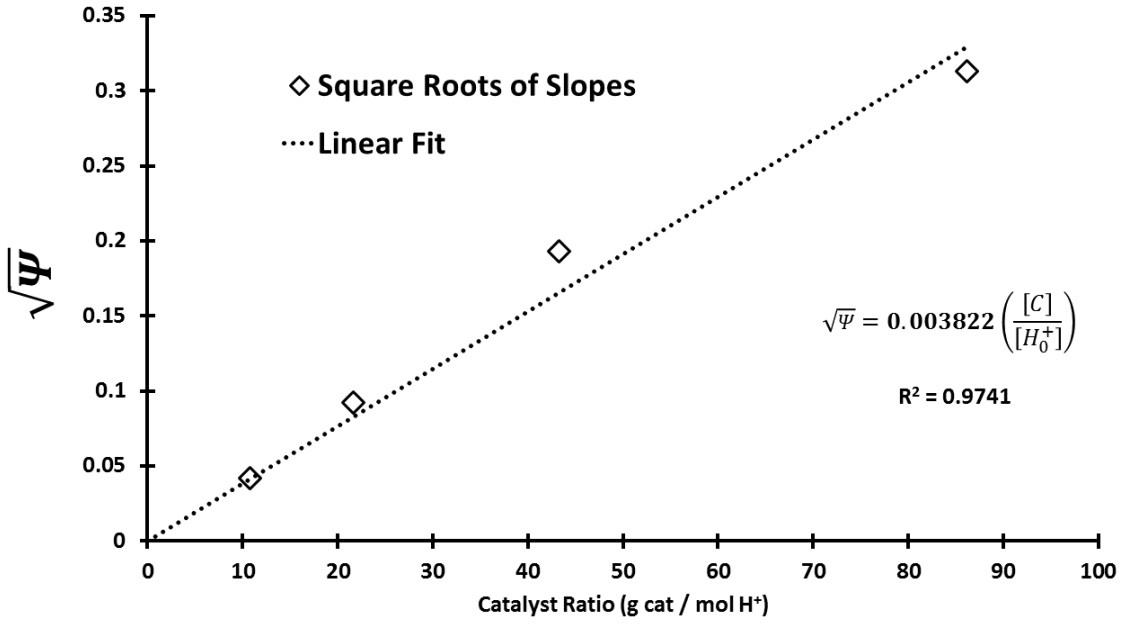

Figure 3.14. *Square roots of the slopes of second-order fits at different catalyst loadings, plotted against the catalyst ratio. Linearity indicates that the reaction is second-order with respect to some function of catalyst loading. In this model, that function is the ratio of catalyst to titratable acids. Using the catalyst concentration for the model fits as well; however, such a model breaks down when compared against data at different pyrolysis oil concentrations.*

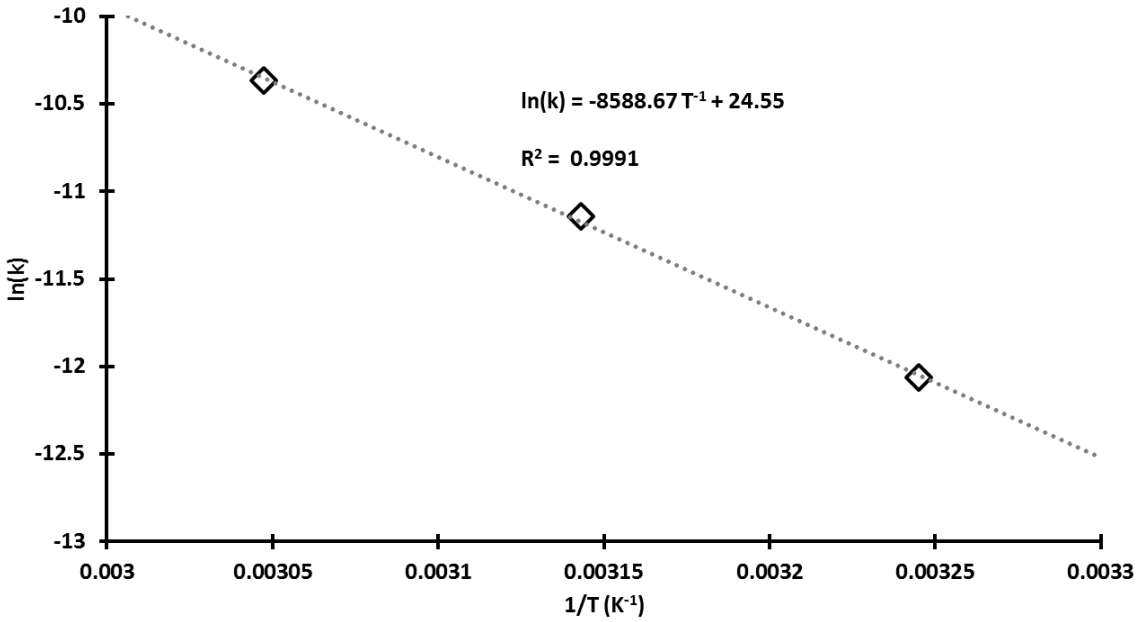

Figure 3.15. *Arrhenius plot for pyrolysis oil esterification, indicating an apparent activation energy of 71.41 kJ/mol.*

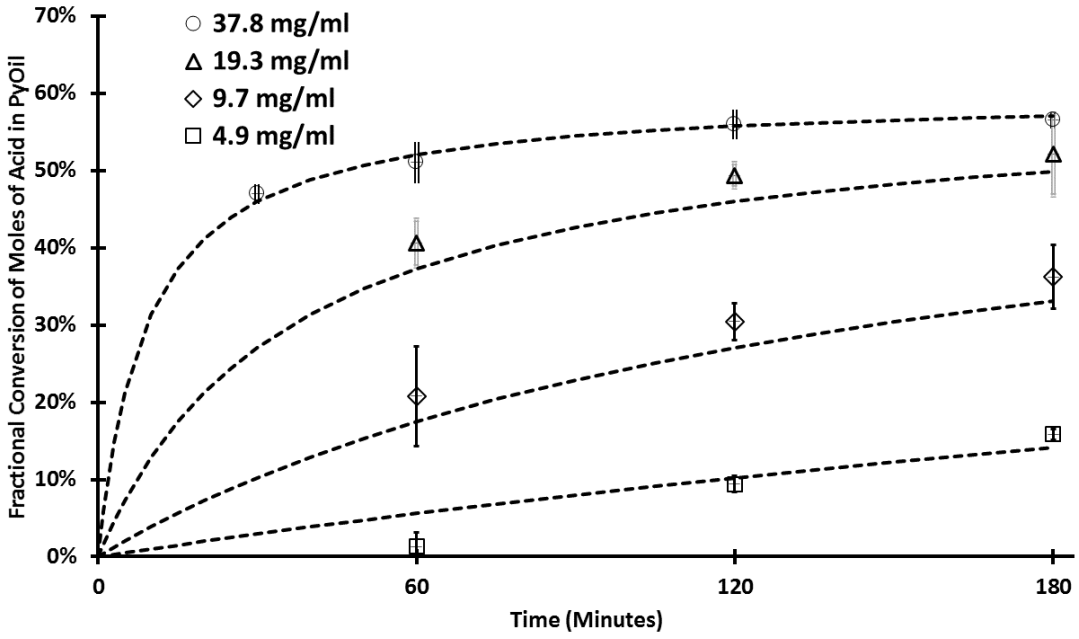

Figure 3.16. *Fractional conversion of pyrolysis oil acid over time, at different catalyst loadings. Dashed curves show predictions of model. The semi-empirical model is a strong fit for the data it was derived from.*

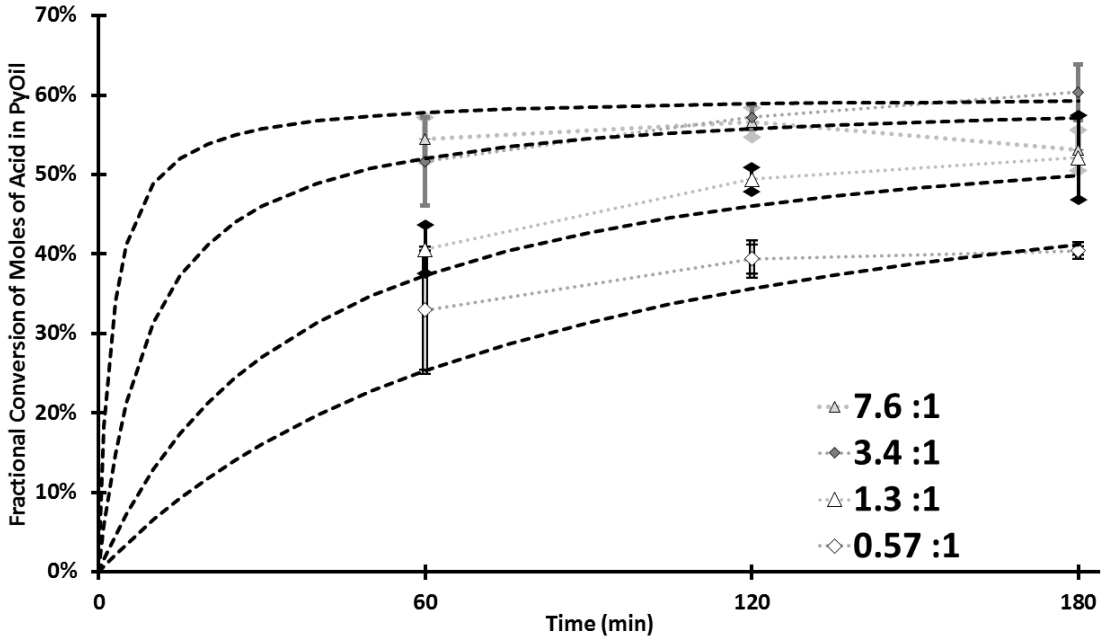

Figure 3.17. *Fractional conversion of pyrolysis oil acid over time, at different MeOH/PyOil weight ratios. Dashed curves show predictions of model. Except for the "1.3:1" data set, these data were not employed in constructing the model, yet still fit the model fairly well.*

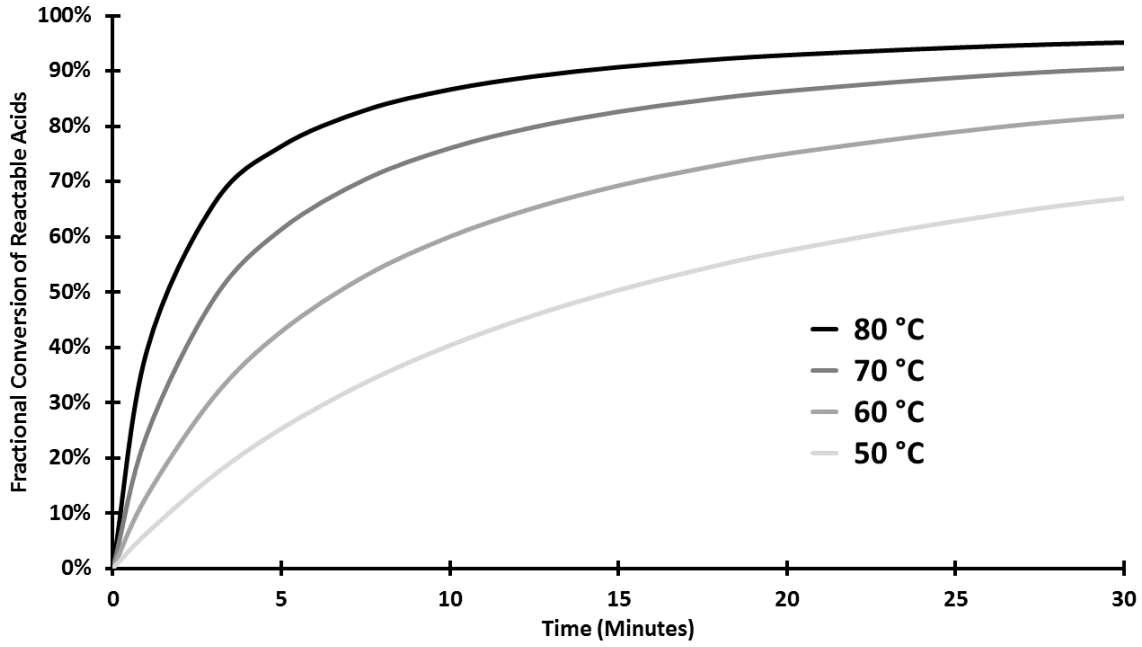

Figure 3.18. *Kinetic model's prediction for the fractional conversion of reactable acids (fractional conversion of titratable acids, divided by 0.60) at different temperatures, showing significant levels of acids mitigation even at mild conditions and short reaction times. Catalyst loading is 10 wt % relative to the pyrolysis oil loading. Higher temperatures improve reaction performance.*

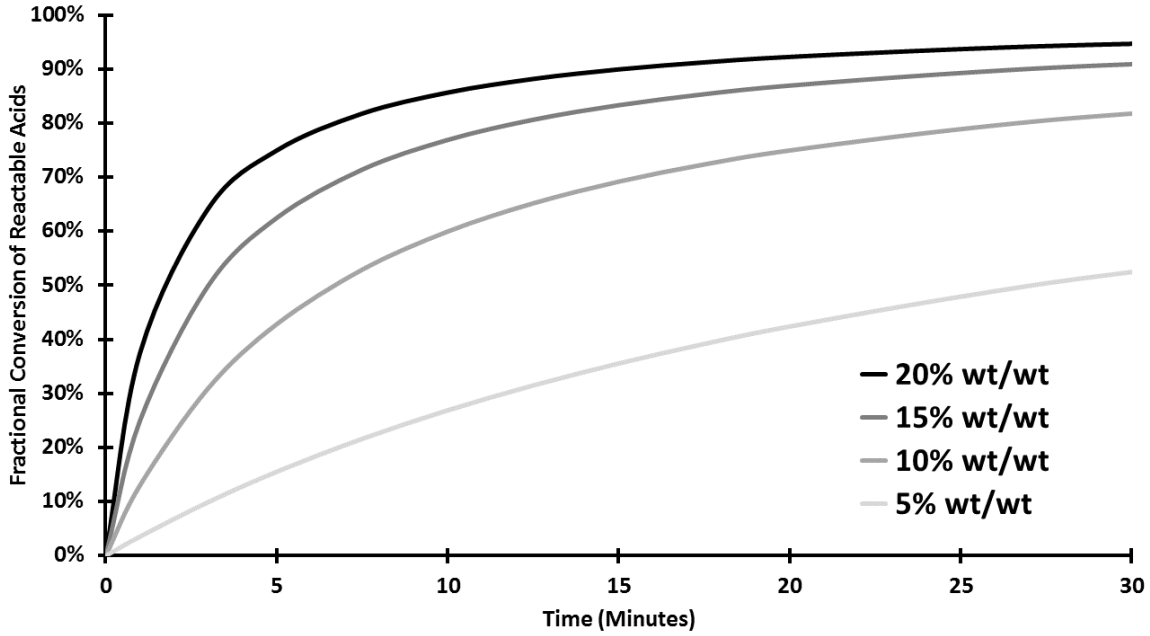

Figure 3.19. *Kinetic model's prediction for the fractional conversion of reactable acids (fracitonal conversion of titratable acids, divided by 0.60) at different catalyst loadings (as wt % relative to pyrolysis oil loading), showing significant levels of acids mitigation even at mild conditions and short reaction times. Temperature is 60 °C.*

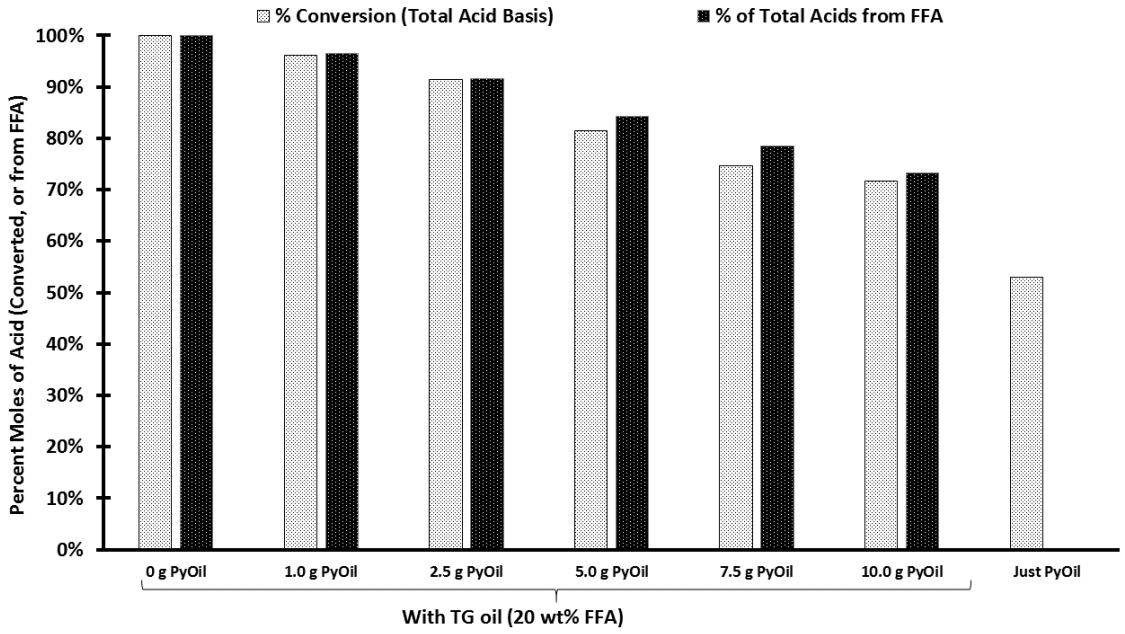

Figure 3.20. *Results of single runs of 50 g of 20 wt % nonanoic acid in canola oil with 20.0 g of methanol, varying amounts of pyrolysis oil, and 524 mg of catalyst, reacted in a single step at 60 °C. Fractional conversion of total acids is plotted next to the fraction of acids contributed by nonanoic acid. A similar run employing 10.0 g of pyrolysis oil without any nonanoic acid or corn oil is shown for comparison.*

Table 3.3. *Summary of reactor loadings for one-pot two-step coprocessing experiment. Concentrations are tabulated on a zero-conversion basis, even though some pyrolysis oil and methanol will have been consumed by the time the TG/FFA is added.*

	Catalyst	**MeOH**	**PyOil**	**FFA**
Loading	524 mg	10.0 g	5.00 g	2.50 g
Before TG/FFA	28.6 mg/ml	546 mg/ml	273 mg/ml	--
	$52.0\ \frac{\text{g cat}}{\text{mol acid}}$	$31.0\ \frac{\text{mol MeOH}}{\text{mol acid}}$	$0.550\ \frac{\text{mol acid}}{\text{kg}}$	--
After TG/FFA	11.4 mg/ml	218 mg/ml	109 mg/ml	54.5 mg/ml
	$20.2\ \frac{\text{g cat}}{\text{mol acid}}$	$12.1\ \frac{\text{mol MeOH}}{\text{mol acid}}$	$0.220\ \frac{\text{mol acid}}{\text{kg}}$	$0.344\ \frac{\text{mol acid}}{\text{kg}}$

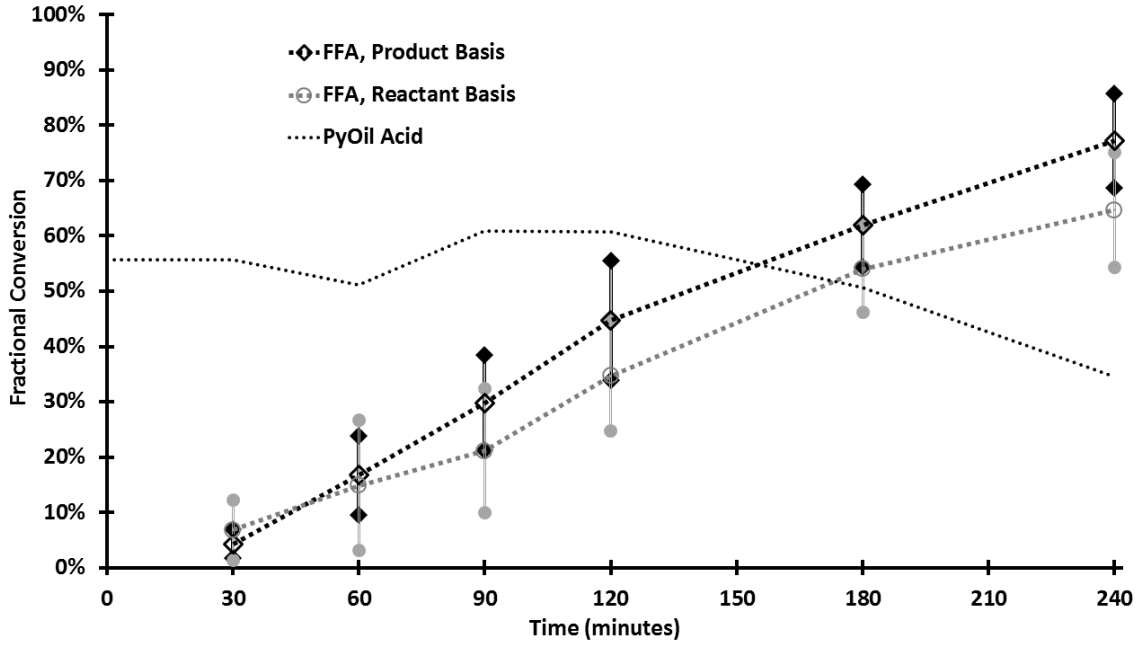

Figure 3.21. *Fractional conversion of nonanoic acid in the two-step coprocessing scheme. Conversion was calculated based on the measured concentration of nonanoic acid ("Reactant Basis") as well as on the measured concentration of methyl nonanoate ("Product Basis"). t = 0 min was the moment the TG/FFA mixture was added to the flask. Error bars show the standard deviation of the data, and the circular and diamond-shaped markers are used to make the endpoints of the standard deviation more visible. Conversion of PyOil acids is shown for comparison.*

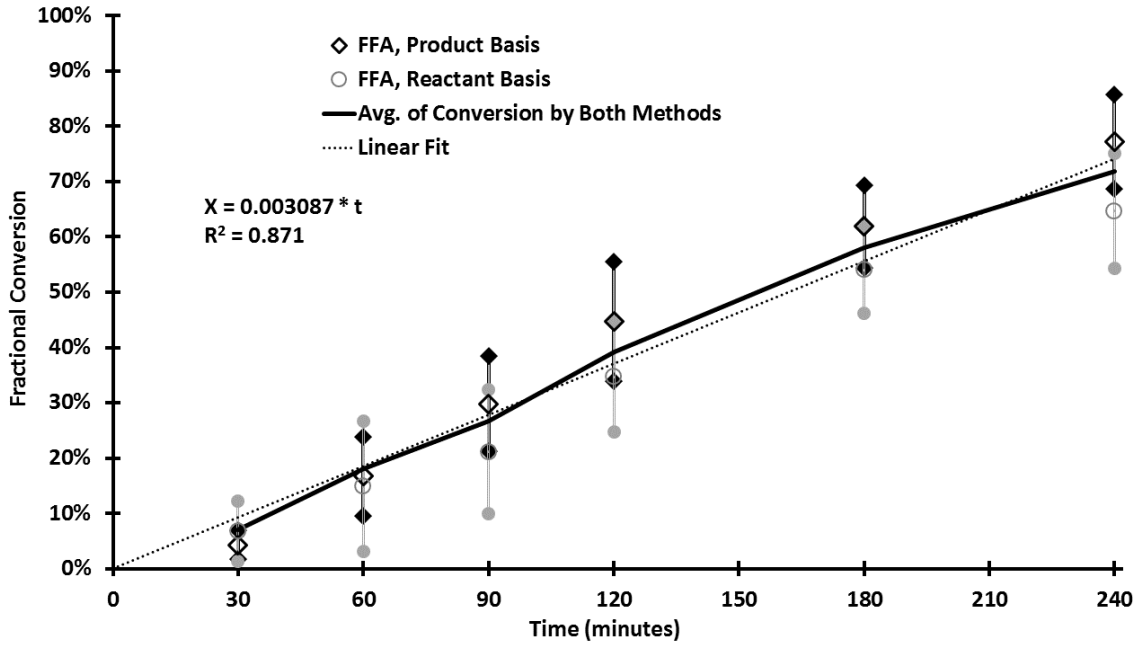

Figure 3.22. *A simple linear fit to the fractional conversion of FFA during the one-pot, two-step coprocessing with pyrolysis oil shows the zero-order rate dependence on fatty acid concentration, indicating that the catalyst's low concentration in the appropriate liquid phase is limiting this reaction at the conditions tested.* R^2 *is calculated relative to all data points and not just their averages.*

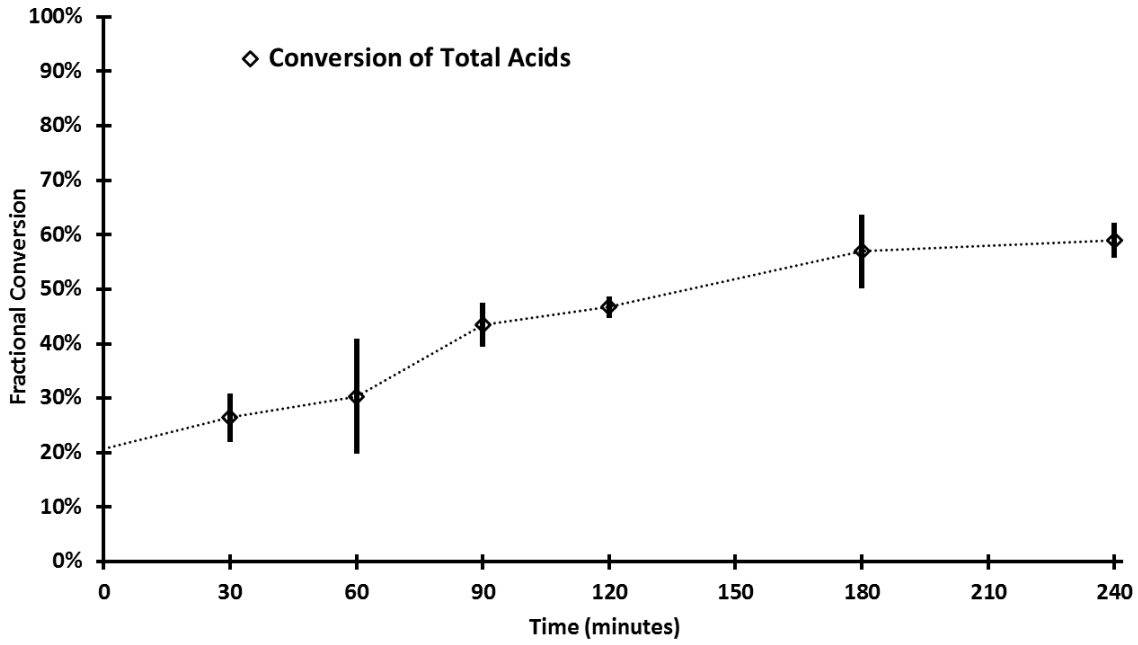

Figure 3.23. *Fractional conversion of total acids in the two-step processing scheme, as measured by titration. The conversion at t = 0 min is an estimation based on the weight ratio of catalyst to pyrolysis oil and the pretreatment time (2 hours), using the model previously derived. Error bars show the standard deviation of the data. Measurement of total acids by titration was necessary to estimate the conversion of pyrolysis oil acids.*

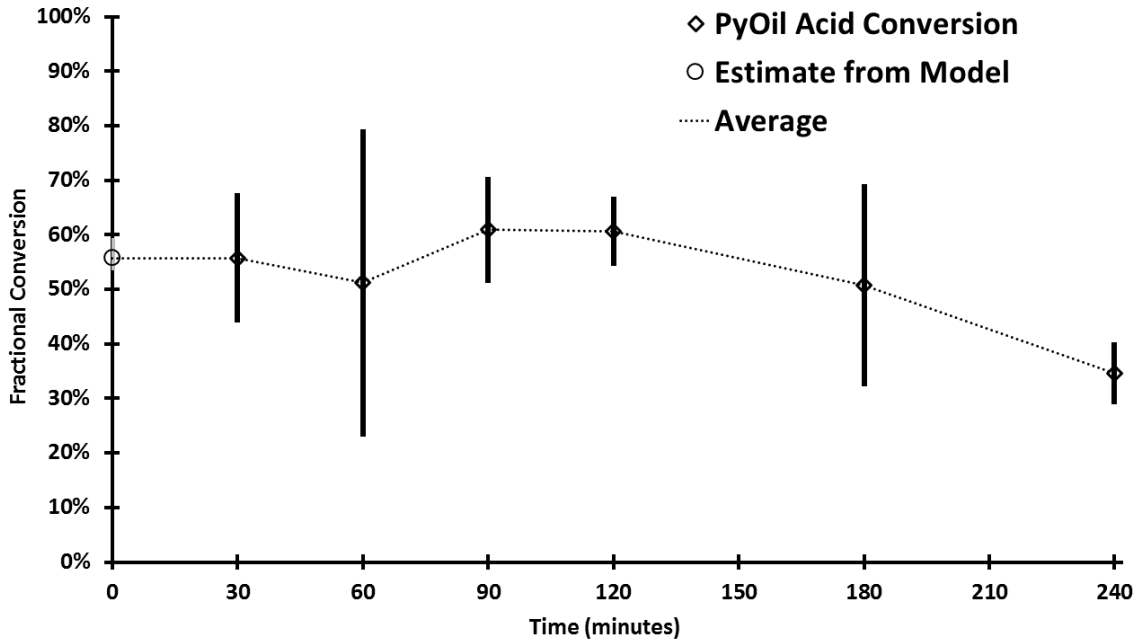

Figure 3.24. *Fractional conversion of moles of acid from pyrolysis oil during the time following the addition of TG/FFA mixture to the reaction flask. The conversion at t = 0 min is an estimation based on the weight ratio of catalyst to pyrolysis oil and the pretreatment time (2 hours), using the model previously derived. Other data points were calculated based on total moles of acids, as measured by titration, corrected by the moles of acid from FFA, as calculated from the average of the fractional conversions calculated on both an FFA and FAME basis. Error bars show the spread of the results. The conversion achieved prior to adding the TG/FFA appears to remain stable for 2 hours before reversing.*

CHAPTER 4

CONCLUSIONS AND CONSIDERATIONS FOR FUTURE WORK

4.1. Introduction

In this work, a newly-developed ionic liquid catalyst was shown to have excellent potency for the esterification of free fatty acids to produce biodiesel, as well as the versatility to achieve the esterification of acids in a pyrolysis liquid. Kinetic models describing the behavior of both reactions were derived and compared to the data, and a novel coprocessing scheme was shown to allow both pyrolysis oil mitigation and the deacidification of high-FFA triglyceride oils to proceed in a single process, demonstrating the catalyst's broad potential for the upgrading of waste biomass to value-added products.

4.2. Relative Potency of Ionic Liquid Catalyst

In order to compare the esterification performance of the ionic liquid catalyst examined in this work ($[BHSO_3AIM][CF_3SO_3]$ or *1-sulfobutyl-3-allylimidazolium triflate*) to other catalysts in the literature, data from several papers were added to a spreadsheet for analysis. The data were given the same treatment as the first-order analysis in Chapter 2, except the model was modified to account for differences in methanol excess, assuming first-order behavior with respect to methanol concentration.

The first-order linear fit is then given by:

$$-\ln\left(\frac{\beta(1-\mathrm{X_{FFA}})}{\beta-\mathrm{X_{FFA}}}\right)=\mathrm{F([C])}\frac{M_{\mathrm{MeOH}}}{M_{\mathrm{FFA}}}(\beta-1)\,t \tag{4.1}$$

β is the molar ratio of methanol to fatty acid, and M_i is the molecular weight of species i. $\mathrm{F([C])}$ is some function containing the catalyst dependency, either determined to be the catalyst concentration itself, or interpolated from data taken at different catalyst loadings. If a sufficiently-developed model was given in the paper, then that model was used instead of this first-order fit.

The catalysts are summarized in Table 4.1, along with the approaches used for comparison with the results of this work. Aghabarari et al. (2013) tested four candidate ionic liquid catalysts of similar molecular structure and chose the most promising, IL8B, for further analysis. Figure 4.1 shows the conversion over time data presented in that paper, along with the fitted model described in Equation 4.1. Fractional conversions at different catalyst loadings for a given reaction time were used to similarly calculate fitted slopes (albeit fitted by drawing a line from the origin through a single datum at each tested condition). Plotting these slopes against the catalyst concentration, as in Figure 4.2, demonstrates that the assumption of first-order behavior with respect to catalyst loading holds up well.

Li et al. (2014) tested seven candidate ionic liquid catalysts and chose the most promising, [$BHSO_3MIM$][HSO_4^-], for further testing. Figure 4.3 shows conversion over time data presented in that paper, along with the fitted model described in Equation 4.1. The behavior at different catalyst loadings did not appear to fit a straightforward reaction

order, so the effect of catalyst loading was accounted for by interpolating between the calculated first-order fitted slopes versus the catalyst concentration. Activation energies were calculated from data at different temperatures, as before.

The papers concerning homogeneous strong acid catalysts presented their own kinetic models, and these were employed for comparison with the results of this work. The catalysts are drawn in Figure 4.4 with their names color coded to correspond with the predicted fractional conversion curves of Figure 4.5 and Figure 4.6, which compare the predicted performance of the catalysts at the same reaction conditions, with catalyst loading consistent on either a mass or mole basis.

Regardless of whether the catalysts are compared on a mass/mass or a mole/mole basis, the catalyst from this work drastically outperforms other ionic liquid catalysts, exhibiting a potency on par with the homogeneous strong acid catalysts. While not all catalysts were tested on the same FFA, catalytic testing on different FFAs usually yields comparable results, with longer-chain fatty acids generally having better performance than shorter-chain acids, within a spread of no more than ~10 % conversion. Therefore, it is unlikely that the relative performance of the different catalysts would seem different had they all been tested on the same fatty acid, and it is clear that the catalyst exhibits remarkable potency as an ionic liquid for FFA esterification.

4.3. Original Contributions of This Work

This work demonstrates the versatility of a new ionic liquid catalyst in the upgrading of waste biomass to value-added products, presents a new approach to kinetic analysis of the esterification of acids in a complex bio-oil derived from fast pyrolysis, and

explores the feasibility of as-yet untested coprocessing schemes for the deacidification of bio-oils derived from drastically different upgrading processes and with potentially very different downstream fates. The research is presented within the paradigm of integrating the treatment of biomass products commonly treated as waste, in order to improve the potential for utilization of untapped feedstocks as well as open new opportunities for downstream processing of existing biomass products. From a purely chemical-engineering perspective, this research may be seen as the testing of an esterification catalyst on pure carboxylic acids before subsequent testing on a real-world mixture of carboxylic acids: a straightforward "point A to point B" approach. However, the results and analysis demonstrate broad applicability of the catalyst to biomass upgrading, and the relation between the pure carboxylic acids—fatty acids characteristic of low-quality biodiesel feedstocks—and the real bio-oil draws a unique connection between two avenues for biomass upgrading that deal with very different feedstocks and reaction products.

4.3.1. Potency of Catalyst for FFA Esterification

The ionic liquid catalyst was tested on the esterification of pure fatty acids in methanol. While this aspect of the work involves tried-and-true methods and a straightforward kinetic treatment of a well-studied reaction, it is still notable for the sheer potency demonstrated by the catalyst. On a molar basis, the catalyst's performance is comparable to that of homogeneous strong acids and far superior to other acidic ionic liquids reported in the literature.

4.3.2. Kinetic Treatment of Pyrolysis Oil Acids

While esterification studies on pyrolysis oil are reported in the literature, a kinetic description of the reaction is lacking, likely due to the complexity of pyrolysis oil mixtures and the sheer diversity of compositions among all pyrolysis oils. This work initially aimed simply to characterize the esterification performance of the catalyst and note the effects of varying certain process parameters. Surprisingly, however, treating the panoply of pyrolysis oil compounds as a single acidic reactant—taken as some fraction of the total titratable acids—allows the derivation of a kinetic model with a remarkable level of simplicity for its predictive power.

The model is semi-empirical, using a dependency on catalyst-to-acids ratio (rather than merely a catalyst concentration) to account for a dependency on some unknown ghost parameter. However, the kinetic analysis unambiguously reveals that the reaction is second-order with respect to acids and second-order with respect to catalyst loading, and calculation of activation energy using data across a 20 °C range was as straightforward as any reaction with pure components. A review of the literature reveals no such kinetic treatment of pyrolysis oil esterification.

4.3.3. Avenues for Integrating Pyrolysis Oil Upgrading with Biodiesel Production

Biodiesel blends with pyrolysis oil have been examined in the literature; however, the deacidification of both component oils using a single catalyst without an intermediate recovery step is a new approach. The range of viable compositions for blends is limited by numerous properties, such as viscosity, heating value, and emulsion stability; however, by mitigating the corrosiveness and reactivity of the pyrolysis oil, it is likely that blends with higher pyrolysis oil concentrations could be employed for a given

application. The two-step, one-pot coprocessing scheme examined in this work shows promise for an as-yet unexplored approach to biomass upgrading, and it is an important first step towards the development of novel processes utilizing next-generation catalysts to achieve the upgrading of waste biomass to value-added products.

4.4. Considerations for Future Work

4.4.1. Catalyst Recovery

One of the most important features of a catalyst is its reusability; however, this work is lacking extensive study on catalyst recovery and the performance of the recovered catalyst. The catalyst is extremely soluble in methanol, so it does not phase-separate from a homogeneous reaction mixture, and the minute amounts involved in the testing of fatty acid esterification precluded the use of solvent extraction to recover the catalyst after use in esterification. A preliminary examination of the catalyst's phase distribution in liquid systems indicates that the catalyst greatly prefers the polar phase of oil/methanol, oil/water, and oil/methanol/water systems (~97 % partitioning into the polar phase, determined by titration). This result, however, contrasts with the observation that, in the one-step, one-pot coprocessing scheme tested, the catalyst only effected the esterification of fatty acids and not the acidic compounds in pyrolysis oil. Larger batches of catalyst must be synthesized in order for study of the catalyst's bulk liquid-liquid phase behavior to guide the design of recovery schemes. Recovery will be crucial, as the cost of the catalyst far exceeds that of other homogeneous catalysts; the precursors alone can cost \$300–\$400 per mole of catalyst, while sulfuric acid (whose catalytic potency per mole is the same) can be sourced for roughly \$0.05–\$5.00 per mole of H_2SO_4, depending

on the quantity and purity (Alfa Aesar 2017; Alibaba 2017).

4.4.2. Kinetic Analysis Using Different Pyrolysis Oils and Catalysts

The kinetic treatment of pyrolysis oil presented in Chapter 3 exhibits remarkable accuracy for its simplicity relative to the complex composition of pyrolysis oil, with integer reaction orders being definitively confirmed by experimental data. That a reaction taking place among a complex panoply of species would lend itself so well to the straightforward kinetic analysis characteristic of single-phase, pure-component reactions is a surprising result. It would only require testing at four or five (depending on the desired level of confidence in calculated activation energies) experimental conditions to determine appropriate parameters (k, ϕ, *and* E_a) to model the esterification of a different pyrolysis liquid, and possibly using a different homogeneous catalyst as well. If the model holds up well across different bio-oil and catalyst combinations, with only those three parameters being varied, it would be useful to tabulate the values of these parameters for different bio-oil sources and esterification catalysts.

Perhaps the model could be expanded to account for moisture content in a pyrolysis oil (likely a contributing factor to the "ghost parameter" being accounted for by the $[H_0^+]^{-n}$ factor in the semi-empirical rate law), and correlations could be drawn between biomass treatment conditions and the kinetic parameters describing the esterification of the resulting pyrolysis liquid fractions. Such studies would be relatively uncharted territory for pyrolysis oil research, and it would not even require sophisticated equipment, relying on straightforward titration with NaOH and phenolphthalein to measure the progress of the reaction.

4.4.3. Characterization of Coprocessing Reaction

While this work presents a preliminary demonstration of the feasibility of coprocessing pyrolysis liquid with high-FFA triglyceride feedstocks, more extensive study of the effects of different process parameters and methodologies is necessary. The failure of the one-step, one-pot scheme—in contrast to the performance of the two-step, one-pot scheme—demands an explanation that may come to light with more extensive study of different feed parameters. The addition of a co-solvent to overcome diffusion limitations could lead to dramatically improved performance, as the catalyst available for FFA esterification appears to be the limiting factor in the reaction at the conditions tested.

The addition of water to the feed would allow characterization of the reverse reaction's role in the overall performance, as well as the effect of pyrolysis oil moisture content on the reaction. Also, removing water from the pyrolysis liquid could have a beneficial effect on reaction performance. Furthermore, simply varying the relative amounts of methanol, pyrolysis oil, catalyst, and TG/FFA could shed light on what is really happening both mechanistically and from a mass transfer perspective by determining parameters for which FFA esterification is *not* zero-order with respect to fatty acid concentration, or for which the pyrolysis oil esterification does not reverse—or even continues—with the addition of TG/FFA.

4.4.4. Downstream Processing of Mitigated Pyrolysis Oil and De-acidified TG/FFA

Downstream treatment of the coprocessing products will depend on the final products desired. If the kinetic limitations of coprocessing can be effectively overcome without permanent/prolonged homogenization or emulsification of the reaction mixture,

then the biodiesel from FFA esterification and the unreacted triglyceride will phase-separate from the methanol and pyrolysis oil, allowing separate downstream processing of the mitigated pyrolysis oil and the unreacted triglyceride. Conversion to biodiesel will require either additional methanol or recovery of methanol from the mitigated pyrolysis oil product, as shown in the integrated approach to waste biomass utilization diagrammed in Figure 4.7.

Processing pyrolysis oil with a high-FFA triglyceride feedstock undoubtedly causes pyrolysis oil compounds (and their esterification/acetalization products) to partition into the oil/biodiesel liquid phase. This contamination may be acceptable for downstream conversion of triglyceride to biodiesel; however, the effect of these compounds in the final product will have to be characterized.

If there is demand for a blend of biodiesel and pyrolysis liquid for a fuel application, then phase separation of the coprocessing products may not be desired; however, the degree of pyrolysis oil deacidification must be calibrated to the process chosen for triglyceride transesterification, since the complex mixture of functional groups in the pyrolysis oil will be available to the catalyst. If a traditional transesterification catalyst, such as a strong, homogeneous base, is to be used, then its effects on the mitigated pyrolysis oil must be understood. Other next-generation catalysts, however, may open the door to selective treatment of triglyceride even in an emulsion or solution of triglyceride, biodiesel, methanol, and deacidified pyrolysis oil.

Figure 4.8 shows an integrated approach to waste biomass utilization in which a catalytic coprocessing scheme is used as a more direct pathway to biodiesel/PyOil blends, allowing the excess methanol from the pyrolysis oil treatment to be used in triglyceride

transesterification as well.

4.5 Final Conclusions

Thermal treatment of biomass by fast pyrolysis is one means of upgrading lignocellulosic material. It is a tried-and-true process for producing biochar, a value-added product with great potential for upgrading to other value-added products; however, the pyrolysis liquids that are inevitably produced by the same processes—although the relative amount generated may be somewhat tuned by varying process parameters—present a problem for the economic and environmental impacts of biomass pyrolysis. This problem, however, also presents an opportunity: a relatively untapped fuel source with the potential to be carbon-neutral.

Catalytic esterification and transesterification of oils to generate biodiesel is one means of upgrading biomass. Biodiesel production is a growing area of research, and the generation of biodiesel from low-FFA feedstocks using homogeneous strong base catalysts, along with the treatment of higher-FFA feedstocks using homogenous strong acid catalysts, have seen some success with commercialization. However, the handling of traditional homogeneous catalysts and the limitations on feedstock choice presented by traditional processes cause biodiesel to struggle against high production costs. Ideal feedstocks for biodiesel production are generally high-quality triglyceride oils that double as food products in the marketplace, severely hampering the growth of the biodiesel industry in the absence of subsidies or fuel mandates. Next-generation processes that would allow low-cost conversion of high-FFA feedstocks—waste oils and the oils extracted from waste products (e.g., spent coffee grounds)—would help to eliminate

reliance on oil products with other uses, open the door to the utilization of untapped feedstocks, and be an overall boon to the biodiesel industry.

This work presents an ionic liquid catalyst with broad applicability to biomass upgrading. The results presented in Chapter 2 demonstrate that the catalyst has a remarkable potency for the esterification of pure carboxylic acids, and the choice of carboxylic acids tested—long-chain fatty acids—indicates that these results are especially relevant to the treatment of high-FFA triglyceride oils. The results presented in Chapter 3 show that the catalyst can achieve carboxylic acid esterification within a real-world pyrolysis oil, with the aim of mitigating the corrosiveness and instability of the bio-oil. A straightforward kinetic treatment of the reaction produces the remarkable result that the reaction—taken as the conversion of a specified fraction of titratable acids—is unequivocally second-order with respect to pyrolysis oil and second-order with respect to the ratio of catalyst to initial pyrolysis oil loading, despite actually being several reactions that take place among a complex panoply of different compounds with various functional groups. The use of the catalyst ratio in the model, rather than the catalyst concentration, likely accounts for compounds in the pyrolysis oil that inhibit the reaction, and the analysis produces a model with good predictive power in light of its simplicity. Recommendations for future work suggest that tabulating fitted kinetic parameters using other pyrolysis oil sources or even other catalysts would be a straightforward task that might shed light on the relevant processing parameters and feedstock characteristics to optimize a pyrolysis oil mitigation process to readily handle bio-oils from different sources.

Since pyrolysis liquid and high-FFA triglyceride oils both can be better utilized

following deacidification by esterification, Chapter 3 explored the possibility of coprocessing these feedstocks with the same catalyst, without an intermediate recovery step. The results showed diminished performance relative to the treatment of either bio-oil on its own; however, preliminary feasibility was demonstrated. Recommendations for future work show an obvious path forward if coprocessing is to be explored further, and there is a possibility that a more integrated treatment of bio-oils through catalytic coprocessing could be a promising new avenue for waste biomass utilization.

Table 4.1. *Summary of catalysts and kinetic models used to compare the results of this work to other esterification catalysts from the literature. "PFAD" is Palm Fatty Acid Distillate, composed primarily of palmitic acid and oleic acid.*

Reference	Catalyst	FFA	Model
This work	$[BHSO_3AIM][CF_3SO_3]$	Nonanoic	Adjusted from what was derived in this work
This work	$[BHSO_3AIM][CF_3SO_3]$	Palmitic	Adjusted from what was derived in this work
Aghabarari et al., 2013	ILB8	Oleic	Fitted to Equation 4.1. 1st Order on Catalyst
Li et al., 2014	$[BHSO_3MIM][HSO_4]$	Oleic	Fitted to Equation 4.1. Interpolation for catalyst dependence.
Alegria et al., 2015	4-DBSA	Oleic	Model and Parameters Given in Paper
Chabukswar et al., 2013	Sulfuric Acid	PFAD	Model and Parameters Given in Paper
Heer et al., 2015	Tosylic Acid	PFAD	Model and Parameters Given in Paper

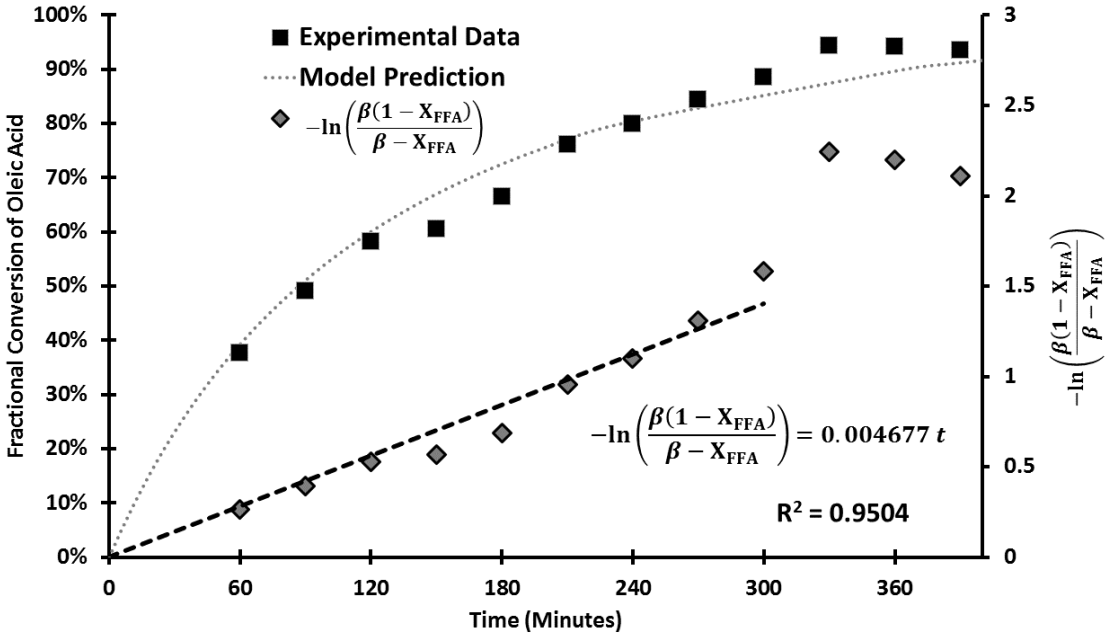

Figure 4.1. *Fitting the kinetic model to reported data on the esterification of oleic acid with IL8B acidic ionic liquid catalyst (Aghabarari, 2013). Temperature was 50 °C, Methanol:FFA molar ratio was 2:1, and catalyst loading was 7.50 mol % (20.7 wt %). The three latest points were excluded from the model and the calculation of* R^2.

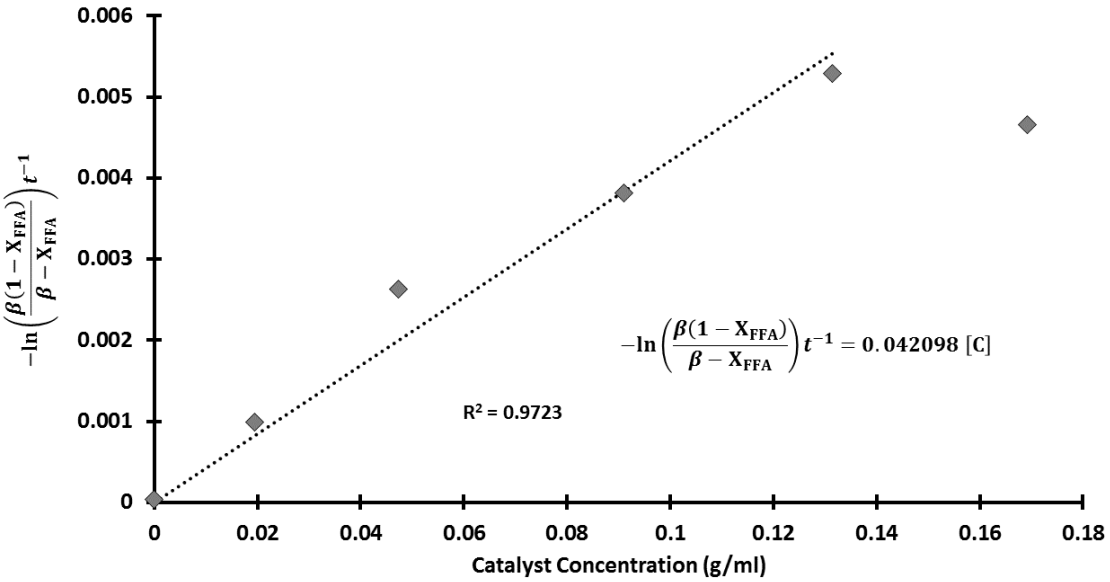

Figure 4.2. *A linear fit of first-order linear slopes versus catalyst concentration, based on reported data on the esterification of oleic acid with IL8B acidic ionic liquid catalyst (Aghabarari et al., 2013). The highest catalyst loading was excluded from the fit and the calculation of R^2. At the relevant range of concentrations, the reaction is first-order with respect to catalyst loading. Since the outlier excluded from this analysis reflects a decrease in performance, the model does not risk predicting unfairly poor performance for the reported catalyst.*

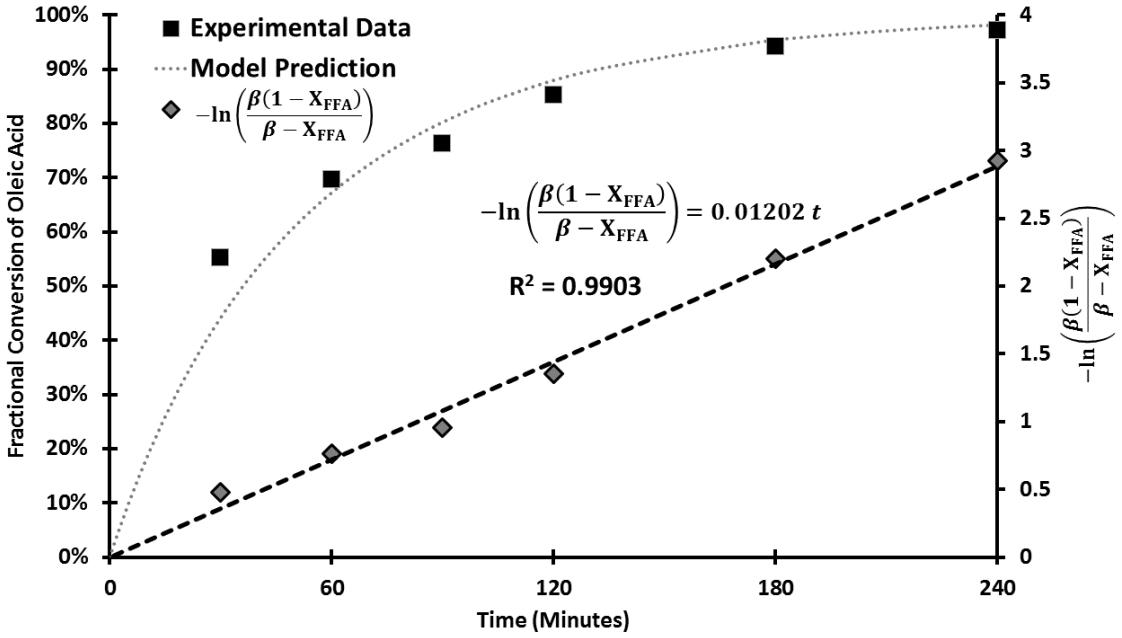

Figure 4.3. *Fitting the kinetic model to reported data on the esterification of oleic acid with [$BHSO_3MIM$][HSO_4^-] acidic ionic liquid catalyst (Li et al., 2014). Temperature was 130 °C, Methanol:FFA molar ratio was 2:1, and catalyst loading was 8.93 mol % (10.0 wt %).*

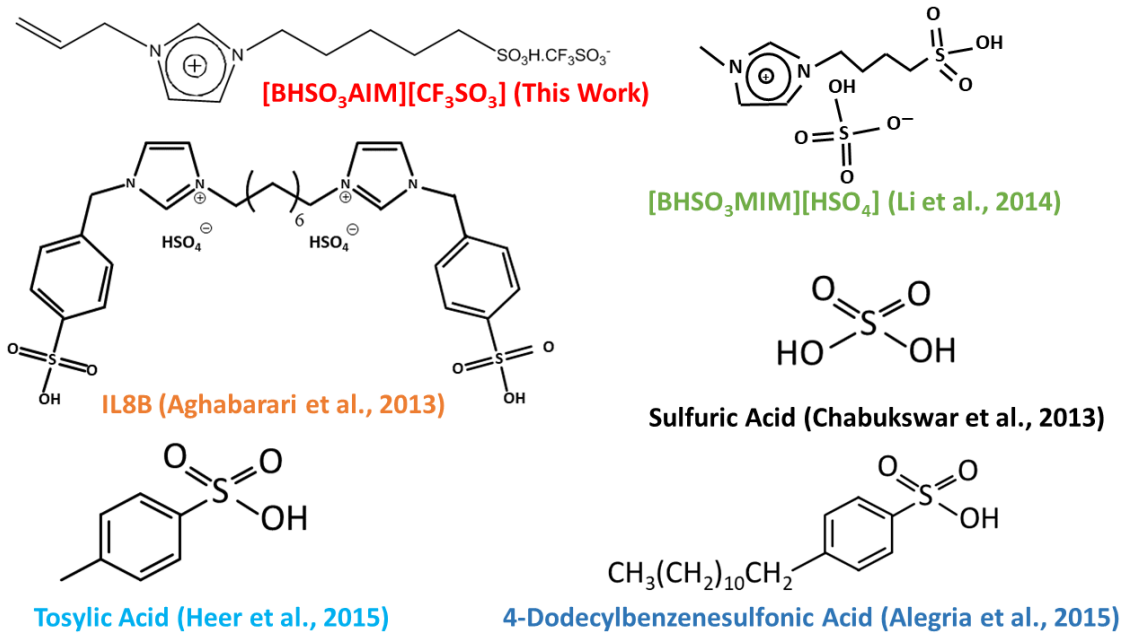

Figure 4.4. *The catalysts used in the comparison. IL8B was the most promising of four ionic liquids presented in the cited work. [BHSO3MIM][HSO4⁻] was the most promising of seven ionic liquids presented in the cited work. The name of each catalyst is color coded to the corresponding curves drawn in Figure 4.5 and Figure 4.6.*

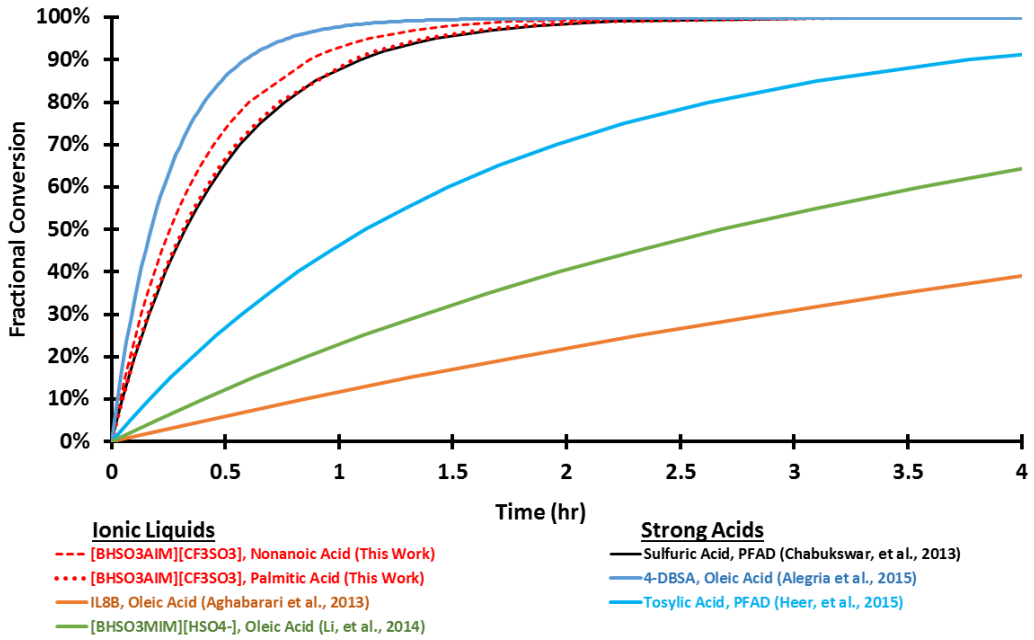

Figure 4.5. *Molar-basis comparison of catalyst from this work to other catalysts in the literature. Temperature = 60 °C, Methanol:FFA Ratio = 21:1, Catalyst Loading = 1.0 % (molar ratio of catalyst to FFA). [$BHSO_3AIM$][CF_3SO_3] is on par with homogeneous strong acid catalysts and superior to other ionic liquid catalysts.*

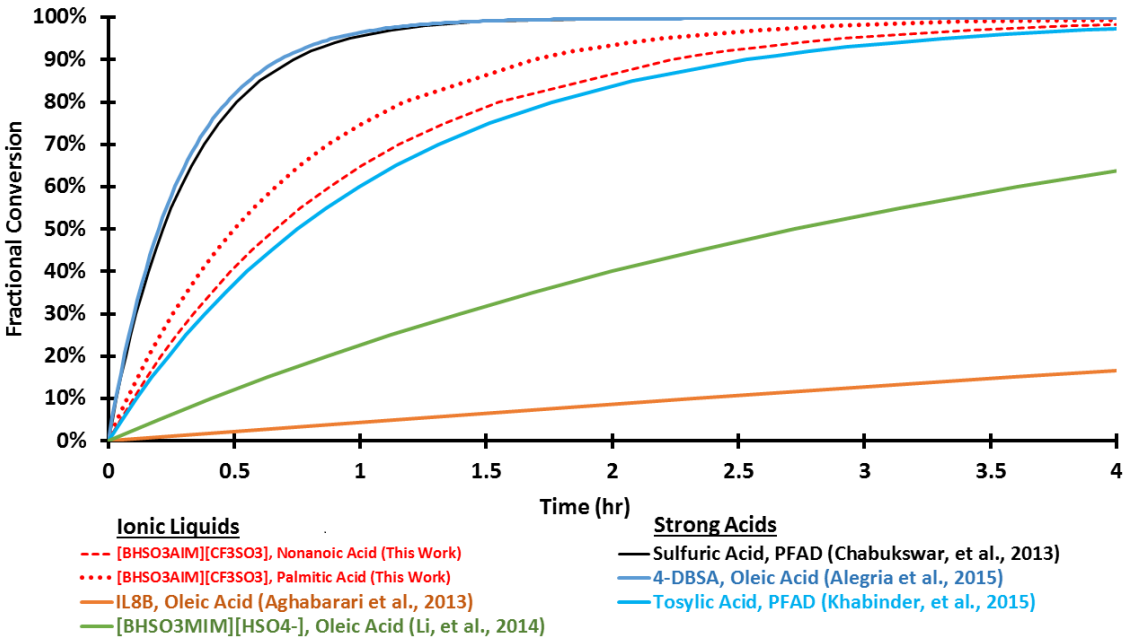

Figure 4.6. *Mass-basis comparison of catalyst from this work to other catalysts in the literature. Temperature = 60 °C, Methanol:FFA Ratio = 21:1, Catalyst Loading = 1.0 % (mass ratio of catalyst to FFA). [$BHSO_3AIM$][CF_3SO_3] is on par with homogeneous strong acid catalysts and superior to other ionic liquid catalysts.*

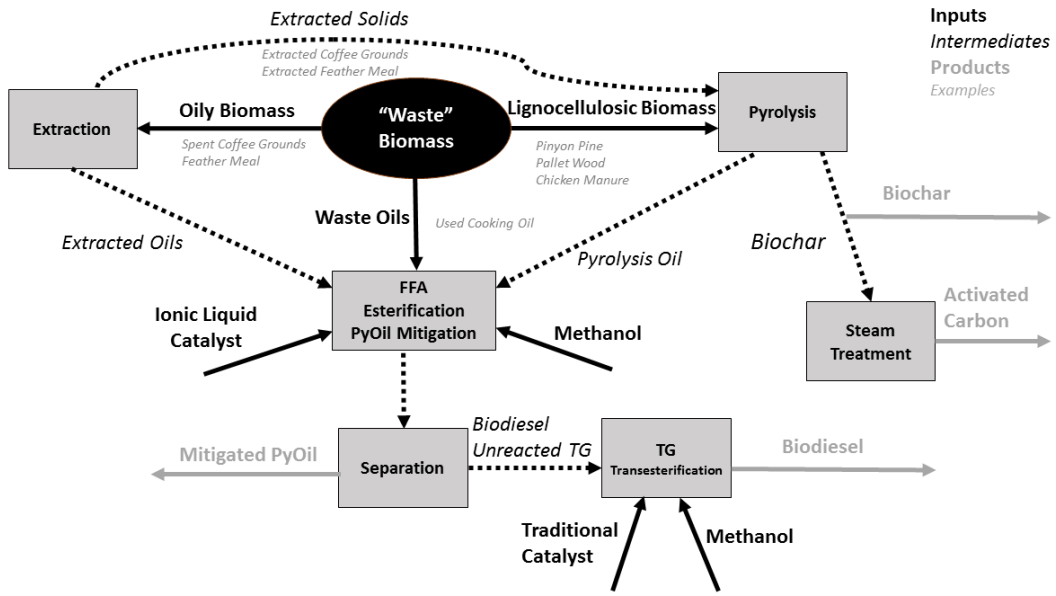

Figure 4.7. *An integrated approach to waste biomass utilization in which the ionic liquid catalyst is used for catalytic coprocessing of pyrolysis liquid with a high-FFA triglyceride feedstock. Subsequent phase separation of the deacidified mixture allows separate downstream treatment: conversion of unreacted triglyceride to biodiesel, and outright utilization or further treatment of the pyrolysis oil product.*

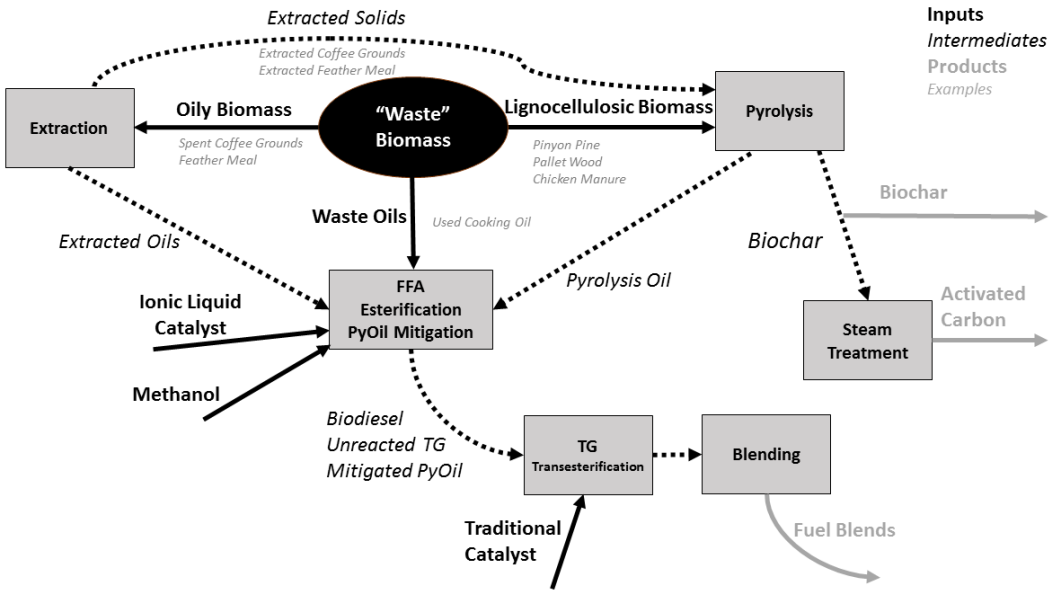

Figure 4.8. *An integrated approach to waste biomass utilization in which the ionic liquid catalyst is used for catalytic coprocessing of pyrolysis liquid with a high-FFA triglyceride feedstock to produce a single-phase product mixture as a more direct pathway to creating biodiesel/PyOil blends.*

REFERENCES

Aghabarari, B.; Dorostkar, N.; Ghiaci, M.; Amini, S.G.; Rahimi, E.; Martinez-Huerta, M.V. Esterification of fatty acids by new ionic liquids as acid catalysts. *Journal of the Taiwan Institute of Chemical Engineers.* **2014**, *45*, 431–435

Akhtar, J.; Amin, N. A review on operating parameters for optimum liquid oil yield in biomass pyrolysis. *Renewable and Sustainable Energy Reviews*. **2012**, *16*, 5101–5109

Alcala, A.; Bridgwater, A.V. Upgrading fast pyrolysis liquids: Blends of biodiesel and pyrolysis oil. *Fuel*. **2013**, *109*, 417–426.

Alegría, A.; Cuellar, J. Esterification of oleic acid for biodiesel production catalyzed by 4-dodecylbenzenesulfonic acid. *Applied Catalysis B: Environmental*. **2015**, *179*, 530–541

Alfa Aesar. http://www.alfa.com/en/ (Accessed June 10, 2017)

Alibaba. Wholesale Sulfuric Acid for Sale For Suppliers and Manufacturers. https://www.alibaba.com/showroom/wholesale-sulfuric-acid-for-sale.html (Accessed June 10, 2017)

Alsalme, A.; Kozhevnikova, E.F.; Kozhevnikov, I.V. Heteropoly acids as catalysts for liquid-phase esterification and transesterification. *Applied Catalysis A: General*. **2008**, *349*, 170–176

Andreani, L.; Rocha, J.D. Use of ionic liquids in biodiesel production: a review. *Brazillian Journal of Chemical Engineering.* **2012**, *29*(1), 1–13

Andrijanto, E.; Dawson, E.A.; Brown, D.R. Hypercrosslinked polystyrene sulphonic acid catalysts for the esterification of free fatty acids in biodiesel synthesis. *Applied Catalysis B: Environmental.* **2012**, *115–116*, 261–268

Antunes, W.M.; Veloso, C.O.; Henriques, C.A. Transesterification of soybean oil with methanol catalyzed by basic solids. *Catalysis Today.* **2008,** *133–135*, 548–554

Atadashi, I.M.; Aroua, M.K.; Aziz, A.R.A; Sulaiman, N.M.N. Production of biodiesel using high free fatty acid feedstocks. *Renewable and Sustainable Energy Reviews*. **2012**, *16(5)*, 3275–3285

Balat, M.; Balat, H. Progress in biodiesel processing. *Applied Energy*. **2010**, *87*, 1815–1835

Bridgwater, A.V., Review of fast pyrolysis of biomass and product upgrading. *Biomass and Bioenergy.* **2012**, *38*, 68–94.

Chabukswar, D.D.; Heer, P.K.K.S.; Gaikar, V.G. Esterification of palm fatty acid distillate using heterogeneous sulfonated microcrystalline cellulose catalyst and its comparison with H_2SO_4 catalyzed reaction. *Industrial & Engineering Chemistry Research.* **2013**, *52*, 7316–7326

Chiaramonti, D.; Bonini, M.; Fratini, E.; Tondi, G.; Gartner, K.; Bridgwater, A.V.; Grimm, H.P.; Soldaini, I.; Webster, A.; Baglioni, P. Development of emulsions from biomass pyrolysis liquid and diesel and their use in engines—Part 1: emulsion production. *Biomass and Bioenergy.* **2003**, *25*, 85–99.

Chiaramonti, D.; Bonini, M.; Fratini, E.; Tondi, G.; Gartner, K.; Bridgwater, A.V.; Grimm, H.P.; Soldaini, I.; Webster, A.; Baglioni, P. Development of emulsions from biomass pyrolysis liquid and diesel and their use in engines—Part 2: tests in diesel engines. *Biomass and Bioenergy*. **2003**, *25*, 101–111.

Chongkhong, S.; Tongurai, C.; Chetpattananondh, P. Continuous esterification for biodiesel production from palm fatty acid distillate using economical process. *Renewable Energy.* **2009**, *34*, 1059–1063

Chouhan, A.P.S.; Sarma, A.K.; Modern heterogeneous catalysts for biodiesel production: A comprehensive review. *Renewable and Sustainable Energy Reviews*. **2011**, *15*, 4378–4399

Czernik, S.; Bridgwater, A.V. Overview of applications of biomass fast pyrolysis oil. *Energy & Fuels.* **2004**, *18*, 590–598

Garcia, C.M.; Teixeira, S.; Marciniuk, L.L.; Schuchardt, U. Transesterification of soybean oil catalyzed by sulfated zirconia. *Bioresource Technology.* **2008**, *99*, 6608–6613

Di Serio, M.; Tesser, R.; Pengmei, L. Heterogeneous catalysts for biodiesel production. *Energy & Fuels.* **2008**, *22*, 207–217.

Furuta, S.; Matsuhashi, H.; Arata, K. Biodiesel fuel production with solid amorphous-zirconia catalysis in fixed bed reactor. *Biomass and Bioenergy*. **2006**, *30*, 870–873

Gunawan, R.; Li, X.; Larcher, A.; Hu, X.; Mourant, D.; Chaiwat, W.; Wu, H.; Li, C. Hydrolysis and glycosidation of sugars during the esterification of fast pyrolysis bio-oil. *Fuel*. **2012**, *95*, 146–151

Hayyan, A.; Mjalli, F.; Mirghani, M.; Hashim, M.; Hayyan, M.; AlNashef, I.; Al-Zahrani, S. Treatment of acidic palm oil for fatty acid methyl esters production. *Chemical Papers.* **2012**, *66*(1), 39–46

He, L.; Qin, S.; Chang, T.; Sun, Y.; Gao, X. Biodiesel synthesis from the esterification of free fatty acids and alcohol catalyzed by long-chain Bronsted acid ionic liquid. *Catalyst Science & Technology.* **2013**, *3*, 1002–1107

Heer, P.K.K.S.; Chabukswar, D.D.; Gaikar, V.G. Intrinsic kinetics of esterification of fatty acids catalyzed by supported ionic liquid catalysts. *Chemical Engineering and Technology*. **2015**, *38*(8) 1416–1424

Hilten, R.N.; Bibens, B.P.; Kastner, J.R.; Das, K.C. In-line esterification of pyrolysis vapor with ethanol improves bio-oil quality. *Energy and Fuels*. **2010**, *24*, 673–682.

Huber, G.W.; Iborra, S.; Corma, A. Synthesis of transportation fuels from biomass: chemistry, catalysis and engineering. *Chemical Reviews.* **2006**, *106*(9), 4044–4098

Hu, X.; Gunawan, R.; Mourant, D.; Hasan, M.D.M.; Wu, L.; Song, Y.; Lievens, C.; Li, C. Upgrading of bio-oil via acid-catalyzed reactions in alcohols—a mini review. *Fuel Processing Technology.* **2017**, *155*, 2–19

Ikura, M.; Stanciulescu, M.; Hogan, E. Emulsification of pyrolysis derived bio-oil in diesel fuel. *Biomass and Bioenergy.* **2003**, *24*, 221–232.

Issariyakul, T.; Kulkarni, M.G.; Dalai, A.K.; Bakhshi, N.N. Production of biodiesel from waste fryer grease using mixed methanol/ethanol system. *Fuel Processing Technology.* **2007**, *88*, 429–436

Jacobson, K.; Gopinath, R.; Meher, L.C.; Dalai, A.K. Solid acid catalyzed biodiesel production from waste cooking oil. *Applied Catalysis B: Environmental.* **2008**, *85*, 86–91

Jeguirim, M.; Limousy, L.; Dutournie, P. Pyrolysis kinetics and physiochemical properties of agropellets produced from spent ground coffee blended with conventional biomass. *Chemical Engineering Research and Design.* **2014**, *92*, 1876–1882

Kondamudi, N.; Mohapatra, S.K.; Misra, M. Spent coffee grounds as a versatile source of green energy. *Journal of Agricultural and Food Chemistry.* **2008**, *56*, 11757–11760

Kondamundi, N.; Strull, J.; Misra, M.; Mohapatra, S.K. A green process for producing biodiesel from feather meal. *Journal of Agricultural and Food Chemistry.* **2009**, *57*(14), 6163–6166

Kondamudi, N.; Mohapatra, S.K.; Misra, M. Quintinite as a bifunctional heterogeneous catalyst for biodiesel synthesis. *Applied Catalysis A: General.* **2011**, *393*(1-2), 36–43.

Kouzu, M.; Kasuno, T.; Tajika, M.; Sugimoto, Y.; Yamanaka, S.; Hidaka, J. Calcium oxide as a solid base catalyst for transesterification of soybean oil and its application to biodiesel production. *Fuel*. **2008**, *87*, 2798–2806

Leung, D.Y.C.; Guo, Y. Transesterification of neat and used frying oil: optimization for biodiesel production. *Fuel Processing Technology.* **2006**, *87*, 883–890

Li,Y.; Hu, S.; Cheng, J.; Lou, W. Acidic ionic liquid-catalyzed esterificatoin of oleic acid for biodiesel synthesis. *Chinese Journal of Catalysis.* **2014**, *35*, 396–406

Lotero, E.; Liu, Y.; Lopez, D.E.; Suwannakarn, K., Bruce, D.A., Goodwin, J.G. Synthesis of biodiesel via acid catalysts. *Industrial & Engineering Chemistry Research*. **2005**, *44*, 5353–5363

Mahfud, F.H.; Melian-Cabrera, I.; Manurung, R.; Heeres, H.J. Upgrading of flash pyrolysis oil by reactive distillation using a high boiling alcohol and acid catalysts. *Trans IChemE, Part B, Process Safety and Environmental Protection.* **2007**, *85*(B5), 466–472

Manya, J. Pyrolysis for biochar purposes: a review to establish current knowledge gaps and research needs. *Environmental Science and Technology*. **2012**, *46*(15), 7939–7954.

Moens, L.; Black, S.K.; Myers, M.D.; Czernik, S. Study of the neutralization and stabilization of a mixed hardwood bio-oil. *Energy & Fuels.* **2009**, *23*, 2695–2699.

Nakagaki, S.; Bail, A.; dos Santos, V.C.; de Souza, V.H.R.; Vrubel, H.; Nunes, F.S.; Ramos, L.P. Use of anhydrous sodium molybdate as an efficient heterogeneous catalyst for soybean oil methanolysis. *Applied Catalysis A: General.* **2008**, *351*, 267–274

Nakajima, K.; Hara, M. Amorphous carbon with SO_3H groups as a solid bronsted acid catalyst. *ACS Catalysis.* **2012**, *2*(7), 1296–1304

Nebel, B.A.; Mittelbach, M. Biodiesel from extracted fat out of meat and bone meal. *European Journal of Lipid Science and Technology.* **2006**, *108*(5), 398–403

Park, Y.; Lee, D.; Kim, D.; Lee, J.; Lee, K. The heterogeneous catalyst system for the continuous conversion of free fatty acids in used vegetable oils for the production of biodiesel. *Catalysis Today.* **2008**, *131*, 238–243

Qi, Z.; Jie, C.; Tiejun, W.; Ying, X. Review of biomass pyrolysis oil properties and upgrading research. *Energy Conversion and Management.* **2007**, *48*, 87–92.

Qiao, K.; Hagiwara, H.; Yokoyama, C. Acidic ionic liquid modified silica gel as novel solid catalysts for esterification and nitration reactions. *Journal of Molecular Catalysis A: Chemical.* **2006**, *246*(1-2), 65–69

Roberts, G.W. *Chemical Reactions and Chemical Reactors*, first ed. John Wiley & Sons, New Jersey, 2009.

Russbueldt, B.M.E.; Hoelderich, W.F. New sulfonic acid ion-exchange resins for the preesterification of different oils and fats with high content of free fatty acids. *Applied Catalysis A: General.* **2009**, *362*, 47–57

Semwai, S.; Arora, A.K.; Badoni, R.P.; Tuli, D.K. Biodiesel production using heterogeneous catalysts. *Bioresource Technology.* **2011**, *102*, 2151–2161

Shi, H.; Wang, Y.; Hua, R. Acid-catalyzed carboxylic acid esterification and ester hydrolysis mechanism: acylium ion as a sharing active intermediate via a spontaneous trimolecular reaction based on density functional theory calculation and supported by electrospray ionization-mass spectrometry. *Physical Chemistry Chemical Physics*. **2015**, *17*, 30279–30291

Sreeprasanth, P.S.; Srivastava, R.; Srinivas, D.; Ratnasamy, P.. Hydrophobic, solid acid catalysts for production of biofuels and lubricants. *Applied Catalysis A: General*. **2006**, *314*, 148–159

Sun, H.; Ding, Y.; Duan, J.; Zhang, Q.; Wang, Z.; Lou, H.; Zheng, X.. Transesterification of sunflower oil to biodiesel on ZrO_2 supported La_2O_3 catalyst. *Bioresource Technology*. **2010**, *101*, 953–958

Tesser, R.; Di Serio, M.; Guida, M.; Nastasi, M.; Santacesaria, E. Kinetics of oleic acid esterification with methanol in the presence of triglycerides. *Industrial & Engineering Chemistry Research*. **2005**, *44*, 7978–7982

Vafaeezadeh, M.; Fattahi, A. DFT investigations for "Fischer" esterification mechanism over silica-propyl-SO_3H catalysts: Is the reaction reversible? *Computation and Theoretical Chemistry.* **2015**, *1071*, 27–32

Veljkovic, V.B.; Lakicevic, S.H.; Stamenkovic, O.S.; Todorovic, Z.B.; Lazic, M.L. Biodiesel production from tobacco (Nicotiana tabacum L.) seed oil with a high content of free fatty acids: Short communication. *Fuel*. **2006**, *85*, 2671–2675

Wang, C.; Hu, Y.; Chen, Q.; Lv, C.; Jia, S. Bio-oil upgrading by reactive distillation using p-toluene sulfonic acid catalyst loaded on biomass activated carbon. *Biomass and Bioenergy.* **2013**, *56*, 405–411

Watson, H.B. *Modern Theories of Organic Chemistry* **1937**. Oxford University Press. Oxford, England, U.K., 1937. pp 130–211.

Xiong, W.; Zhu, M.; Deng, L.; Fu, Y.; Guo, Q. Esterification of organic acid in bio-oil using acidic ionic liquid catalysts. *Energy & Fuels.* **2009**, *23*, 2278–2283

Yoo, S.J.; Lee, H.; Veriansyah, B.; Kim, Jaehoon; Kim, Jae-Duck; Lee, Y.; Synthesis of biodiesel from rapeseed oil using supercritical methanol with metal oxide catalysts. *Bioresource Technology*. **2010**, *101*, 8686–8689

Zhang, Q.; Chang, J.; Wang, T.; Xu, Y. Upgrading bio-oil over different solid catalysts. *Energy & Fuels*. **2006**, *20*, 2717–2720

Zhang, Z.; Wang, Q.; Tripathi, P.; Pittman, C.U. Catalytic upgrading of bio-oil using 1-octene and 1-butanol over sulfonic acid resin catalysts. *Green Chemistry*. **2011**, *13*, 940–949